2008

OXIDATIVE STRESS AND THE GUANOSINE NUCLEOTIDE TRIPHOSPHATE POOL: IMPLICATIONS FOR A BIOMARKER AND MECHANISM OF IMPAIRED CELL FUNCTION

Celeste Maree Bolin
The University of Montana

OXIDATIVE STRESS AND THE GUANOSINE NUCLEOTIDE TRIPHOSPHATE POOL: IMPLICATIONS FOR A BIOMARKER AND MECHANISM OF IMPAIRED CELL FUNCTION

By

Celeste Maree Bolin

B.A. Chemistry, Whitman College, Walla Walla, WA 2001

Dissertation

presented in partial fulfillment of the requirements
for the degree of

Doctor of Philosophy
in Toxicology

The University of Montana
Missoula, Montana

Spring 2008

Approved by:

Dr. David A. Strobel, Dean
Graduate School

Dr. Fernando Cardozo-Pelaez, Chair
Department of Biomedical and Pharmaceutical Sciences

Dr. Diana Lurie,
Department of Biomedical and Pharmaceutical Sciences

Dr. Richard Bridges
Department of Biomedical and Pharmaceutical Sciences

Dr. Darrell Jackson
Department of Biomedical and Pharmaceutical Sciences

Dr. Kent Sugden
Department of Chemistry

Oxidative stress and the guanosine nucleotide triphosphate pool: implications for a biomarker and mechanism of impaired cell function

Chairperson: Fernando Cardozo-Pelaez, Ph.D.

Oxidation of the guanosine (G) moiety, yielding the oxidized lesion 8-hydroxy-2'-deoxyguanosine (oxo^{8}2dG), in DNA has become a hallmark biomarker in assessing cellular outcomes induced by oxidative stress. It is well established that the guanosine nucleotide triphosphate pool is also susceptible to oxidative stress and suggested to be more available for oxidation than DNA due to the lack of protective histones and robust repair mechanisms for reducing the levels of all the products of oxidation. The oxidation of guanosine in the nucleotide triphosphate pool, resulting in oxidized guanosine 5'-triphoshate (oxo^{8}GTP), has been overlooked due to the lack of a reliable method. Oxo^{8}GTP has been shown to precede oxidation to G incorporated into DNA and modulate cell processes such as G-protein signaling and RNA synthesis. Evidence is presented in this study of a reliable method to quantify oxo^{8}GTP, a proposed mechanism for the oxidative modification of GTP in the presence of copper and L-ascorbic acid, and evidence of oxo^{8}GTP as an inhibitor of soluble guanylyl cyclase (sGC). A significant induction of oxo^{8}GTP in cell-free preparations as well as in PC12 and HEK 293T cells exposed to physiologically relevant oxidative conditions generated with 10 μM copper sulphate and 1mM L-Ascorbic Acid (Cu/Asc) is also reported. Exposure to oxidative conditions by Cu/As leads to elevations in oxo^{8}GTP significant enough to result in a reduction of the sGC product, cyclic guanosine monophosphate (cGMP), by as much as half in pure sGC and PC12 cells. GTP is protected from oxidation in the presence of reduced glutathione and this subsequently rescues sGC activity. This suggests that oxo^{8}GTP is produced by free radicals *in vivo* and can significantly impact neuronal cell functions regulated by sGC activity in the central nervous system such as synaptic plasticity. Alterations in copper homeostasis and oxidative stress have been implicated in several neurodegenerative disorders including Alzheimer's and Parkinson's diseases as well as Amyotrophic Lateral Sclerosis. Based upon evaluation of the data presented herein, we hypothesize that neuronal deficiencies in such disorders might be due to oxidation of the GTP pool and the ensuing effects on neuronal function.

ACKNOWLEDGEMENTS

Thank you to my parents, John and Christine Bolin, for their unconditional love and constant motivation to pursue my dreams even in a place far away from home in more ways than one. I would also like to thank all my friends for their encouragement of my scientific and life pursuits, especially my partner, JC Schneider who has been holding the other end of the rope during the hardest part of my PhD ascent.

I would also like to thank my advisor, Dr. Fernando Cardozo-Pelaez who told me he would fire me if I didn't go to graduate school. I have found a place in science that fulfills me more than I thought possible, and the opportunities he has granted me to challenge my abilities sewed the seeds of that inspiration.

I would like to further thank the Center for Environmental Health Sciences and the Department of Pharmaceutical and Biomedical Sciences at The University of Montana for the educational and funding resources necessary to pursue my graduate degree. I would also like to thank the members of my committee Dr. Diana Lurie, Dr. Darrell Jackson, Dr. Richard Bridges, and Dr. Kent Sugden for their mentorship, expertise, and all their invested time during my graduate school educational experience.

Addditional gratitude to the following funding sources during my PhD: P.E.O International, AFPE, and NSF EPScOR.

TABLE OF CONTENTS

LIST OF FIGURES

LIST OF TABLES

INTRODUCTION

Maintenance of Cellular Oxidative Status

The careful balance between reductants and oxidants in the cellular pool is collectively referred to as cellular redox status. The redox status of a cell influences normal cell functioning processes such as proliferation, differentiation as well as intra- and extracellular signaling. It is also thought to play a role in deleterious processes such as cell death and carcinogenesis. Cellular redox status is a dynamic state dependent on the levels of free radicals, highly reactive molecular species that contain one or more unpaired electrons. The most oxidizing free radical found in cells is the hydroxyl radical ($^{\bullet}OH$) which belongs to a class of oxygen –containing compounds termed reactive oxygen species (ROS). The superoxide radical ($O_2^{\bullet -}$) and hydrogen peroxide (H_2O_2) are also given this designation of abundant cellular ROS. As shown in Table 1 and discussed in detail below, there are several cellular sources of these ROS as well as complementary antioxidants and free radical scavengers regulating their relative concentration. The loss of balance between ROS and antioxidants in the cellular milieu which results in a deleterious impact on cell function and fate is defined as oxidative stress (Sies 1991).

Table 1. Cellular sources and respective antioxidant and free radical scavengers maintaining the concentration of the most abundant cellular reactive oxygen species.

Reactive Oxygen Species	Cellular Source	Cellular Antioxidant Enzymes and Small Molecule Antioxidants
Hydroxyl radical, $^{\bullet}OH$	Reaction of transition metals with H_2O_2 (Fenton Reaction) 1) $Fe^{2+} + H_2O_2 \rightarrow Fe^{3+} + {}^{\bullet}OH + {}^{-}OH$ 2) $Cu^{+} + H_2O_2 \rightarrow Cu^{2+} + {}^{\bullet}OH + {}^{-}OH$	α-Tocopherol (vitamin E) Ascorbate (vitamin C)
Superoxide Radical, $O_2^{\bullet-}$	Mitochondrial electron transport chain Enzymes including NADPH oxidase and nitric oxide synthase Auto-oxidation reactions Heme proteins heme-Fe^{2+}-$O_2 \rightarrow$ heme$Fe^{3+} + O_2^{\bullet-}$	Superoxide Dismutase (SOD) $2O_2^{\bullet-} + 2H^{+} \rightarrow H_2O_2 + O_2$
Hydrogen Peroxide, H_2O_2	Mitochondrial electron transport chain (dismutation of $O_2^{\bullet-}$) Enzymes including xanthine, urate, monoamine and D-amino oxidases such as SOD	Catalase $2H_2O_2 \rightarrow 2H_2O + O_2$ Glutathione Peroxidase (GPx) $H_2O_2 + 2GSH \rightarrow GSSG + 2H_2O$

Adapted from (Halliwell 2007)

The hydroxyl radical is the ROS with the highest reduction potential (2.31V) and therefore is the most oxidizing (Buettner 1993). Most of the $^{\bullet}OH$ produced in the cell is a result of the reduction of transition metals such as Fe(II) and Cu(I) in the presence of H_2O_2 via the Fenton reaction (Table 1) (Liochev 1999). The initial oxidation of Fe(III) and Cu(II) to their Fenton-reactive species requires the presence of abundant cellular reductants such as ascorbate. Superoxide also catalyzes this oxidation of Fe(III) and Cu(II) thus combining the Fenton reaction with the Haber-Weiss reaction ($O_2^{\bullet-} + H_2O_2 \rightarrow O_2 + {}^{\bullet}OH + {}^{-}OH$). However, under normal physiological conditions it is thought that concentrations of $O_2^{\bullet-}$ are too low to facilitate this reaction (Haber and Weiss 1934; Halliwell 2007). The cellular concentration of these transition metals in their redox-active, "free" states is also tightly regulated within physiological limits. This is accomplished by metal binding proteins such as hemoglobin, myoglobin, and ferritin for Fe(II) and albumin, cerruloplasmin, and copper chaperones for Cu(II). However, an increased body burden of both of these Fenton-reactive metals is known to occur with toxicological insult and disease pathologies which will be discussed later.

Likely due to the extremely short half life of $^{\bullet}OH$ which is on the order of nanoseconds, and its high reactivity *in vivo*, there are no antioxidant enzymes with the specific function of removing $^{\bullet}OH$ (Pastor, Weinstein et al. 2000). Most scavenging of this ROS is accomplished by small molecule antioxidants such as α-tocopherol (vitamin E) and ascorbate (vitamin C) maintained through dietary sources. Oxidative modification of biomolecules such as proteins, lipids, and DNA is often associated with attack by $^{\bullet}OH$ and the byproducts have been used biomarkers of cellular oxidative stress. These will be discussed in detail. Recently, it was reported that the major byproduct from the repair of

oxidatively modified DNA, measured in urine, showed an inverse correlation with blood plasma levels of vitamins E and C in healthy subjects (Foksinski, Gackowski et al. 2007).

The superoxide radical is far less reactive than $^{\bullet}OH$ with a much lower reduction potential (0.94V) although it has a high rate of physiological production in mitochondria (Buettner 1993). The mitochondria is the main source of energy production in the form of ATP synthesis for the cell. This is accomplished by transfer of electrons through the mitochondrial electron transport chain. Complexes I and III of the electron transport chain can leak electrons directly to O_2 producing $O_2^{\bullet-}$. Other sources of $O_2^{\bullet-}$ are listed in Table 1 including production by endogenous enzymes, auto-oxidation reactions of biological molecules such as the neurotransmitters adrenalin and dopamine, and a small amount of intermediary heme-Fe(III)- $O_2^{\bullet-}$ formed when O_2 binds to iron in hemoglobin or myoglobin (Yeh and Alayash 2003). There are two main forms of superoxide dismutase (SOD) responsible for maintaining low intracellular concentrations of $O_2^{\bullet-}$: Copper-zinc SOD (CuZn SOD) located in the cytoplasm, also referred to as SOD1 and manganese SOD (Mn SOD) located in the mitochondria, also referred to as SOD2. The function of these enzymes is to catalyze the dismutation of $O_2^{\bullet-}$ to H_2O_2 and O_2 each forming an enzyme-metal intermediate with either Cu or Mn (Table 1). The importance of these antioxidant enzymes has been emphasized in studies of transgenic mice lacking SOD activity. Deficiency in MnSOD results in perinatal fatality in mice due to severe central nervous system (CNS) and cardiac degeneration (Lebovitz, Zhang et al. 1996). Additionally, ablation of the gene for CuZn SOD in mice results in severe damage to the CNS and vascular dysfunction along with hepatocarcinogenesis and skeletal muscle atrophy over the life-span of the animals (Reaume, Elliott et al. 1996; Didion, Ryan et al.

2002; Elchuri, Oberley et al. 2005; Jackson 2006; Muller, Song et al. 2006). Overexpression of human CuZn SOD has been shown to attenuate age-related increases in oxidative damage (Cardozo-Pelaez, Song et al. 1998). Conversely, elevated wild-type CuZn SOD has also been shown to increase oxidative burden in mice potentially due to the increase in the ROS byproduct of SOD reactions, H_2O_2 (Peled-Kamar, Lotem et al. 1997).

Hydrogen peroxide is the only ROS discussed that is not, by definition, a free radical and therefore it is far less reactive than $^{\bullet}OH$ or $O_2^{\bullet-}$ and is a very weak oxidant with a reduction potential of only 0.32V (Buettner 1993). However, H_2O_2 is ubiquitous in physiological tissues and steady-state concentrations have been suggested to be as high as 10^{-7}M (Halliwell 2007). Due to the ease with which H_2O_2 crosses cell membranes and its integral participation in forming the highly damaging $^{\bullet}OH$ via the Fenton reaction, levels are regulated by the presence of specific antioxidant enzymes including catalase and glutathione peroxidase (GPx) which catalyze the detoxification of H_2O_2 to H_2O and O_2 (Table 1). Deficiencies in catalase in humans, acatalasemia, does not result in overt pathology although it has been associated with increased risk for the development of diabetes and vascular disease (Leopold and Loscalzo 2005). Similarly, deletion of the gene encoding catalase in mice is not fatal although apparently increases susceptibility to H_2O_2 generating toxins and cancer development with age (Ho, Xiong et al. 2004). The lack of overt pathology is likely due to the redundancy in H_2O_2 scavenging enzymes within the cell with deficiencies in catalase compensated for by enzymes such as GPx. Knockout mice lacking GPx show similar susceptibilities to oxidative insults as the catalase knockout phenotype (Fu, Cheng et al. 1999).

Another highly active reductant in the cell capable of scavenging free radicals is the thiol-containing antioxidant reduced glutathione (GSH). GSH, in addition to being a cofactor for GPx reactions, is also an important small molecule antioxidant independent of this role. GSH has been shown to interact with $^{\bullet}$OH *in vitro*, but its primary role in maintaining redox balance is thought to be by preventing protein thiol groups from oxidation thus preventing deleterious protein cross-linking. A deficiency in the rate-limiting enzyme for GSH synthesis, γ-glutamylcysteine synthetase, in transgenic mice is embryonic lethal and a decrease in tissue GSH levels is associated with a range of human diseases such as Wilson's disease, Parkinson's disease, and pulmonary fibrosis (Summer and Eisenburg 1985; Jenner 1993; Dalton, Dieter et al. 2000; Hudson 2004).

Fluctuations in the redox status of the cell are associated with normal processes of development and aging as well as the pathogenesis of several diseases and outcomes of toxicological insult. Levels of ROS are highly influential over this redox status participating in both beneficial and pathological cellular processes. In order to better characterize the latter, biomarkers of oxidative stress are often quantified as oxidative lesions in macromolecules such as DNA. These biomarkers serve a dual role as both tools with diagnostic potential for diseases and toxicological insults that do not exhibit signs of obvious pathology and as mechanistic endpoints which could help in the search for more specific therapeutic interventions.

Oxidative Damage and Repair of Guanine Incorporated into DNA

The oxidative modification of DNA by ROS can generate a number of possible DNA lesions. Of the two purine DNA bases, guanine and adenine, and the two pyrimidine DNA bases, cytosine and thymine, guanine has the lowest reduction potential

and therefore is the most readily oxidized (Devasagayam, Steenken et al. 1991; Steenken 1997; Milligan, Aguilera et al. 2001). Two-electron oxidation of the C8 position of guanosine, the guanine base with associated ribose sugar, facilitated by $^{\bullet}$OH attack results in the formation of 8-oxoguanosine (oxo^{8}G) (Table 2). A tautomeric form of this adduct, 8-hydroxyguanosine (OH^{8}G), is the major oxidation product of guanosine oxidation at low pH conditions similar to those employed in most analytical detection methods (Figure 1) (Culp, Cho et al. 1989; Breen and Murphy 1995). However, at physiological pH = 7.4, oxo^{8}G is the predominant form.

FIGURE 1

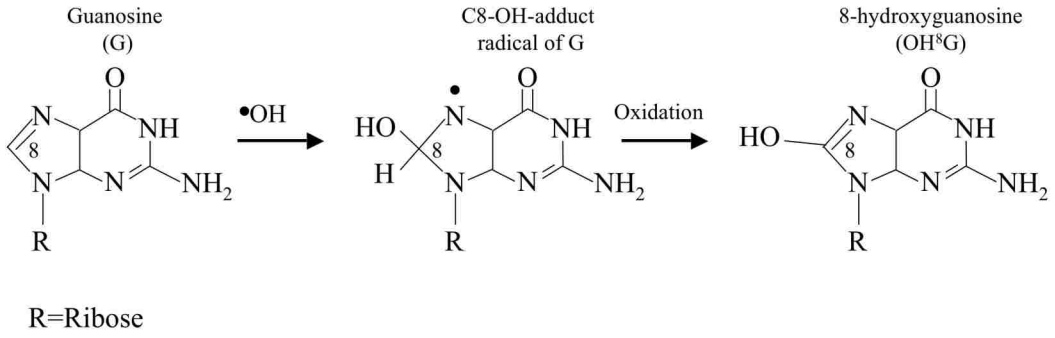

Adapted from (Breen and Murphy 1995; Dizdaroglu, Jaruga et al. 2002)

Figure 1. Mechanism of two-electron oxidation of guanosine.

Hydroxyl radical attack at the C8 position of guanine causes electron abstraction from the N7 position forming a C8-OH-adduct reactive intermediate which undergoes oxidation to form 8-hydroxyguanosine.

In the 2'-deoxyguanosine (2-dG) form found in DNA, guanine base with associated deoxyribose sugar, this same mechanism of oxidation by $^{\bullet}$OH results in the formation of the 8-oxo-2'-deoxyguanosine (oxo^{8}2dG) lesion (Kasai and Nishimura 1983). A summary clarifying the nomenclature of these guanine-containing moieties and their oxidized counterparts is outlined in Table 2.

Table 2. Nomenclature and description of guanine and oxidized guanine compounds

Name	Abbr	Compound Description	Classification
Guanine	Gua	Guanine base	Purine
8-oxo-7,8-dihydroguanine	Oxo^8Gua	Oxidized guanine base	Oxidized purine
Guanosine	G	Guanine attached to ribose	Nucleoside
8-oxoguanosine	Oxo^8G	Oxidized guanosine	Oxidized Nucleoside
2'-deoxyguanosine	2-dG	Guanine attached to a 2'-deoxyribose	Nucleoside
8-oxo-2'-deoxyguanosine	Oxo^8dG	Oxidized 2'-deoxyguanosine	Oxidized Nucleoside
Cyclic guanosine 5'-monophosphate	cGMP	Cyclic guanine nucleoside monophosphate	Nucleotide
Guanosine 5'-triphosphate	GTP	Guanosine with 3 phosphate groups	Nucleoside Triphosphate
8-oxoguanosine 5'-triphosphate	Oxo^8GTP	Oxidized guanosine nucleoside triphosphate	Oxidized Nucleoside Triphosphate
Deoxyguanosine 5'-triphosphate	dGTP	2'-deoxyguansine with 3 phosphate groups	Nucleoside Triphosphate
8-oxo-2'-deoxyguanosine 5'-triphosphate	Oxo^8dGTP	Oxidized 2'-deoxyguanosine nucleoside triphosphate	Oxidized Nucleoside Triphosphate

Adapted from (Halliwell 2007)

The oxo^{8}2dG adduct is one of the most frequently studied of the over twenty oxidized DNA base products characterized and it attracts considerable interest as a biomarker of oxidative stress associated with a host of normal and disease-associated physiological processes including aging, diabetes, and cancer (Dandona, Thusu et al. 1996; Dizdaroglu, Jaruga et al. 2002; Chiou, Chang et al. 2003). The ultimate consequences of oxo^{8}dG accumulation are unclear; however, it is known to have deleterious effects in both proliferating and differentiated cells, leading to the initiation step of carcinogenesis in the former and apoptosis in the latter. Several reports have shown that oxo^{8}dG can preclude cellular transformation in proliferating cells, as it has been frequently identified in the p53 tumor suppressor gene observed in lung and liver cancer (Hollstein, Sidransky et al. 1991). The consequences of oxo^{8}dG accumulation in postmitotic cells such as neurons appear to be errors in transcription (Chen and Bogenhagen 1993). Oxo^{8}dG accumulation has been associated with aging and neurodegenerative disease. Basal levels of oxo^{8}dG have been shown to increase with aging in various rodent tissues, as well as in animal models of neurological disease (Fraga, Shigenaga et al. 1990; Chen and Bogenhagen 1993; Cardozo-Pelaez, Song et al. 1999; Bogdanov, Andreassen et al. 2001). In age-related neurodegenerative diseases such as Alzheimer's (AD) and Parkinson's Disease (PD), a significant increase in oxo^{8}2dG levels in impacted brain regions and in cerebral spinal fluid (CSF) as compared to age-matched controls has been demonstrated in post-mortem tissue (Table 3).

Table 3. Percent of oxo^{8}2G relative to unmodified 2-dG significantly increased compared to age-matched controls in Alzheimer's and Parkinson's Disease brains.

Percent Oxo^{8}2dG/ 2dG in Nuclear DNA

CNS Sample	Age-Matched Control	Alzheimer's Disease	Reference
Ventricular CSF	0.617%	3.200%	Lovell et. al., 1999
Frontal Lobe	0.309%	0.926%	Gabbita et.al., 1998
Frontal Lobe	0.005%	0.013%	Wang et. al., 2005
Temporal Lobe	0.309%	1.230%	Gabbita et.al., 1998
Parietal Lobe	0.309%	0.770%	Gabbita et.al., 1998
Parietal Lobe	0.077%	0.154%	Lyras et. al., 1997
Parietal Lobe	0.005%	0.008%	Wang et. al., 2005
CNS Sample	**Age-Matched Control**	**Parkinson's Disease**	**Reference**
Substantia Nigra	0.463%	0.926%	Alam et. al., 1997
Substantia Nigra	0.002%	0.005%	Sanchez-Ramos et. al., 1994
Medial Putamen	0.386%	0.540%	Alam et. al., 1997
Caudate	0.002%	0.006%	Sanchez-Ramos et. al., 1994

Oxidative stress is recognized as an important pathological hallmark of both AD and PD although the percent of oxo^{8}2dG relative to unmodified 2-dG in nuclear DNA from the brains of patients is as low as 0.005% with an upper limit of only around 1% (Table 3). The significance of these small percentages of oxo^{8}dG in DNA in disease suggests that relatively low levels of oxidation may indeed have drastic cellular consequences, especially in a post-mitotic neuronal cell. Also, given the fact that guanine is more abundant in other cellular compartments, it raises the possibility that oxidation of guanine in the genomic DNA pool is not the most robust biomarker of oxidative status. The free-radical theory of aging first introduced in 1956 by Denham Harman suggests that aging results from the accumulation of oxidative damage to tissue by free radicals. This theory is supported by the observation that there is an inverse relationship between metabolic rate and subsequent O_2 consumption and lifespan. Measurements of the oxidized guanine DNA base excision repair product, 8-oxo-7,8-dihydroguanine (oxo^{8}Gua), excreted into urine verified a positive correlation with metabolic rate and negative correlation with lifespan which was specific for this lesion as compared to other oxidative DNA repair products (Foksinski, Rozalski et al. 2004).

There are two mechanisms by which oxo^{8}dG can be incorporated into DNA: (1) direct modification of DNA by oxyradical attack or (2) by oxidative modification of 2'-deoxyguanosine triphosphate (dGTP) substrate used by DNA polymerases during DNA replication (Figure 2).

FIGURE 2

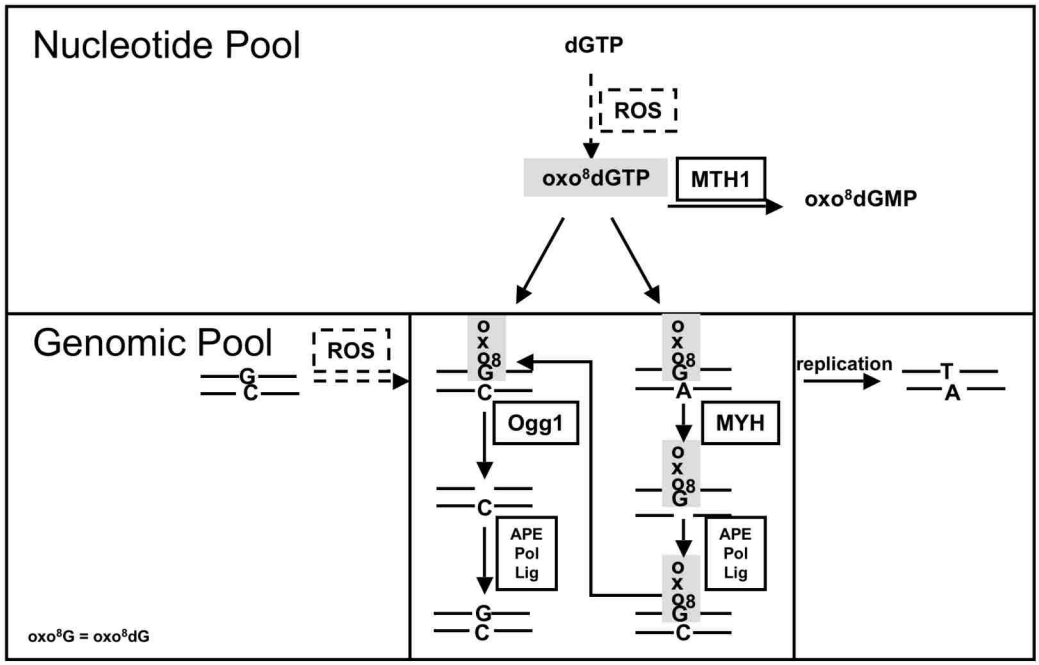

Adapted from (Nakabeppu, Tsuchimoto et al. 2007)

Figure 2. Repair enzymes for oxo^{8}dG lesions in the nucleotide and genomic pool. Oxo^{8}dG can be incorporated into DNA either by oxidation of dGTP in the nucleotide pool or direct oxidition to the guanine base in DNA. This can result in G:C to T:A transversions due to the ability of oxo^{8}dG to pair with adenosine in DNA. MTH1 is the dGTPase responsible for recognizing and hydrolyzing oxo^{8}dGTP from this nucleotide pool as a first line of defense against this lesion making its way into DNA. However, once incorporated into DNA, the Ogg1 glycosylase enzyme recognizes and cleaves this lesion paired with cytosine and with the help of an apurinic endonuclease (APE), DNA polymerase (Pol) and DNA ligase (Lig) the DNA is fully repaired. If the oxo^{8}dG lesion is paired with adenosine after replication, another glycosylase, MutY, will cleave the adenosine which can then be replaced with cytosine by APE, Pol, and Lig enabling oxo^{8}dG to be recognized and removed by the activity of Ogg1.

Oxo^{8}dG is pro-mutagenic due to its tendency to preferentially pair with adenine over cytosine during DNA replication, leading to G:C to T:A transversions (Hollstein, Sidransky et al. 1991; Shibutani, Takeshita et al. 1991; Cheng, Cahill et al. 1992). If antioxidant systems fail to prevent oxidation of G in the dGTP pool or in DNA, cells have a redundant system of enzymes that catalyze the sanitation of either the oxidized guanosine nucleotide pool (MTH1), remove oxo^{8}dG from DNA (Ogg1), or after replication remove the mispaired A to the oxo^{8}dG (MYH).

Oxo^{8}dG is cleaved from DNA by enzymes of the base excision repair (BER) pathway. BER is initiated by the activity of a bifunctional glycosylase/ AP lyase enzyme. This enzyme, 8-oxoguanine DNA glycosylase 1 (Ogg1), is able to recognize the oxidized guanine base (oxo^{8}dG) and cleave it out of the DNA chain (Radicella, Dherin et al. 1997). The human form of Ogg1 (hOgg1) is a bifunctional glycosylase with a mitochondrial as well as nuclear form which have recently been shown to differentially regulate cell death under conditions of oxidative stress (Oka, Ohno et al. 2008). The inactivation of the gene that codes for mouse Ogg1 (mOgg1) has been shown to result in an accumulation of oxo^{8}dG in mitochondrial and nuclear DNA isolated from liver as well as decrease the excretion of the Ogg1 cleavage product oxo^{8}Gua (Klungland, Rosewell et al. 1999; Minowa, Arai et al. 2000; de Souza-Pinto, Eide et al. 2001; Osterod, Hollenbach et al. 2001; Rozalski, Siomek et al. 2005) (Table 4). Increased susceptibility to manganese in brain tissue from Ogg1 knock-out mice as compared to wild-type control has also been demonstrated by a greater loss of dopamine in caudate putamen and a significantly higher increase in oxo^{8}2dG from nuclear DNA isolated from midbrain (Cardozo-Pelaez et. al. 2005).

Table 4. Oxidative modifications in tissue from mice deficient in DNA repair enzymes

DNA Repair Enzyme Knock-Out Mouse Model	Biological Source	Markers of Increased Oxidative Modifications Compared to Wild-Type	References
8-oxoguanine DNA glyclosylase (Ogg1)	Liver	Increased oxo^{8}dG lesions in nuclear DNA	Klungland et. al., 1999 Minowa et. al., 2000
	Liver	Increased oxo^{8}dG lesions in mitochondrial DNA	de Souza-Pinto et. al., 2001
	Urine	Decrease in excretion of Ogg1 cleavage product (oxo^{8}Gua)	Rosalski et. al., 2005
	Brain	Increased oxo^{8}dG lesions in nuclear DNA and dopamine loss with Manganese exposure	Cardozo-Pelaez et. al., 2005
Adenine/2-hydroxyadenine DNA glycosylase (MYH)	Liver	Increased oxo^{8}dG lesions in nuclear DNA	Russo et. al., 2004 Russo et. al., 2007
Ogg1/MYH	Liver Small Intestine Lung	Increased oxo^{8}dG lesions in nuclear DNA	Russo et. al., 2007
Oxidized purine nucleoside triphosphatase (MTH1)	Brain	Increased oxo^{8}dG lesions in nuclear DNA and oxo^{8}G lesions in RNA under conditions of induced of oxidative stress	Kajitani et. al., 2006 Nakebeppu et al., 2007

Additionally, the activity of mOgg1 in specific brain regions appears to be the determinant of the level of oxo^{8}dG present; conditions that modulate mOgg1 activity in C57Bl/6J mouse brain and differentiated rat pheochromocytoma (PC12) cells, a cell culture model of neuronal cells, lead to alterations in oxo^{8}dG levels (Cardozo-Pelaez, Brooks et al. 2000; Stedeford, Cardozo-Pelaez et al. 2001; Cardozo-Pelaez, Stedeford et al. 2002). If DNA replication ensues without removal of the oxo^{8}dG from the parent strand, oxo^{8}dG will preferentially pair with adenosine. Then, the first step in BER will be initiated by MutY homologue (MYH), an adenine/2-hydroxyadenine glycosylase mismatch and BER enzyme that will excise adenine and 2-hydroxyadenine paired with oxo^{8}2dG (Figure 2). As with Ogg1, the MYH gene codes for nuclear and mitochondrial forms (Ohtsubo, Nishioka et al. 2000). Livers isolated from mice deficient in MYH have been shown to accumulate significantly higher levels of oxo^{8}2dG as compared to wild-type, and double knock-out mice lacking Ogg1 and MYH show significant accumulation of the oxo^{8}dG lesion in liver, small intestine, and lung in adult animals (Table 4) (Russo, De Luca et al. 2004; Russo, De Luca et al. 2007). The levels of oxo^{8}2dG in the brain of these Ogg1/MYH knock-out animals reveal a trend of increasing oxo^{8}2dG accumulation although not as significant as in organs with proliferating cells.

The oxidized nucleotide triphosphatase, Mut T homolog-1 (MTH1), responsible for the hydrolysis of 8-oxo-2'deoxyguanosine triphosphate (oxo^{8}dGTP) to its inactive form, 8-oxo-2'deoxyguanosine monophosphate (oxo^{8}GMP), is the third enzyme that prevents oxo^{8}2dG accumulation in DNA at the level of the nucleotide pool (Mo, Maki et al. 1992; Sakumi, Furuichi et al. 1993). Mice deficient in MTH1 have been extensively studied in models of neurotoxicity and demonstrate increased oxo^{8}2dG accumulation in

DNA as well as oxo^{8}G accumulation in RNA in response to oxidative stress from kainate-induced excitotoxicity or exposure to 1 -methyl-4-phenyl-1,2,3,6-tetrahydropyridine (MPTP) (Kajitani, Yamaguchi et al. 2006; Nakabeppu, Tsuchimoto et al. 2007) (Table 4). In addition to oxo^{8}dGTP and to a much lesser extent 8-oxo-guanosine triphosphate (oxo^{8}GTP) , the MTH1 protein is capable of hydrolyzing oxidized adenine moieties including 2-oxo-deoxyadenosine triphosphate (oxo^{2}dATP), 2-oxo-ATP (oxo^{2}ATP), 8-oxo-dATP (oxo^{8}dATP), and 8-oxo-ATP (oxo^{8}ATP) (Fujikawa, Kamiya et al. 1999; Fujikawa, Kamiya et al. 2001). However, the specific activity of MTH1 for each of these modified purines is not equal: oxo^{2}dATP > oxo^{2}ATP > oxo^{8}dGTP > oxo^{8}dATP >> oxo^{8}GTP > oxo^{8}ATP (Fujikawa, Kamiya et al. 2001). In fact, the catalytic efficiency for oxo^{8}dGTP has been shown to be between forty and fifty times greater than that for oxo^{8}GTP (Hayakawa, Hofer et al. 1999; Fujikawa, Kamiya et al. 2001). To date, there are no specific repair mechanisms that compensate for this inefficiency of MTH1 to remove oxo^{8}GTP from the nucleotide pool. Given the volume of literature that has been devoted to characterizing the levels and fate of oxo^{8}2dG in DNA and the significant evidence of its association with cancer and neurodegenerative disease, there appears to be a disproportionate deficit in research attention to the ribonucleotide form of guanosine, GTP, and the fate of its oxidized counterpart, oxo^{8}GTP. The few studies aimed at evaluating cellular consequences of increased oxo^{8}GTP in the cell or to test its relative abundance under conditions of oxidized stress are summarized below.

Cellular Fate of Oxo^{8}GTP

Guanosine 5'-triphosphate (GTP) participates in several critical physiological functions including but not limited to, RNA synthesis, protein synthesis, cell signaling

through activation of GTP-binding proteins, and the production of the second messenger cyclic guanosine monophosphate (cGMP). Oxo^{8}GTP as shown in Figure 3 is the major product of oxidation to the guanosine moiety of this nucleoside triphosphate.

FIGURE 3

8-hydroxyguanosine 5'-triphosphate
(Oxo^{8}GTP)

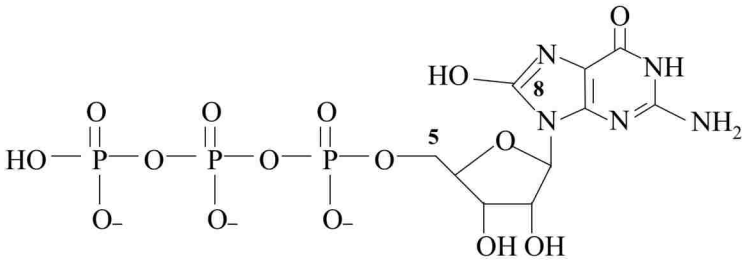

It is assumed that oxidation of guanosine incorporated into GTP is by a similar ROS-catalyzed mechanism as shown in Figure 1. Additionally, it has been previously shown that $^{\bullet}$OH is produced by electron transfer by Fe(II), Fe(III), and Cu(II) complexed with nucleotide triphosphates such as GTP in the presence of the abundant cellular reductant ascorbate (Biaglow, Held et al. 1996). Such Cu complexes are known to affect signal transduction by acting as second messengers, and depending on their concentration and the target protein, may be the ultimate factor influencing cell survival or cell death responses (Filomeni, Rotilio et al. 2005; Filomeni, Cerchiaro et al. 2007). On average, the concentration of ribonucleotide triphosphate (ATP, GTP, CTP, and UTP) RNA precursors has been shown to be a hundred times higher than that of deoxyribonucleotide triphosphate DNA percursors (dATP, dGTP, dCTP, and dTTP). GTP is representative of this with an average concentration of 468 ± 224 μM reported in mammalian cells compared to an average concentration for dGTP of 5.2 ± 4.5 μM (Traut 1994). Figure 4 outlines what has been previously determined in research literature regarding the generation, elimination, and incorporation of oxo^{8}GTP in the cellular milieu.

FIGURE 4

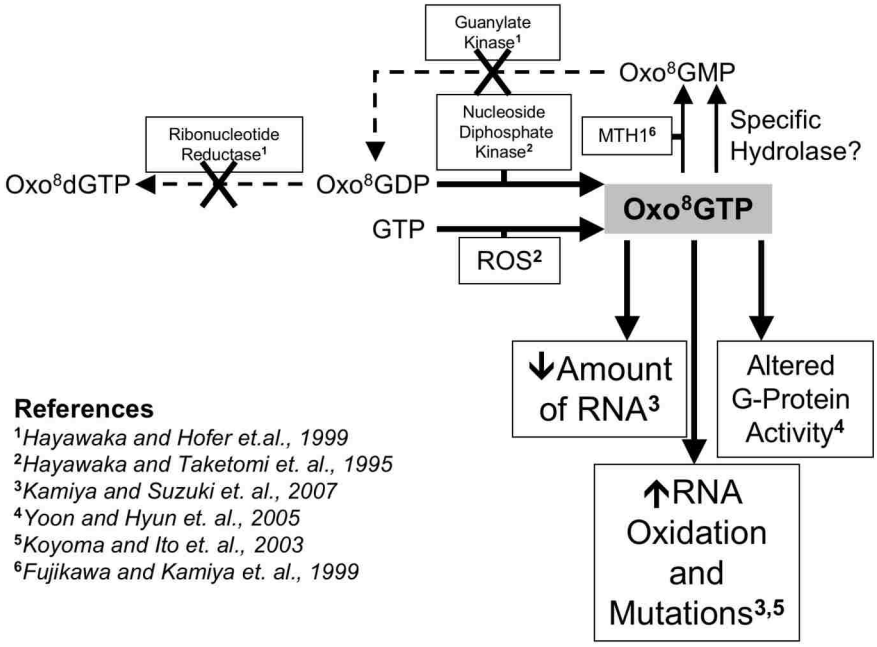

References

[1]*Hayawaka and Hofer et.al., 1999*
[2]*Hayawaka and Taketomi et. al., 1995*
[3]*Kamiya and Suzuki et. al., 2007*
[4]*Yoon and Hyun et. al., 2005*
[5]*Koyoma and Ito et. al., 2003*
[6]*Fujikawa and Kamiya et. al., 1999*

Figure 4. Mechanisms of oxo^{8}GTP production, elimination, and utilization.

Oxo^{8}GTP can be formed either by direct modification of the GTP pool, thought to be the major pathway, or by phosphorylation of oxo^{8}GDP by nucleotide diphosphate kinase. Ribonucleotide reductase cannot form oxo^{8}dGTP from oxo^{8}GDP. Once in the cellular pool, oxo^{8}GTP can by hydrolyzed to oxo^{8}GMP by MTH1 although with very low efficiency. Oxo^{8}GMP is not a viable substrate for guanylate kinase to produce oxo^{8}GDP. A more efficient hydrolyase specific for oxo^{8}GTP has not been identified to date. Cellular effects of oxo^{8}GTP reported so far are a decreasae in total mRNA, increase in mutations in mRNA oxidation and mutations as well as altered G-protein signaling.

Because guanosine has been well established as a viable substrate for oxidative modification by ROS in the forms of dGTP, DNA, or RNA, it has been assumed that oxo^{8}GTP is produced in the cytoplasm by direct oxidation by GTP although the data presented herein is the first to specifically verify this oxidative modification of GTP by ROS in a cell culture system (Hayakawa, Taketomi et al. 1995). Oxo^{8}GTP has also been shown to be a viable substrate for nucleotide diphosphate kinase, and therefore high levels of oxo^{8}GDP could also promote elevated oxo^{8}GTP (Hayakawa, Hofer et al. 1999). Early studies confirmed that oxo^{8}GTP is an active substrate for RNA polymerase II and that it can be misincorporated into RNA opposite adenine instead of cytosine, inducing translational errors in the resulting protein (Taddei, Hayakawa et al. 1997). Recently, studies have confirmed these errors in transcription induced by oxidative modification of RNA precursors. It was demonstrated that the addition of oxo^{8}GTP to *in vitro* transcription reactions reduces the total amount of mRNA synthesized as well as increases the number of mutations in the mRNA (Kamiya, Suzuki et al. 2007). These findings have substantial implications for post-mitotic cells such as neurons that depend on RNA fidelity for the maintenance of cellular protein expression and function. It has been suggested that expression of transcription elongation factor S-II confers resistance to transcriptional errors induced with oxidative stress by cleaving out misincorporated bases (Koyama, Ito et al. 2003). However, there has not been a specific RNA repair mechanism identified for recognizing and excising oxidized bases and as stated above, the activity of MTH1 is not sufficient to prevent the formation of substantial amounts of oxidized RNA precursors such as oxo^{8}GTP. The deleterious implication of this is emphasized by evidence of increased levels of oxidized RNA adducts in the brains of

idiopathic neurodegenerative disease patients including Alzheimer's disease, Parkinson's disease, and Lewy body disease (Nunomura, Perry et al. 1999; Zhang, Perry et al. 1999; Nunomura, Chiba et al. 2002; Shan, Tashiro et al. 2003; Shan and Lin 2006). Oxo^{8}GTP can also affect G-protein signaling although currently there is only one study that has investigated this. Yoon et. al. demonstrated that incubating purified, recombinant Ras or cell lysates from human embryonic kidney (HEK 293T) cells with oxo^{8}GTP resulted in an increased Ras activity by as much as two times the level induced by the unmodified GTP substrate (Yoon, Hyun et al. 2005). Given that oxo^{8}GTP is more potent than the native substrate of Ras, the authors suggest that oxo^{8}GTP is not simply a by-product formed with oxidative stress but a physiologically-active molecule that participates in cell signaling. Interestingly, the effects of oxo^{8}GTP were not consistent amongst the other GTP-binding proteins analyzed. When oxo^{8}GTP was incubated with purified Rac1, purified Cdc 42, or cell lysates from HEK 293T cells there was no detectable activity (Yoon, Hyun et al. 2005). Therefore, it appears that oxo^{8}GTP does interact with GTP-binding proteins although the effects are not uniform and this poses the question of whether GTP might be a target for oxidative modification as a mediator of the cellular response.

Roles of GTP with a Focus on the Nervous System

Cellular consequences of oxo^{8}GTP in post-mitotic neurons are completely unknown. A cellular target of GTP important for neurotransmission as well as physiological processes such as vasodilation and platelet aggregation is soluble guanylyl cyclase (sGC) [E.C. 4.6.1.2.] (Moncada, Palmer et al. 1991). To stay within the scope of this introduction, the discussion of sGC will focus on implications for the central

nervous system. sGC is a heterodimer consisting of an α and β subunit and is activated by the co-factor nitric oxide (NO) binding to a heme prosthetic group on the β subunit which then facilitates the conversion of the substrate GTP to the product cyclic guanosine 5'-monophosphate (cGMP) (Craven and DeRubertis 1978; Gerzer, Bohme et al. 1981). sGC is located in the cytoplasm and is distinct from the particulate or membrane-bound guanylyl cyclase which is differentially regulated and insensitive to NO (Waldman and Murad 1987). Figure 5 depicts the regulation of sGC as well as the targets of cGMP, the intracellular messenger product of sGC activation. The ultimate fate of generated cGMP from sGC activation is stimulation of cGMP-dependent kinases, cGMP-regulated ion channels, and cGMP-regulated phosphodiesterases (Francis, Blount et al. 2005) (Figure 5).

FIGURE 5

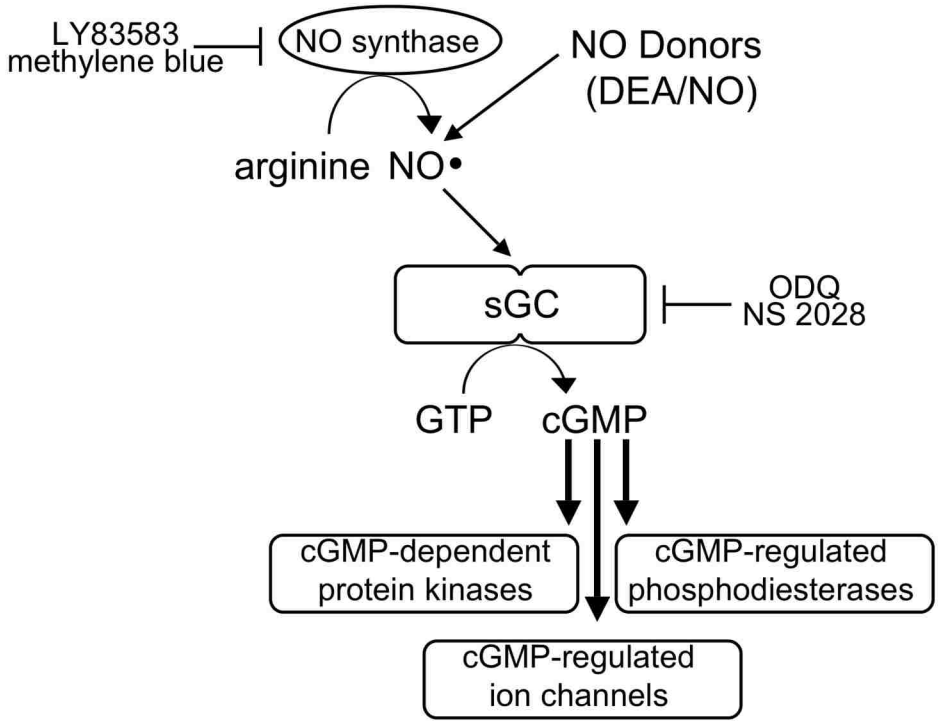

Adapted from (Friebe and Koesling 2003)

Figure 5. Regulation and cellular fate of soluble guanylyl cyclase activity.

Nitric oxide (NO) synthase is the endogenous enzyme that catalyzes the production of NO from L-arginine for use by soluble guanylyl cyclase (sGC). Synthetic NO donors including DEA/NO are often used in experimental settings to activate sGC. Inhibitors of NO synthase and therefore sGC activity include LY83583 and methylene blue. NO is a necessary co-factor for the conversion of GTP to cGMP by sGC. Specific inhibitors that interfere with NO binding to a heme-binding domain of sGC include ODQ and NS 2028. The product of cGMP activation acts on several downstream targets including cGMP-dependent kinases, cGMP-regulated phosphodiesterases, and cGMP-regulated ion channels.

Several synthetic stimulators and inhibitors of sGC have been used for experimental and therapeutic investigations (Gruetter, Kadowitz et al. 1981; Garthwaite, Southam et al. 1995; Schrammel, Behrends et al. 1996; Olesen, Drejer et al. 1998; Hobbs 2002). Table 5 lists the two synthetic inhibitors of sGC, ODQ and NS2028, that have shown specificity for the enzyme as opposed to interference with available NO.

Table 5. Kinetic properties of synthetic sGC inhibitors.

Inhibitor	Maximum Velocity (V_{max})	Michealis-Menton Constant (K_m)	IC_{50}	Reference
ODQ 1*H*-[1,2,4]Oxadiazolo[4,3-*a*]quinoxalin-1-one	3.49 ± 0.07 cGMP(μmol)/mg/min -500 μM GTP	82 ± 20 nM DEA/NO	0.72 ± 0.18μM -3 μM DEA/NO -500 μM GTP	Schrammel et. al., 1996
NS 2028 4*H*-8-bromo-1,2,4-oxadiazolo(3,4-d)benz(b)(1,4)oxazin-1-one	384 ± 10 cGMP (nmol)/mg/min -30 μM GTP	20 ± 3 μM GTP	200nM -100 μM SIN-1 -100μM GTP	Olesen et. al., 1998

Methylene blue and 6-anilino-5,8-quinolinedione (LY83583) have also been employed in investigations ablating the NO/sGC/cGMP pathway however, they are known to inhibit neuronal nitric oxide synthase (NOS), the endogenous enzyme responsible for converting L-arginine to NO in neurons, as opposed to direct interaction with the sGC protein (Luo, Das et al. 1995) (Figure 5). Table 6 lists the effects of pharmacological inhibition of sGC on endpoints of neurotoxicity that have been evaluated.

Table 6. The effects of pharmacological inhibition of sGC on endpoints of neurotoxicity.

Model	Pharmacological Inhibition of Soluble Guanylyl Cyclase	Neurotoxicity Endpoint	References
Rat Hippocampal Neurons	LY85358 *ex vivo*	Inhibition of long -term potentiation (LTP) with tetanic stimuli	Arancio et. al., 1995
Rat Hippocampal Slices	ODQ *ex vivo*	Reduction of LTP with tetanic stimuli	Boulton et. al., 1995
	NS 2028 *ex vivo*	Reduction of LTP with tetanic stimuli	Monfort et. al, 2002
Guinea Pig Hippocampal Slices	LY85358 *ex vivo*	Reduction of LTP with tetanic stimuli	Zhuo et. al., 1994
Rat Cerebellar Neurons	ODQ *ex vivo*	Inhibition of long-term depression with low-frequency stimuli	Boxall et. al., 1996
Salamander retinal neurons	ODQ *ex vivo*	Reduction in the number of neuritic processes from cone cells	Zhang et. al., 2005
Ferret Cortical Tissue	ODQ *in vivo*	Inhibition of sublamination in the dorsal lateral geniculate nucleus	Leamey et. al., 2001

Modification of the NO/sGC/cGMP pathway has been shown to elicit deleterious consequences in the central nervous system (CNS) including reduced neuronal activation, impairment of long term potentiation (LTP), inhibition of long-term depression (LTD), and the disruption of neurodevelopmental processes (Table 6) (Zhuo, Hu et al. 1994; Arancio, Kandel et al. 1995; Boulton, Southam et al. 1995; Tanaka, Markerink-van Ittersum et al. 1997; Bidmon, Starbatty et al. 2004; Boess, Hendrix et al. 2004; Monfort, Munoz et al. 2004; Yamazaki, Chiba et al. 2006). A lot of emphasis has been placed on the NO/sGC/cGMP pathway as an essential mechanism for observed increases in long-lasting synaptic plasticity defined as long-term potentiation (LTP), the physiological correlate of learning (Bliss and Collingridge 1993). There are several biochemical processes that take place during synaptic strengthening as a conequence of LTP but they all appear to converge with respect to signaling by NO that leads to the eventual increase in expression of proteins necessary for the strengthening of the synaptic connectivity. This is exemplified by the fact that animals deficient in neuronal NOS show reduced LTP and demonstrate significant cognitive impairment in learning and memory tasks as compared to wild-type controls (Son, Hawkins et al. 1996; Kirchner, Weitzdoerfer et al. 2004). As a neuronal target of NO, sGC plays an important role amongst these processes. It has been shown that pharmacological inhibition of sGC prevents LTP in the hippocampus of rats and guinea pigs, a region of the brain highly associated with learning and memory processes (Table 6) (Zhuo, Hu et al. 1994; Arancio, Kandel et al. 1995; Boulton, Southam et al. 1995; Son, Lu et al. 1998; Monfort, Munoz et al. 2002). Similar LTP impairment has been shown to occur in primary hippocampal neurons isolated from rat brain (Table 6). It is hypothesized that sGC activation leads to an increase in

available cGMP required to activate cGMP-dependent kinases that go on to phosphorylate transcription factors such as cAMP responsive element (CRE)-binding protein (CREB) which in turn promotes an increase in RNA synthesis necessary to increase proteins required for synaptic strengthening (Lu, Kandel et al. 1999). Co-localization of NOS and sGC on pre and post-synaptic densities in hippocampal neurons strengthens the conclusions of the integral role that sGC plays in the cellular mechanisms that lead to LTP (Burette, Zabel et al. 2002). Modulations in NO-responsive sGC expression and activity have also been associated with a variety of disorders including cardiovascular disease and neurological diseases such as Alzheimer's Disease (AD), Creutzfeldt-Jakob disease, and multiple sclerosis, all of which include a component of oxidative stress in their pathologies (Bonkale, Winblad et al. 1995; Baltrons, Pifarre et al. 2004; Puzzo, Vitolo et al. 2005; Moncada and Higgs 2006). This oxidative stress is hypothesized to be mediated, in part, by an aberrant increase in Fenton-reactive metals such as copper in AD brains (Lovell, Robertson et al. 1998; Huang, Atwood et al. 1999; Maynard, Cappai et al. 2002; Bush 2003; Rossi, Arciello et al. 2006). However, the oxidative stress hypothesis associated with increases in transition metal-induced increases in ROS has not been evaluated in terms of the sGC/cGMP pathway.

Copper, ROS, and Alzheimer's Disease

All of the main neurodegenerative diseases that manifest in cognitive deficiencies include a component of aberrant protein folding and aggregation in their pathology. In the brain of Alzheimer's disease (AD) patients, the misfolded proteins collect into amyloid beta (Aβ) plaques. Protein plaques also denote the hallmark feature of prion disease (PrPD) and in Parkinson's disease (PD) intracellular aggregates are identified as Lewy bodies

(Taylor, Hardy et al. 2002). Additionally, in familial amyotrophic lateral sclerosis (ALS), the presence of Bunina bodies verify disease state (Taylor, Hardy et al. 2002). Another unifying feature of these diseases, facilitated by the collection of these proteins, is altered homeostasis of one or more metal ions, namely Zn (II), Cu(II), and Fe(III) (Bush 2003). However, analysis of postmortem brain tissue from patients with some of these neurodegenerative diseases is either unavailable or misleading due to the lack of a reliable methodology (i.e. without acid sample preparation required for inductively-coupled plasma mass spectrometry (ICP-MS) to measure these metal ions complexed to proteins in tissue (Corrigan, Reynolds et al. 1993; Wong, Chen et al. 2001). However, AD tissue has been analyzed using micro-PIXE analysis in stained tissue which overcomes this methodology obstacle. Lovell et. al. reported a 30% increase in copper in senile plaques of AD brain as compared to plaque-free regions as well as a 400% increase in copper in neutropils of AD as compared to age-matched, healthy controls (Lovell, Robertson et al. 1998). The interactions of the Aβ peptide, both insoluble $A\beta_{1-42}$ and soluble $A\beta_{1-40}$, with copper has been described (Atwood, Scarpa et al. 2000). There are two basic hypothesis about the reactions of metal-protein complexes in these diseases: (1) the presence of metal ions facilitates the aggregation of misfolded proteins or (2) metal ions catalyze reactions producing ROS that cause cellular damage via oxidative stress (Gaggelli, Kozlowski et al. 2006). These hypotheses are not mutually exclusive however and it is suggested that oxidative processes lead to protein damage that further exacerbates the progression of the disease causing an auto-destructive process (Bayer, Schafer et al. 2006). There is a massive amount of information available in the research literature regarding these hypothesis as they relate to several neurodegenerative diseases

and metals ions, including the ones listed above (Molina-Holgado, Hider et al. 2007). However, to stay within the scope of this study, focus will be placed on the production of ROS by Cu(II) specifically in relation to the pathology of AD.

Sources of ROS in AD brain tissue include Aβ-catalyzed H_2O_2 generation through the reduction of Cu^{2+} using O_2 and biological reducing agents such as ascorbic acid as substrates (Huang, Atwood et al. 1999). Reduced copper ions (Cu^{+}) can then participate in the Fenton reaction with H_2O_2 to produce the highly reactive $OH^{\cdot}$ radical. In fact, it has been shown that the Aβ peptide does not produce toxic amounts of H_2O_2 in the absence of Cu(II) (Opazo, Huang et al. 2002). However, it has been suggested that Aβ might be part of a normal metal clearance mechanism which becomes unregulated when there is excessive metal concentration that overwhelms this clearance system, causing aggregation and pro-oxidant behavior (Bush 2003). This could help explain evidence of Aβ plaques in normal, non-demented elderly brains (Katzman, Terry et al. 1988; Arriagada, Marzloff et al. 1992; Giannakopoulos, Hof et al. 1995; Davis, Schmitt et al. 1999). Additionally, the Tg2576 transgenic mouse models of AD that express the Swedish mutation of human amyloid precursor protein (APP) and collect significant levels of Aβ plaque by 12 months of age fail to present consistent behavioral measures of age-dependent cognitive decline or gross neuronal death (Irizarry, McNamara et al. 1997; Chen, Chen et al. 2000; Westerman, Cooper-Blacketer et al. 2002; Lesne, Kotilinek et al. 2008). Support for the role of copper in conferring toxicity of the Aβ peptide also comes from successful investigations of copper chelation. The copper chelator iodochlorhydroxyquin (clioquinol) has been investigated in human AD patients in clinical

trials as well as mouse models of AD and shown to have potential therapeutic benefit (Cherny, Atwood et al. 2001; Ritchie, Bush et al. 2003).

As suggested earlier, there is a careful balance between Aβ, copper, and ROS that exists in normal aging brain physiology that appears to be severely disrupted in AD. An increasing amount of evidence has been presented proposing that the onset of AD is preceded by an interim phase of dementia pathology termed Mild Cognitive Impairment (MCI) (Petersen and Negash 2008). Analysis of CSF, urine, and blood of MCI patients reveals an increase in lipid peroxidation compared to age-matched controls (Pratico, Clark et al. 2002; Wang, Markesbery et al. 2006). Evidence of early oxidative events in AD has also been supported by analysis of urine, plasma, and brain tissue of Tg2576 mice that show an elevation in lipid peroxidation, a biomarker of oxidative stress also found in AD patients (Pratico, Clark et al. 2000). This lipid peroxidation precedes the formation of amyloid plaques and exhibits an age-dependent increase that parallels amyloid pathology in this model (Pratico, Uryu et al. 2001). Unfortunately, analysis of copper content in the brains of these mice have excluded protein-bound levels of Cu(II) and prevent correlation with early oxidative events (Maynard, Cappai et al. 2002). Identifying the triggers and endpoints of this unbalanced copper homeostasis can aid in AD research in two important avenues: (1) identification of biomarkers of sporadic AD that lead to earlier diagnosis and (2) development of therapeutic intervention strategies that inhibit these initial events in AD that precede gross neuronal loss. Anaylsis of GTP, dGTP and their oxidized counterparts oxo^{8}GTP and oxo^{8}dGTP could generate a substantial amount of information to forward research in these avenues.

The hypothesis that is presented and tested herein is that oxo^{8}GTP is produced under physiological conditions and it is increased during oxidative stress induced by toxicological insult or neurodegenerative disease. A consequence of elevated oxo^{8}GTP levels is a reduction in available cyclic guanosine monophosphate (cGMP) due to its activity as a pathological inhibitor of soluble guanylyl cyclase (sGC). This hypothesis will be tested with the following specific aims:

Specific Aim 1. Determine the levels of oxo^{8}GTP produced in cell-free GTP preparations and cytosolic extracts from cells in culture under conditions of oxidative stress induced by ascorbate and copper using a novel HPLC-EC methodology.

Specific Aim 2. Determine the specific mechanism of oxidation to GTP induced by ascorbate and copper using EPR.

Specific Aim 3. Evaluate the consequences of increased levels of oxo^{8}GTP on sGC activity.

References

Arancio, O., E. R. Kandel, et al. (1995). "Activity-dependent long-term enhancement of transmitter release by presynaptic 3',5'-cyclic GMP in cultured hippocampal neurons." Nature **376**(6535): 74-80.

Arriagada, P. V., K. Marzloff, et al. (1992). "Distribution of Alzheimer-type pathologic changes in nondemented elderly individuals matches the pattern in Alzheimer's disease." Neurology **42**(9): 1681-8.

Atwood, C. S., R. C. Scarpa, et al. (2000). "Characterization of copper interactions with alzheimer amyloid beta peptides: identification of an attomolar-affinity copper binding site on amyloid beta1-42." J Neurochem **75**(3): 1219-33.

Baltrons, M. A., P. Pifarre, et al. (2004). "Reduced expression of NO-sensitive guanylyl cyclase in reactive astrocytes of Alzheimer disease, Creutzfeldt-Jakob disease, and multiple sclerosis brains." Neurobiol Dis **17**(3): 462-72.

Bayer, T. A., S. Schafer, et al. (2006). "A vicious circle: role of oxidative stress, intraneuronal Abeta and Cu in Alzheimer's disease." Clin Neuropathol **25**(4): 163-71.

Biaglow, J. E., K. D. Held, et al. (1996). "Role of guanosine triphosphate in ferric ion-linked Fenton chemistry." Radiat Res **145**(5): 554-62.

Bidmon, H. J., J. Starbatty, et al. (2004). "Cerebral expression of the alpha2-subunit of soluble guanylyl cyclase is linked to cerebral maturation and sensory pathway refinement during postnatal development." Neurochem Int **45**(6): 821-32.

Bliss, T. V. and G. L. Collingridge (1993). "A synaptic model of memory: long-term potentiation in the hippocampus." Nature **361**(6407): 31-9.

Boess, F. G., M. Hendrix, et al. (2004). "Inhibition of phosphodiesterase 2 increases neuronal cGMP, synaptic plasticity and memory performance." Neuropharmacology **47**(7): 1081-92.

Bogdanov, M. B., O. A. Andreassen, et al. (2001). "Increased oxidative damage to DNA in a transgenic mouse model of Huntington's disease." J Neurochem **79**(6): 1246-9.

Bonkale, W. L., B. Winblad, et al. (1995). "Reduced nitric oxide responsive soluble guanylyl cyclase activity in the superior temporal cortex of patients with Alzheimer's disease." Neurosci Lett **187**(1): 5-8.

Boulton, C. L., E. Southam, et al. (1995). "Nitric oxide-dependent long-term potentiation is blocked by a specific inhibitor of soluble guanylyl cyclase." Neuroscience **69**(3): 699-703.

Breen, A. P. and J. A. Murphy (1995). "Reactions of oxyl radicals with DNA." Free Radic Biol Med **18**(6): 1033-77.

Buettner, G. R. (1993). "The pecking order of free radicals and antioxidants: lipid peroxidation, alpha-tocopherol, and ascorbate." Arch Biochem Biophys **300**(2): 535-43.

Burette, A., U. Zabel, et al. (2002). "Synaptic localization of nitric oxide synthase and soluble guanylyl cyclase in the hippocampus." J Neurosci **22**(20): 8961-70.

Bush, A. I. (2003). "The metallobiology of Alzheimer's disease." Trends Neurosci **26**(4): 207-14.

Cardozo-Pelaez, F., P. J. Brooks, et al. (2000). "DNA damage, repair, and antioxidant systems in brain regions: a correlative study." Free Radic Biol Med **28**(5): 779-85.
Cardozo-Pelaez, F., S. Song, et al. (1998). "Attenuation of age-dependent oxidative damage to DNA and protein in brainstem of Tg Cu/Zn SOD mice." Neurobiol Aging **19**(4): 311-6.
Cardozo-Pelaez, F., S. Song, et al. (1999). "Oxidative DNA damage in the aging mouse brain." Mov Disord **14**(6): 972-80.
Cardozo-Pelaez, F., T. J. Stedeford, et al. (2002). "Effects of diethylmaleate on DNA damage and repair in the mouse brain." Free Radic Biol Med **33**(2): 292-8.
Cardozo-Pelaez, F., D. P. Cox, et al. (2005). "Lack of the DNA repair enzyme OGG1 sensitizes dopamine neurons to manganese toxicity during development." Gene Expr **12**(4-6): 315-23.
Chen, G., K. S. Chen, et al. (2000). "A learning deficit related to age and beta-amyloid plaques in a mouse model of Alzheimer's disease." Nature **408**(6815): 975-9.
Chen, Y. H. and D. F. Bogenhagen (1993). "Effects of DNA lesions on transcription elongation by T7 RNA polymerase." J Biol Chem **268**(8): 5849-55.
Cheng, K. C., D. S. Cahill, et al. (1992). "8-Hydroxyguanine, an abundant form of oxidative DNA damage, causes G----T and A----C substitutions." J Biol Chem **267**(1): 166-72.
Cherny, R. A., C. S. Atwood, et al. (2001). "Treatment with a copper-zinc chelator markedly and rapidly inhibits beta-amyloid accumulation in Alzheimer's disease transgenic mice." Neuron **30**(3): 665-76.
Chiou, C. C., P. Y. Chang, et al. (2003). "Urinary 8-hydroxydeoxyguanosine and its analogs as DNA marker of oxidative stress: development of an ELISA and measurement in both bladder and prostate cancers." Clin Chim Acta **334**(1-2): 87-94.
Corrigan, F. M., G. P. Reynolds, et al. (1993). "Hippocampal tin, aluminum and zinc in Alzheimer's disease." Biometals **6**(3): 149-54.
Craven, P. A. and F. R. DeRubertis (1978). "Restoration of the responsiveness of purified guanylate cyclase to nitrosoguanidine, nitric oxide, and related activators by heme and hemeproteins. Evidence for involvement of the paramagnetic nitrosyl-heme complex in enzyme activation." J Biol Chem **253**(23): 8433-43.
Culp, S. J., B. P. Cho, et al. (1989). "Structural and conformational analyses of 8-hydroxy-2'-deoxyguanosine." Chem Res Toxicol **2**(6): 416-22.
Dalton, T. P., M. Z. Dieter, et al. (2000). "Knockout of the mouse glutamate cysteine ligase catalytic subunit (Gclc) gene: embryonic lethal when homozygous, and proposed model for moderate glutathione deficiency when heterozygous." Biochem Biophys Res Commun **279**(2): 324-9.
Dandona, P., K. Thusu, et al. (1996). "Oxidative damage to DNA in diabetes mellitus." Lancet **347**(8999): 444-5.
Davis, D. G., F. A. Schmitt, et al. (1999). "Alzheimer neuropathologic alterations in aged cognitively normal subjects." J Neuropathol Exp Neurol **58**(4): 376-88.
de Souza-Pinto, N. C., L. Eide, et al. (2001). "Repair of 8-oxodeoxyguanosine lesions in mitochondrial dna depends on the oxoguanine dna glycosylase (OGG1) gene and 8-oxoguanine accumulates in the mitochondrial dna of OGG1-defective mice." Cancer Res **61**(14): 5378-81.

Devasagayam, T. P., S. Steenken, et al. (1991). "Formation of 8-hydroxy(deoxy)guanosine and generation of strand breaks at guanine residues in DNA by singlet oxygen." Biochemistry **30**(25): 6283-9.
Didion, S. P., M. J. Ryan, et al. (2002). "Increased superoxide and vascular dysfunction in CuZnSOD-deficient mice." Circ Res **91**(10): 938-44.
Dizdaroglu, M., P. Jaruga, et al. (2002). "Free radical-induced damage to DNA: mechanisms and measurement." Free Radic Biol Med **32**(11): 1102-15.
Elchuri, S., T. D. Oberley, et al. (2005). "CuZnSOD deficiency leads to persistent and widespread oxidative damage and hepatocarcinogenesis later in life." Oncogene **24**(3): 367-80.
Filomeni, G., G. Cerchiaro, et al. (2007). "Pro-apoptotic activity of novel Isatin-Schiff base copper(II) complexes depends on oxidative stress induction and organelle-selective damage." J Biol Chem **282**(16): 12010-21.
Filomeni, G., G. Rotilio, et al. (2005). "Disulfide relays and phosphorylative cascades: partners in redox-mediated signaling pathways." Cell Death Differ **12**(12): 1555-63.
Foksinski, M., D. Gackowski, et al. (2007). "Effects of basal level of antioxidants on oxidative DNA damage in humans." Eur J Nutr **46**(3): 174-80.
Foksinski, M., R. Rozalski, et al. (2004). "Urinary excretion of DNA repair products correlates with metabolic rates as well as with maximum life spans of different mammalian species." Free Radic Biol Med **37**(9): 1449-54.
Fraga, C. G., M. K. Shigenaga, et al. (1990). "Oxidative damage to DNA during aging: 8-hydroxy-2'-deoxyguanosine in rat organ DNA and urine." Proc Natl Acad Sci U S A **87**(12): 4533-7.
Francis, S. H., M. A. Blount, et al. (2005). "Molecular properties of mammalian proteins that interact with cGMP: protein kinases, cation channels, phosphodiesterases, and multi-drug anion transporters." Front Biosci **10**: 2097-117.
Fu, Y., W. H. Cheng, et al. (1999). "Cellular glutathione peroxidase protects mice against lethal oxidative stress induced by various doses of diquat." Proc Soc Exp Biol Med **222**(2): 164-9.
Fujikawa, K., H. Kamiya, et al. (1999). "The oxidized forms of dATP are substrates for the human MutT homologue, the hMTH1 protein." J Biol Chem **274**(26): 18201-5.
Fujikawa, K., H. Kamiya, et al. (2001). "Human MTH1 protein hydrolyzes the oxidized ribonucleotide, 2-hydroxy-ATP." Nucleic Acids Res **29**(2): 449-54.
Gaggelli, E., H. Kozlowski, et al. (2006). "Copper homeostasis and neurodegenerative disorders (Alzheimer's, prion, and Parkinson's diseases and amyotrophic lateral sclerosis)." Chem Rev **106**(6): 1995-2044.
Garthwaite, J., E. Southam, et al. (1995). "Potent and selective inhibition of nitric oxide-sensitive guanylyl cyclase by 1H-[1,2,4]oxadiazolo[4,3-a]quinoxalin-1-one." Mol Pharmacol **48**(2): 184-8.
Gerzer, R., E. Bohme, et al. (1981). "Soluble guanylate cyclase purified from bovine lung contains heme and copper." FEBS Lett **132**(1): 71-4.
Giannakopoulos, P., P. R. Hof, et al. (1995). "Regional distribution of neurofibrillary tangles and senile plaques in the cerebral cortex of very old patients." Arch Neurol **52**(12): 1150-9.

Gruetter, C. A., P. J. Kadowitz, et al. (1981). "Methylene blue inhibits coronary arterial relaxation and guanylate cyclase activation by nitroglycerin, sodium nitrite, and amyl nitrite." Can J Physiol Pharmacol **59**(2): 150-6.

Haber, F. and J. Weiss (1934). "The catalytic decomposition of hydrogen peroxide by iron salts." Proc. R. Soc. London, Ser. A. **147**: 332-351.

Halliwell, B. G., J. M. (2007). Free Radicals in Biology and Medicine. New York, Oxford University Press Inc.

Hayakawa, H., A. Hofer, et al. (1999). "Metabolic fate of oxidized guanine ribonucleotides in mammalian cells." Biochemistry **38**(12): 3610-4.

Hayakawa, H., A. Taketomi, et al. (1995). "Generation and elimination of 8-oxo-7,8-dihydro-2'-deoxyguanosine 5'-triphosphate, a mutagenic substrate for DNA synthesis, in human cells." Biochemistry **34**(1): 89-95.

Ho, Y. S., Y. Xiong, et al. (2004). "Mice lacking catalase develop normally but show differential sensitivity to oxidant tissue injury." J Biol Chem **279**(31): 32804-12.

Hobbs, A. J. (2002). "Soluble guanylate cyclase: an old therapeutic target re-visited." Br J Pharmacol **136**(5): 637-40.

Hollstein, M., D. Sidransky, et al. (1991). "p53 mutations in human cancers." Science **253**(5015): 49-53.

Huang, X., C. S. Atwood, et al. (1999). "The A beta peptide of Alzheimer's disease directly produces hydrogen peroxide through metal ion reduction." Biochemistry **38**(24): 7609-16.

Hudson, V. M. (2004). "New insights into the pathogenesis of cystic fibrosis: pivotal role of glutathione system dysfunction and implications for therapy." Treat Respir Med **3**(6): 353-63.

Irizarry, M. C., M. McNamara, et al. (1997). "APPSw transgenic mice develop age-related A beta deposits and neuropil abnormalities, but no neuronal loss in CA1." J Neuropathol Exp Neurol **56**(9): 965-73.

Jackson, M. J. (2006). "Lack of CuZnSOD activity: a pointer to the mechanisms underlying age-related loss of muscle function, a commentary on "absence of CuZn superoxide dismutase leads to elevated oxidative stress and acceleration of age-dependent skeletal muscle atrophy"." Free Radic Biol Med **40**(11): 1900-2.

Jenner, P. (1993). "Altered mitochondrial function, iron metabolism and glutathione levels in Parkinson's disease." Acta Neurol Scand Suppl **146**: 6-13.

Kajitani, K., H. Yamaguchi, et al. (2006). "MTH1, an oxidized purine nucleoside triphosphatase, suppresses the accumulation of oxidative damage of nucleic acids in the hippocampal microglia during kainate-induced excitotoxicity." J Neurosci **26**(6): 1688-98.

Kamiya, H., A. Suzuki, et al. (2007). "Effects of 8-hydroxy-GTP and 2-hydroxy-ATP on in vitro transcription." Free Radic Biol Med **43**(5): 837-43.

Kasai, H. and S. Nishimura (1983). "Hydroxylation of the C-8 position of deoxyguanosine by reducing agents in the presence of oxygen." Nucleic Acids Symp Ser(12): 165-7.

Katzman, R., R. Terry, et al. (1988). "Clinical, pathological, and neurochemical changes in dementia: a subgroup with preserved mental status and numerous neocortical plaques." Ann Neurol **23**(2): 138-44.

Kirchner, L., R. Weitzdoerfer, et al. (2004). "Impaired cognitive performance in neuronal nitric oxide synthase knockout mice is associated with hippocampal protein derangements." Nitric Oxide **11**(4): 316-30.
Klungland, A., I. Rosewell, et al. (1999). "Accumulation of premutagenic DNA lesions in mice defective in removal of oxidative base damage." Proc Natl Acad Sci U S A **96**(23): 13300-5.
Koyama, H., T. Ito, et al. (2003). "Transcription elongation factor S-II maintains transcriptional fidelity and confers oxidative stress resistance." Genes Cells **8**(10): 779-88.
Lebovitz, R. M., H. Zhang, et al. (1996). "Neurodegeneration, myocardial injury, and perinatal death in mitochondrial superoxide dismutase-deficient mice." Proc Natl Acad Sci U S A **93**(18): 9782-7.
Leopold, J. A. and J. Loscalzo (2005). "Oxidative enzymopathies and vascular disease." Arterioscler Thromb Vasc Biol **25**(7): 1332-40.
Lesne, S., L. Kotilinek, et al. (2008). "Plaque-bearing mice with reduced levels of oligomeric amyloid-beta assemblies have intact memory function." Neuroscience **151**(3): 745-9.
Liochev, S. I. (1999). "The mechanism of "Fenton-like" reactions and their importance for biological systems. A biologist's view." Met Ions Biol Syst **36**: 1-39.
Lovell, M. A., J. D. Robertson, et al. (1998). "Copper, iron and zinc in Alzheimer's disease senile plaques." J Neurol Sci **158**(1): 47-52.
Lu, Y. F., E. R. Kandel, et al. (1999). "Nitric oxide signaling contributes to late-phase LTP and CREB phosphorylation in the hippocampus." J Neurosci **19**(23): 10250-61.
Luo, D., S. Das, et al. (1995). "Effects of methylene blue and LY83583 on neuronal nitric oxide synthase and NADPH-diaphorase." Eur J Pharmacol **290**(3): 247-51.
Maynard, C. J., R. Cappai, et al. (2002). "Overexpression of Alzheimer's disease amyloid-beta opposes the age-dependent elevations of brain copper and iron." J Biol Chem **277**(47): 44670-6.
Milligan, J. R., J. A. Aguilera, et al. (2001). "Redox reactivity of guanyl radicals in plasmid DNA." Int J Radiat Biol **77**(3): 281-93.
Minowa, O., T. Arai, et al. (2000). "Mmh/Ogg1 gene inactivation results in accumulation of 8-hydroxyguanine in mice." Proc Natl Acad Sci U S A **97**(8): 4156-61.
Mo, J. Y., H. Maki, et al. (1992). "Hydrolytic elimination of a mutagenic nucleotide, 8-oxodGTP, by human 18-kilodalton protein: sanitization of nucleotide pool." Proc Natl Acad Sci U S A **89**(22): 11021-5.
Molina-Holgado, F., R. C. Hider, et al. (2007). "Metals ions and neurodegeneration." Biometals **20**(3-4): 639-54.
Moncada, S. and E. A. Higgs (2006). "Nitric oxide and the vascular endothelium." Handb Exp Pharmacol(176 Pt 1): 213-54.
Moncada, S., R. M. Palmer, et al. (1991). "Nitric oxide: physiology, pathophysiology, and pharmacology." Pharmacol Rev **43**(2): 109-42.
Monfort, P., M. D. Munoz, et al. (2002). "Long-term potentiation in hippocampus involves sequential activation of soluble guanylate cyclase, cGMP-dependent protein kinase, and cGMP-degrading phosphodiesterase." J Neurosci **22**(23): 10116-22.

Monfort, P., M. D. Munoz, et al. (2004). "Sequential activation of soluble guanylate cyclase, protein kinase G and cGMP-degrading phosphodiesterase is necessary for proper induction of long-term potentiation in CA1 of hippocampus. Alterations in hyperammonemia." Neurochem Int **45**(6): 895-901.

Muller, F. L., W. Song, et al. (2006). "Absence of CuZn superoxide dismutase leads to elevated oxidative stress and acceleration of age-dependent skeletal muscle atrophy." Free Radic Biol Med **40**(11): 1993-2004.

Nakabeppu, Y., D. Tsuchimoto, et al. (2007). "Oxidative damage in nucleic acids and Parkinson's disease." J Neurosci Res.

Nunomura, A., S. Chiba, et al. (2002). "Neuronal RNA oxidation is a prominent feature of dementia with Lewy bodies." Neuroreport **13**(16): 2035-9.

Nunomura, A., G. Perry, et al. (1999). "RNA oxidation is a prominent feature of vulnerable neurons in Alzheimer's disease." J Neurosci **19**(6): 1959-64.

Ohtsubo, T., K. Nishioka, et al. (2000). "Identification of human MutY homolog (hMYH) as a repair enzyme for 2-hydroxyadenine in DNA and detection of multiple forms of hMYH located in nuclei and mitochondria." Nucleic Acids Res **28**(6): 1355-64.

Oka, S., M. Ohno, et al. (2008). "Two distinct pathways of cell death triggered by oxidative damage to nuclear and mitochondrial DNAs." Embo J **27**(2): 421-32.

Olesen, S. P., J. Drejer, et al. (1998). "Characterization of NS 2028 as a specific inhibitor of soluble guanylyl cyclase." Br J Pharmacol **123**(2): 299-309.

Opazo, C., X. Huang, et al. (2002). "Metalloenzyme-like activity of Alzheimer's disease beta-amyloid. Cu-dependent catalytic conversion of dopamine, cholesterol, and biological reducing agents to neurotoxic H(2)O(2)." J Biol Chem **277**(43): 40302-8.

Osterod, M., S. Hollenbach, et al. (2001). "Age-related and tissue-specific accumulation of oxidative DNA base damage in 7,8-dihydro-8-oxoguanine-DNA glycosylase (Ogg1) deficient mice." Carcinogenesis **22**(9): 1459-63.

Pastor, N., H. Weinstein, et al. (2000). "A detailed interpretation of OH radical footprints in a TBP-DNA complex reveals the role of dynamics in the mechanism of sequence-specific binding." J Mol Biol **304**(1): 55-68.

Peled-Kamar, M., J. Lotem, et al. (1997). "Oxidative stress mediates impairment of muscle function in transgenic mice with elevated level of wild-type Cu/Zn superoxide dismutase." Proc Natl Acad Sci U S A **94**(8): 3883-7.

Petersen, R. C. and S. Negash (2008). "Mild cognitive impairment: an overview." CNS Spectr **13**(1): 45-53.

Pratico, D., C. M. Clark, et al. (2000). "Increased 8,12-iso-iPF2alpha-VI in Alzheimer's disease: correlation of a noninvasive index of lipid peroxidation with disease severity." Ann Neurol **48**(5): 809-12.

Pratico, D., C. M. Clark, et al. (2002). "Increase of brain oxidative stress in mild cognitive impairment: a possible predictor of Alzheimer disease." Arch Neurol **59**(6): 972-6.

Pratico, D., K. Uryu, et al. (2001). "Increased lipid peroxidation precedes amyloid plaque formation in an animal model of Alzheimer amyloidosis." J Neurosci **21**(12): 4183-7.

Puzzo, D., O. Vitolo, et al. (2005). "Amyloid-beta peptide inhibits activation of the nitric oxide/cGMP/cAMP-responsive element-binding protein pathway during hippocampal synaptic plasticity." J Neurosci **25**(29): 6887-97.
Radicella, J. P., C. Dherin, et al. (1997). "Cloning and characterization of hOGG1, a human homolog of the OGG1 gene of Saccharomyces cerevisiae." Proc Natl Acad Sci U S A **94**(15): 8010-5.
Reaume, A. G., J. L. Elliott, et al. (1996). "Motor neurons in Cu/Zn superoxide dismutase-deficient mice develop normally but exhibit enhanced cell death after axonal injury." Nat Genet **13**(1): 43-7.
Ritchie, C. W., A. I. Bush, et al. (2003). "Metal-protein attenuation with iodochlorhydroxyquin (clioquinol) targeting Abeta amyloid deposition and toxicity in Alzheimer disease: a pilot phase 2 clinical trial." Arch Neurol **60**(12): 1685-91.
Rossi, L., M. Arciello, et al. (2006). "Copper imbalance and oxidative stress in neurodegeneration." Ital J Biochem **55**(3-4): 212-21.
Rozalski, R., A. Siomek, et al. (2005). "Substantial decrease of urinary 8-oxo-7,8-dihydroguanine, a product of the base excision repair pathway, in DNA glycosylase defective mice." Int J Biochem Cell Biol **37**(6): 1331-6.
Russo, M. T., G. De Luca, et al. (2007). "Different DNA repair strategies to combat the threat from 8-oxoguanine." Mutat Res **614**(1-2): 69-76.
Russo, M. T., G. De Luca, et al. (2004). "Accumulation of the oxidative base lesion 8-hydroxyguanine in DNA of tumor-prone mice defective in both the Myh and Ogg1 DNA glycosylases." Cancer Res **64**(13): 4411-4.
Sakumi, K., M. Furuichi, et al. (1993). "Cloning and expression of cDNA for a human enzyme that hydrolyzes 8-oxo-dGTP, a mutagenic substrate for DNA synthesis." J Biol Chem **268**(31): 23524-30.
Schrammel, A., S. Behrends, et al. (1996). "Characterization of 1H-[1,2,4]oxadiazolo[4,3-a]quinoxalin-1-one as a heme-site inhibitor of nitric oxide-sensitive guanylyl cyclase." Mol Pharmacol **50**(1): 1-5.
Shan, X. and C. L. Lin (2006). "Quantification of oxidized RNAs in Alzheimer's disease." Neurobiol Aging **27**(5): 657-62.
Shan, X., H. Tashiro, et al. (2003). "The identification and characterization of oxidized RNAs in Alzheimer's disease." J Neurosci **23**(12): 4913-21.
Shibutani, S., M. Takeshita, et al. (1991). "Insertion of specific bases during DNA synthesis past the oxidation-damaged base 8-oxodG." Nature **349**(6308): 431-4.
Sies, H. (1991). "Role of reactive oxygen species in biological processes." Klin Wochenschr **69**(21-23): 965-8.
Son, H., R. D. Hawkins, et al. (1996). "Long-term potentiation is reduced in mice that are doubly mutant in endothelial and neuronal nitric oxide synthase." Cell **87**(6): 1015-23.
Son, H., Y. F. Lu, et al. (1998). "The specific role of cGMP in hippocampal LTP." Learn Mem **5**(3): 231-45.
Stedeford, T., F. Cardozo-Pelaez, et al. (2001). "Comparison of base-excision repair capacity in proliferating and differentiated PC 12 cells following acute challenge with dieldrin." Free Radic Biol Med **31**(10): 1272-8.

Steenken, S. (1997). "Electron transfer in DNA? Competition by ultra-fast proton transfer?" Biol Chem **378**(11): 1293-7.
Summer, K. H. and J. Eisenburg (1985). "Low content of hepatic reduced glutathione in patients with Wilson's disease." Biochem Med **34**(1): 107-11.
Taddei, F., H. Hayakawa, et al. (1997). "Counteraction by MutT protein of transcriptional errors caused by oxidative damage." Science **278**(5335): 128-30.
Tanaka, J., M. Markerink-van Ittersum, et al. (1997). "Nitric oxide-mediated cGMP synthesis in oligodendrocytes in the developing rat brain." Glia **19**(4): 286-97.
Taylor, J. P., J. Hardy, et al. (2002). "Toxic proteins in neurodegenerative disease." Science **296**(5575): 1991-5.
Traut, T. W. (1994). "Physiological concentrations of purines and pyrimidines." Mol Cell Biochem **140**(1): 1-22.
Waldman, S. A. and F. Murad (1987). "Cyclic GMP synthesis and function." Pharmacol Rev **39**(3): 163-96.
Wang, J., W. R. Markesbery, et al. (2006). "Increased oxidative damage in nuclear and mitochondrial DNA in mild cognitive impairment." J Neurochem **96**(3): 825-32.
Westerman, M. A., D. Cooper-Blacketer, et al. (2002). "The relationship between Abeta and memory in the Tg2576 mouse model of Alzheimer's disease." J Neurosci **22**(5): 1858-67.
Wong, B. S., S. G. Chen, et al. (2001). "Aberrant metal binding by prion protein in human prion disease." J Neurochem **78**(6): 1400-8.
Yamazaki, M., K. Chiba, et al. (2006). "Differences in neuritogenic response to nitric oxide in PC12 and PC12h cells." Neurosci Lett **393**(2-3): 222-5.
Yeh, L. H. and A. I. Alayash (2003). "Redox side reactions of haemoglobin and cell signalling mechanisms." J Intern Med **253**(5): 518-26.
Yoon, S. H., J. W. Hyun, et al. (2005). "In vitro evidence for the recognition of 8-oxoGTP by Ras, a small GTP-binding protein." Biochem Biophys Res Commun **327**(1): 342-8.
Zhang, J., G. Perry, et al. (1999). "Parkinson's disease is associated with oxidative damage to cytoplasmic DNA and RNA in substantia nigra neurons." Am J Pathol **154**(5): 1423-9.
Zhuo, M., Y. Hu, et al. (1994). "Role of guanylyl cyclase and cGMP-dependent protein kinase in long-term potentiation." Nature **368**(6472): 635-9.

CHAPTER ONE

Assessing biomarkers of oxidative stress: Analysis of guanosine and oxidized guanosine nucleotide triphosphates by high performance liquid chromatography with electrochemical detection

Abstract

Oxidation of the guanosine moiety in DNA has become a hallmark biomarker in assessing oxidative stress. The oxidation of guanosine in the nucleotide triphosphate pool has been overlooked due to the lack of a reliable methodology. This method describes a sample processing and high performance liquid chromatography with electrochemical detection protocol for the analysis of the cellular pool of guanosine triphosphates and oxidized guanosine triphosphates. Validation of this method is demonstrated along with evaluation of these analytes in control and oxidizing conditions in vitro and in HEK 293T cells. Oxidation of this triphosphate pool occurred independently of oxidation to DNA.

Introduction

Oxidative stress is defined as the deleterious impact in cell function as a consequence of the loss in homeostatic balance between reactive oxygen species (ROS) and antioxidants in the cellular milieu (Sies 1991). ROS are formed continuously as a result of normal cellular respiration, enzymatic metabolism, and exogenous insults (Halliwell and Gutteridge 1986). Oxidative stress has been implicated in the onset and development of several pathological processes including cancer and age-related neurodegenerative diseases such as Parkinson's Disease (PD) (Hollstein, Sidransky et al. 1991; Sanchez-Ramos 1994; Alam, Jenner et al. 1997; Beal 2003). The interaction of ROS with DNA has the potential to generate a number of possible DNA lesions. Among the four DNA bases, guanine has the lowest reduction potential and it is the most readily oxidized (Devasagayam, Steenken et al. 1991; Steenken 1997; Milligan, Aguilera et al. 2001). Two-electron oxidation of guanine results in the formation of 8-oxo-2'-deoxyguanosine (oxo^{8}dG), which is the major oxidation product of guanine. This species is one of the most frequently studied oxidized DNA base products, and it has attracted considerable interest as a biomarker of oxidative stress associated with diseases ranging from cancer to neurological deficits (Dizdaroglu, Jaruga et al. 2002; Proteggente, England et al. 2002; Chiou, Chang et al. 2003; Wang, Xiong et al. 2005). It has been shown that oxo^{8}dG is produced by hydroxyl radical ($OH^{\cdot}$) attack, the most oxidizing ROS to arise in biological systems, on the C8 position of 2'-deoxyguanosine (2-dG) in DNA (Kasai and Nishimura 1983; Buettner 1993). Oxo^{8}dG is promutagenic due to its tendency to preferentially pair with adenosine over cytosine during DNA replication, leading to G:C $\rightarrow$ T:A transversions (Cheng, Cahill et al. 1992). Increases in oxo^{8}dG

levels in DNA can also occur after $OH^{\cdot}$ radical attack to the cellular 2'-deoxyguanosine 5'-triphosphate (dGTP) pool producing oxidized 2-dG 5'-triphosphate (oxo^8dGTP) (Hayakawa, Taketomi et al. 1995). Oxo^8dGTP can then be incorporated into DNA during cellular replication or during DNA repair. The dGTP nucleotide pool is mainly located in the cytoplasm; therefore, it is more available for attack by ROS as compared to DNA, which is protected by histones and tightly packaged in the nucleus.

Guanosine 5'-triphosphate (GTP), required for RNA synthesis and several normal cellular functions, can also be modified by ROS. GTP concentrations in the cytoplasm are hundreds of times larger than dGTP (Kornberg 1992). This suggests that under conditions of high ROS levels, significantly more oxidized GTP (oxo^8GTP) than oxo^8dGTP could be produced in the cell. However, due to the lack of a reliable way to quantify these oxidation products, little is know of the degree of oxidation to dGTP or GTP pools after ROS attack and the possible impact of these oxidation products to cellular physiology. Recently it has been shown that the dGTP pool endures greater levels of oxidation after irradiation as compared to DNA (Haghdoost, Czene et al. 2005). Levels of oxo^8dG in cells, tissue, and whole animal have been reported as an important biomarker for oxidative stress when evaluating disease pathologies ranging from cancer to diabetes (Hollstein, Sidransky et al. 1991; Dandona, Thusu et al. 1996). However, most of this evidence has been accrued by assessment of oxo^8dG via antibody technology. It is necessary to investigate the relative contributions of oxidized dGTP and GTP to this biomarker assessment as well as the particular susceptibility of these cellular pools to oxidative stress as compared to DNA.

The following study describes a sample processing and HPLC-EC methodology for the simultaneous determination of dGTP, GTP, oxo^{8}dGTP, and oxo^{8}GTP in cells. Optimization of retention times was achieved by dephosphorylating the compounds to their respective guanosine nucleoside forms 2-deoxyguanosine (2dG), guanosine (G), and their corresponding oxidized forms oxo^{8}dG and oxo^{8}G, and detection selectivity was gained by detection at specific voltages by the coularray detector. Although hydrolysis of guanosine nucleotide triphosphates to their respective guanosine nucleosides by alkaline phosphatase (EC 3.1.3.1) has been reported as a preparative step for HPLC with UV detection, validation of this technique as a reliable assessment of dGTP and GTP concentrations in the cells concomitantly with assessment of their oxidized forms, oxo^{8}dGTP and oxo^{8}GTP, has not been established until now (Cohen, Maybaum et al. 1981). The method described here was used to quantify the basal levels of dGTP and GTP in human embryonic kidney (HEK 293T) and to assess the susceptibility of theses pools to ROS attack. Oxo^{8}dG was quantified in nuclear DNA extracts of the HEK393T cells under oxidizing conditions that impacted the GTP pool, and shown to be equal to that of controls. Thus, these results suggest a novel way of assessing the oxidation of cellular guanosine triphosphates as a biomarker of oxidative stress that occurs independently from oxidation to DNA. The sample processing and chromatographic analysis presented permit us to demonstrate that under conditions in which ROS are produced, the GTP pool can be impacted without noticeable changes to the dGTP pool or the guanine base in DNA.

Materials and Methods

Chemicals and Reagents

All reagents were purchased from Sigma-Aldrich (St. Louis, MO), unless otherwise indicated. 8-oxoguanosine-5'-triphosphate (oxo^{8}GTP) and 8-oxo-2'-deoxyguanosine-5'-triphosphate (oxo^{8}dGTP) were purchased from TriLink Biotechnologies (San Diego, CA). 8-oxoguanosine (oxo^{8}G) was obtained from Cayman Chemical (Ann Arbor, MI). Ultrapure water was obtained from a Milli-Q UF-Plus apparatus (Millipore).

Cell culture

HEK 293T cells purchased from American Type Culture Collection (Menasses, VA) were grown in T75 cell culture flasks (Costar, Corning Inc., Corning, NY) at 37° C, 5% CO_2. Cells were maintained in 1X Dulbecco's Modification of Eagle's Medium with 4.5 g/L glucose and L-glutamine, 10% fetal bovine serum, 1 mM sodium pyruvate, 1X non-essential amino acids, 1000 international units (IU) penicillin – 1 mg/mL streptomycin, and 50 μg/mL gentamicin sulfate. All media reagents were purchased from CellGro® technologies (Mediatec Inc., Herndon, VA, USA). All in vitro experiments were conducted with harvested cells that had reached confluency, approximately 3 x 10^7 cells per flask. Mycophenolic Acid (MPA) was solubilized in ethanol and diluted in cell culture media for MPA experiments. A final concentration of 2 μM MPA was added in a subset of cell colonies and incubated for one hour at 37^{o}C, a dose previously shown not to affect cell viability (Gu, Gathy et al. 2003). For oxidation experiments, control cell populations were incubated in 1mM L-ascorbic acid and oxidation colonies contained 1mM L-ascorbic acid and 10 μM cupric sulfate. All

reagents were prepared in media before addition to flasks and incubation at 37°C for four hours.

dGTP, GTP, oxo^{8}dGTP, and oxo^{8}GTP extraction

All the extraction steps were performed on ice. Immediately prior to processing, confluent flasks of HEK 293T cells were assessed for viability using the tryphan blue exclusion method and counted. After washing three times with ice-cold phosphate-buffered saline (PBS), cells were harvested with the addition of 3 mL of 1X trypsin-EDTA and pelleted by centrifugation at 2,000 x g, 4°C. Cell pellets were pooled from two flasks per sample in 6mL of PBS. Following centrifugation, protein was precipitated using 1.5mL of 6% Trichloroacetic Acid (TCA), vortex-mixed for 20s, ice-bathed for 10 minutes, and vortex-mixed again for 20s. Cell extracts were then centrifuged at 13,000 rpm for 10 minutes at 4°C. The resulting supernatant was neutralized to pH 6 with a solution containing 3M KOH and 3M $KHCO_3$. Samples were stored at -80°C until undergoing the dephosphorylation process.

dGTP, GTP, oxo^{8}dGTP, and oxo^{8}GTP dephosphorylation

Neutralized cell extracts, standards, and in vitro reactions were treated similarly for dephosphorylation. On ice, 25 Units of alkaline phosphatase (dissolved in Tris-HCl pH 8.0), 1.8 mM sodium acetate, and 100mM Tris-HCl, were added to 10μL of sample in total volume of 20 μL. After incubation at 37°C for 1 hour, the dephosphorylation reaction was stopped by placing on ice. This was followed by filtering through Ultrafree-MC (30-kD) tubes (Millipore Corp., Bedford, MA). Quantification of the generated nucleosides (2-dG, G, oxo^{8}dG and oxo^{8}G) was carried out by injecting 10μL of the filtrate into the HPLC-EC for in vitro reactions and 20μL of filtrate for cell extracts.

Instrument and Chromatographic Conditions

Guanosine nucleotide triphosphates, guanosine nucleosides, and oxidized derivatives were resolved by HPLC with a reverse phase YMC basic column (4.6 x 150 mm; particle size 3-micron) (YMC Inc., Wilmington, NC) and quantified using a CoulArray electrochemical detection system (ESA, Inc., Chelmsford, MA). An isocratic mobile phase consisting of 100 mM sodium acetate, pH 5.2, 4% Methanol (HPLC Grade) diluted in water polished with C18 Sep-Pak cartridges (Waters Corp., Milford, MA) was utilized to elute the guanosine nucleotide triphosphates and guanosine nucleosides from the column. The mobile phase was filtered using 0.2 μm nylon filters and degassed by sonication before use with the HPLC. Potentials of the twelve coulometric analytical cells of the CoulArray system, placed in series, were as follows: 50, 125, 175, 200, 250, 380, 500, 700, 785, 850, 890, 900 mV. Data were recorded, analyzed, and stored using CoulArray for Windows data analysis software (ESA Inc., Chelmsford, MA).

Calibration standards

Stock solutions of each analyte were prepared by individually dissolving commercially available, pure guanosine and oxidized guanosine nucleosides as well as guanosine nucleotide triphosphates in mobile phase. For the nucleosides 2-dG and G, the addition of 5 μL of 10M NaOH to 1mL of stock solution was required to achieve adequate solubility. Calibration curves were generated from standards of dGTP, GTP, 2-dG, and G ranging from 5 pmoles to 4 nmoles. Elution of the guanosine-containing analytes was monitored in the 700, 785, and 850 mV channels and their injected amounts were graphed relative to the sum of peak areas. Oxo^{8}dGTP, oxo^{8}GTP, oxo^{8}dG, and oxo^{8}G calibration curves were created from concentrations ranging from 5 to 50 pmoles.

These oxidized guanosine analytes were monitored in the 250 mV channel and their injected amounts were graphed relative to peak area of the corresponding peak. Dephosphorylated calibration standards were treated similarly with the addition of the dephosphorylation steps outlined in 2.4.

Oxidation of GTP in vitro

All reagents for in vitro oxidations were reconstituted in PBS, pH = 7.4, and kept on ice. Control reactions included 1 mM GTP and 1 mM L-ascorbic acid and oxidation reactions contained 1 mM GTP, 1 mM L-ascorbic acid, and 10 μM cupric sulfate in a final volume of 100 μL. All samples were incubated for 4 hours at 37ºC.

DNA isolation

DNA was extracted from confluent flasks of HEK 293T cells, with minor modifications, according to a method previously described (Bolin, Stedeford et al. 2004). Briefly, confluent flasks of control populations were treated with unmodified cell culture media described above (see 2.5). Oxidized populations were exposed to a final concentration of 10 μM cupric sulfate and 1 mM L-ascorbic acid prepared in cell culture media and incubated for 4 hours at 37ºC. After washing three times with ice-cold phosphate-buffered saline (PBS), cells were harvested with the addition of 3 mL of 1X trypsin-EDTA and pelleted by centrifugation at 2,000 x g, 4ºC. Pellets were resuspended in 1 mL of DNA extraction buffer containing 0.1 M Trizma-base, 0.1 M NaCl, and 20 mM EDTA, and lysed by sonication using a Vir Sonic Ultrasonic Cell Disruptor 100 (Virtis Company, Gardiner, NY). Following sonication, 300 μL of DNA extraction buffer containing 33 U of DNase free RNase T1 (EC 3.1.27.3) and 200 μg of RNase A (EC 3.1.27.5) and incubated at 37ºC for 1 hour. After mixing and brief centrifugation at

1,500 x g for 5 minutes, 300 µL of DNA extraction buffer containing 300 µg of Proteinase K (EC 3.4.21.64) and 1% SDS was added to each sample. Following incubation at 37 ^{o}C for 1 hour, the protein fraction was separated from the DNA by three consecutive organic extractions as follows: 700 µL of phenol (stored at –20 ^{o}C saturated in buffer) was added to the mixture and after homogenization and centrifugation the aqueous phase was transferred to 1.5 mL microcentrifuge tubes containing Light Phase Lock Gel (Brinkmann Instruments, Inc., Westbury, NY). The samples were then extracted with phenol:chloroform:isoamyl alcohol (25:24:1), and chloroform:isoamyl alcohol (24:1). The DNA was precipitated from the aqueous phase with two volumes of ice-cold ethanol (with respect to aqueous volume) and stored overnight at -20 ^{o}C.

Extracted DNA was prepared for the HPLC analysis by resolving it into deoxynucleoside components. The DNA was denatured by digestion at 90 ^{o}C for 2 minutes in 100 µL of 20 mM sodium acetate (pH 5.0) then incubating at 37 ^{o}C for 1 hr with 10 U of nuclease P1 (EC 3.1.30.1) (dissolved in 20 mM sodium acetate). Each sample was then treated with 10 U of alkaline phosphatase (dissolved in Tris-HCl pH 8.0) and incubated at 37 ^{o}C for 1 hour. The reaction was stopped by addition of 20 µL of 3 M sodium acetate (pH 5.0), then filtered using Ultrafree-MC (30-kD) tubes and lyophilized. Samples were stored at -80^{o}C and reconstituted in 50 µL of mobile phase before HPLC-EC analysis. Injection volumes for HPLC-EC analysis contained 10 µL of sample.

Statistical Analysis

All data were analyzed using Prism GraphPad 4.0 software (Graph pad Software Inc., San Diego, CA). Calibration curve parameters for each of the analytes were

obtained by linear regression analysis. An unpaired t-test was performed on data from MPA and oxidation experiments; values denoted with an asterisk are significantly different from their corresponding controls ($P < 0.05$).

Results

Detection of guanosine and oxidized guanosine moieties

Our chromatographic conditions allowed for the separation of guanosine (dGTP, GTP, 2-dG, and G) and oxidized guanosine moieties (oxo^{8}dGTP, oxo^{8}dG, oxo^{8}GTP, and oxo^{8}G) of interest. Figure 6A and 6B were obtained by injection of a single standard containing the six guanosine compounds shown (GTP, dGTP, G, 2-dG, Oxo^{8}G, Oxo^{8}dG). Figure 6C was obtained by injection of standards containing known quantities of oxo^{8}dGTP and oxo^{8}GTP. Although the retention times for oxo^{8}dGTP and oxo^{8}GTP overlap with those of dGTP and GTP, selectivity for their analysis is gained by detection at different oxidation potentials. Both compounds, especially oxo^{8}dGTP, do not seem to coelute with any other. Elution of the guanosine triphosphates is monitored in the 700, 785, and 850 mV channels (Figure 6A), while elution of the oxidized forms is monitored in the 250 mV channel where the maximum aplitude signal is observed (Figure 6C). However, when using extracts from biological samples for HPLC-EC analysis, the difference in chemical composition between the mobile phase and biological milieu generates a broad solvent front in the first four minutes of the analysis. This solvent front peak overlaps the elution of peaks generated from the guanosine triphosphates and makes their analysis impossible. Given the good resolution for the analysis of 2-dG and G (Figure 6A) and for oxo^{8}dG and oxo^{8}G (Figure 6B) combined with their low levels in biological systems, we opted to analyze the triphosphates after an additional sample preparation step to dephosphorylate these analytes before injecting them into the HPLC-EC.

FIGURE 6

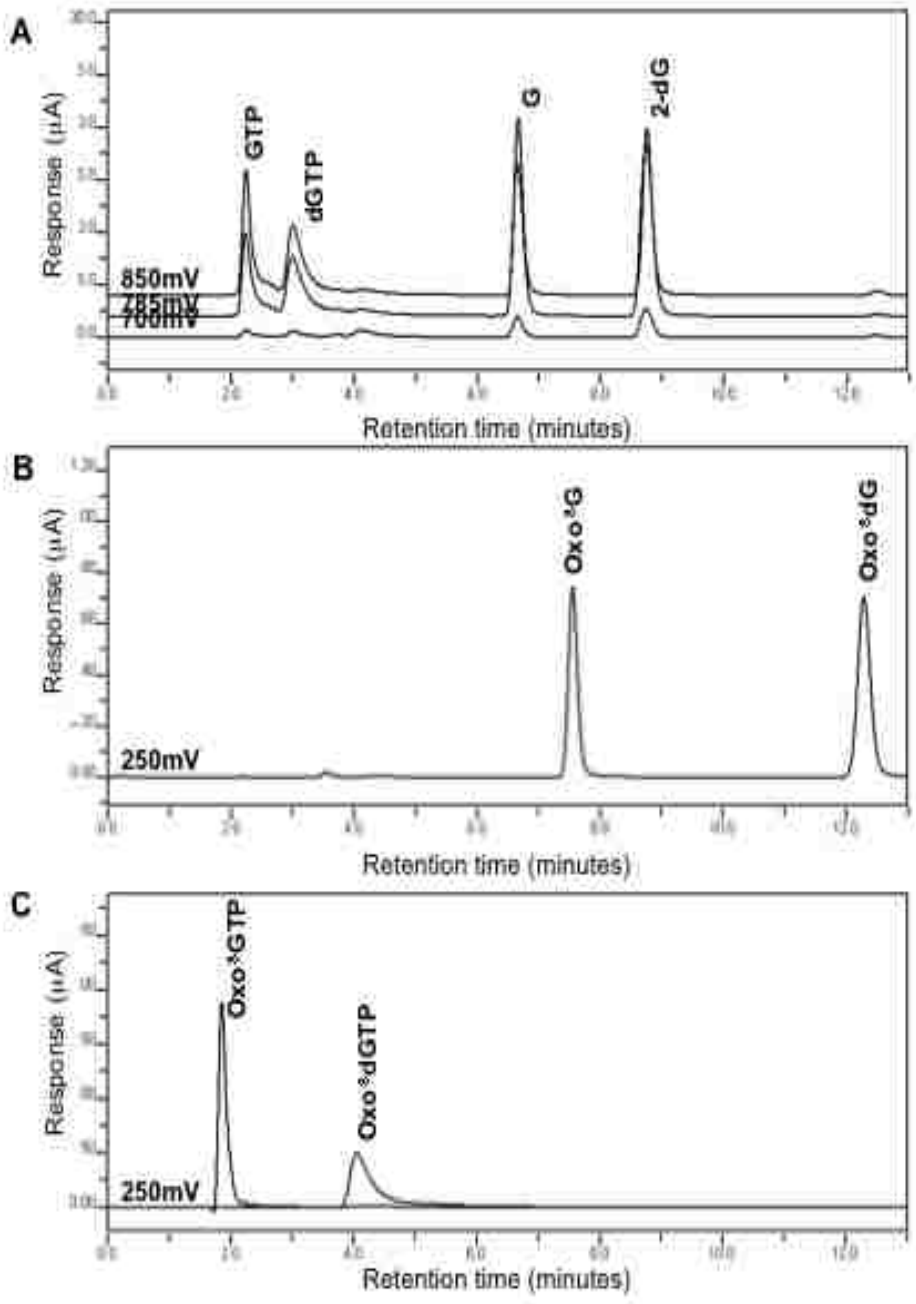
A
Response (μA)
GTP
dGTP
G
2-dG
850mV
785mV
700mV
Retention time (minutes)
B
Response (μA)
Oxo⁸G
Oxo⁸dG
250mV
Retention time (minutes)
C
Response (μA)
Oxo⁸GTP
Oxo⁸dGTP
250mV
Retention time (minutes)

Figure 6. Chromatographic profiles for GTP, dGTP, G, and 2-dG

Chromatographic profiles for a standard containing GTP, dGTP, G, and 2-dG (A) detected in channels set at 700, 785, and 850 mV, a standard containing oxo^{8}G and oxo^{8}dG detected with a channel set at 250 mV (B), and standards of oxo^{8}GTP and oxo^{8}dGTP detected at 250 mV (C).

Validation of preparative sample dephosphorylation

To test whether the dephosphorylation step would interfere with the electrochemical analysis of the analytes, we constructed calibration curves for each of the triphosphate moieties after dephosphorylation and compared their response to injections of equivalent amounts of standards of their respective guanosine nucleosides (Figure 7). Figure 7A compares the response of 2-dG generated from dephosphorylation of dGTP to the response of a prepared 2-dG standard. Figures 7B, 7C, and 7D were constructed similarly to allow for the same comparison for G, oxo^{8}dG, and oxo^{8}G respectively. The calibration curves for the dephosphorylated oxidized guanosine triphosphates and oxidized guanosine nucleosides were built based on a picomolar scale and those for the unmodified guanosine compounds were built based on a nanomolar scale. This is due to the observation that the concentration of oxidized guanosine nucleotide triphosphates (oxo^{8}GTP and oxo^{8}dGTP) and oxidized guanosine nucleosides (oxo^{8}G and oxo^{8}dG) might be several orders of magnitude smaller than their corresponding unmodified guanosine compounds (dGTP, GTP, G, 2-dG) in biologically relevant systems.

FIGURE 7

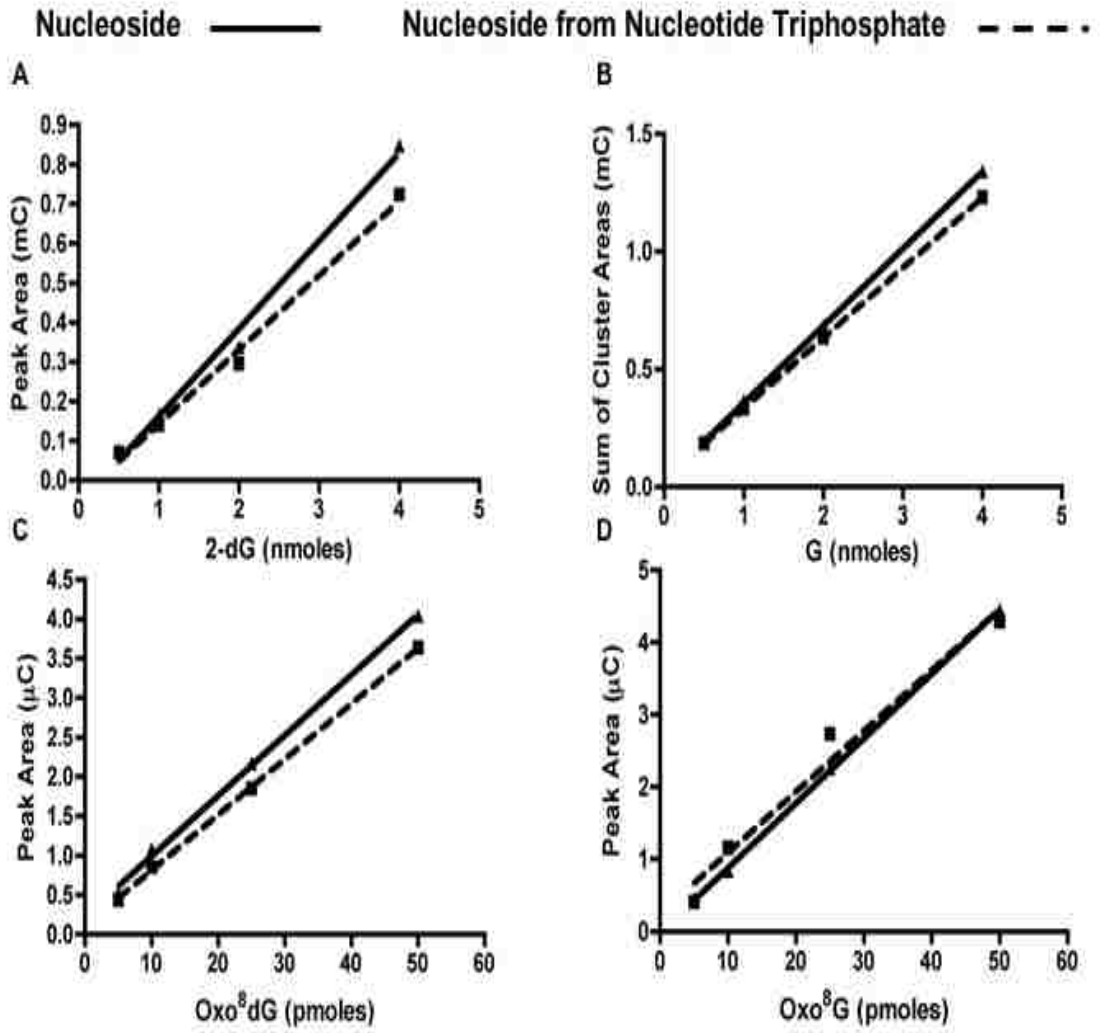
Nucleoside
Nucleoside from Nucleotide Triphosphate
A
Peak Area (mC)
2-dG (nmoles)
B
Sum of Cluster Areas (mC)
G (nmoles)
C
Peak Area (µC)
Oxo8dG (pmoles)
D
Peak Area (µC)
Oxo8G (pmoles)

Figure 7. Calibration curves for 2-dG, G, oxo^{8}dG, and oxo^{8}G

Solid lines are calibration curves built with known amounts of 2-dG(A), G (B), oxo^{8}dG (C), and oxo^{8}G (D). Dashed lines are calibration curves built with equivalent amounts of standards containing dGTP (A), GTP (B), oxo^{8}dGTP (C), and oxo^{8}GTP (D) after alkaline phosphatase treatment. (n = 2).

Table 7 outlines the specific calibration components of each of the dephosphorylated guanosine triphosphates as well as the guanosine nucleoside standards. Each of the calibration curves yielded a coefficient of determination (r^2) greater than 0.9 and an average percent recovery of 95% or greater. The values for the slope and intercept for the dephosphorylated guanosine nucleotide triphosphates as compared to their corresponding standard guanosine nucleoside were not significantly different.

Table 7. Comparison of calibration curve components of guanosine nucleosides and deposhorylated guanosine nucleotides

					Dephosphorylated			
Component	G	Oxo^8G	2-dG	Oxo^8dG	GTP	Oxo^8GTP	dGTP	Oxo^8dGTP
Slope	0.3281	0.08951	0.2224	0.07660	0.2987	0.08418	0.1185	0.07047
Y-intercept	0.02874	-0.01398	-0.06004	0.2302	0.03513	0.2534	-0.04541	0.1106
r^2	0.9998	0.9997	0.9912	0.9978	1.000	0.9729	0.9922	0.9996
Average % Recovery	99.49	100.05	103.68	97.17	100.04	89.63	103.72	99.57

It can be therefore concluded that the dephosphorylation of guanosine and oxidized guanosine triphosphates is complete under these reaction conditions, and that the levels of the resulting nucleoside are equivalent to the levels of the parent nucleotide triphosphate. The limit of detection (LOD) for each nucleoside was determined as the amount giving a signal-to-noise (S/N) ratio of 3:1. The LOD for each compound were 126.83 (G), 167.91 (dG), 40.24 (oxo^8G), and 47.11 (oxo^8dG) fmole, respectively. The limit of quantification (LOQ) for each nucleoside was determined as the amount giving a S/N ratio of 10:1. The LOQ for each compound were 422.80 (G), 559.70 (dG), 134.10 (oxo^8G), and 157.0 (oxo^8dG) fmole, respectively. These detection limits are one to two orders of magnitude lower than the levels of G, dG, oxo^8G, and oxo^8dG measured in biological samples using this methodology (see Sections 3.3 and 3.4).

Detection of guanosine and oxidized guanosine moieties in HEK 293T cells

To test whether the same dephosphorylation process could be applied to the analysis of nucleotide triphosphates in biological samples, we used HEK 293T cells with and without the addition of mycophenolic acid (MPA). MPA is a non-nucleoside, noncompetitive, reversible inhibitor of inosine monophosphate dehydrogenase (IMPDH) (EC 1.1.1.205) (Allison and Eugui 2000). IMPDH is responsible for catalyzing the rate-limiting step in the de novo biosynthesis of guanosine monophosphate (GMP) which is further converted into guanosine diphosphate (GDP) and GTP. Previous studies have shown that concentrations of MPA ranging from 0.2 to 2 μM reduce the levels of GTP in vitro as much as eighty percent without affecting cell viability (Daxecker, Raab et al. 2001; Gu, Gathy et al. 2003). Figure 8A and 8B are representative chromatograms of dephosphorylated cytosolic extracts from control and MPA-treated HEK 293T cells.

Addition of 2 μM MPA for one hour significantly reduced GTP levels by 70% (Fig. 8A and 8C) without affecting the concentration of dGTP (Fig. 8D) or cell viability. Interestingly, oxo^{8}GTP was also significantly reduced by 70% in these same MPA-exposed colonies (Fig. 8E). Oxo^{8}dGTP was undetectable in control and MPA-exposed samples.

FIGURE 8

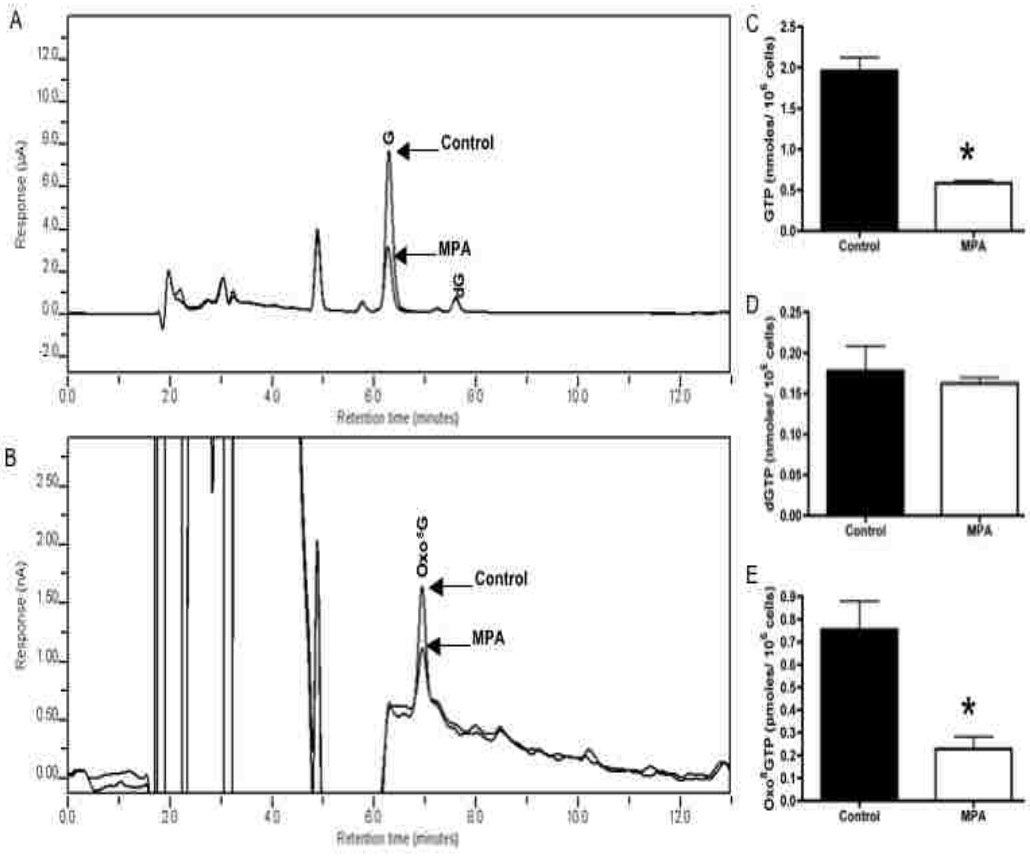
A
Response (μA)
G
Control
MPA
dG
Retention time (minutes)
B
Response (nA)
Oxo⁸G
Control
MPA
Retention time (minutes)
C
GTP (nmoles/ 10⁶ cells)
Control
MPA
D
dGTP (nmoles/ 10⁶ cells)
Control
MPA
E
Oxo⁸GTP (pmoles/ 10⁶ cells)
Control
MPA

Figure 8. Chromatographic profiles of GTP in HEK 293T cell extracts

Typical chromatograhic profiles of cytosolic cellular extracts, after treatment with alkaline phosphatase, obtained from HEK 293T cells in control or MPA-exposed populations (2 μM, 1 hour). Typical retention times for G and 2-dG generated are presented in 3A, and that for oxo^{8}G in 3B (chromatograms reflect a 3D shift for display purposes). Although channels 700, 785, and 850 mV were used for quantitation of GTP and dGTP, only dominant channel 785 mV is shown in this figure for clarity. Bar graphs show cellular levels of GTP (C), dGTP (D), and oxo^{8}GTP (E) in control (black bar) and MPA treated (white bar) cells. Values expressed as nanomoles (dGTP and GTP) or picomoles (oxo^{8}GTP) per 10^{6} cells. Data expressed as the mean ± SEM (n =3-4, ***** $p < 0.05$).

Basal levels of 2-dG, G, oxo^{8}dG, and oxo^{8}G were undetectable in control cell populations that did not undergo the preparative dephosphorylation step (data not shown). Therefore, endogenous concentrations of these free guanosine (2-dG and G) and oxidized guanosine nucleosides (oxo^{8}dG and oxo^{8}G) in the cellular pool do not confound direct detection and analysis of the dephosphorylated guanosine triphosphate. The concentrations of GTP, dGTP, and oxo^{8}GTP based on an average cell volume of 820 μm^3 was calculated at 2.58 mM, 0.139mM, and 0.762 nM, respectively (Tsao, Condon et al., 2000). Thus, we conclude that determination of these nucleosides is a valid approach to determine levels of the original nucleotide triphosphate.

Oxidation of guanosine triphosphates in vitro and in HEK 293T cells

To assess the impact of oxidative damage in the guanosine triphosphates cellular pools, initially we exposed GTP to a known ROS producing system (1 mM L-ascorbic acid and 10 μM cupric sulfate). Figure 9A and 9B are representative chromatograms of the analysis of GTP, after alkaline phosphatase treatment, under control and oxidizing conditions.

FIGURE 9

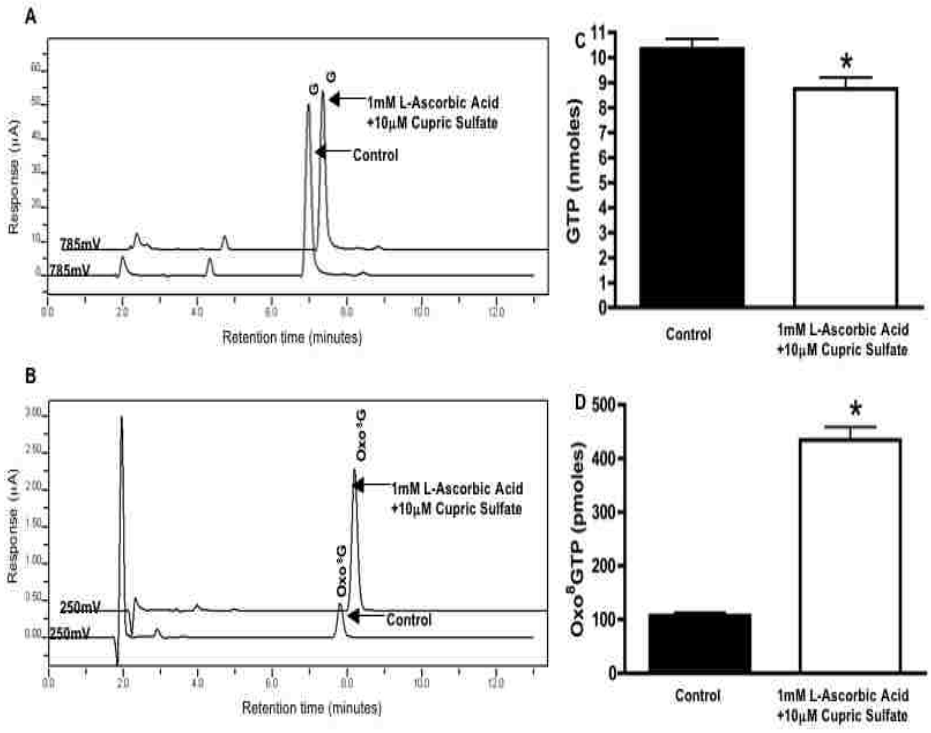
A
Response (μA)
G
G
1mM L-Ascorbic Acid
+10μM Cupric Sulfate
Control
785mV
785mV
Retention time (minutes)
B
Response (μA)
Oxo⁸G
Oxo⁸G
1mM L-Ascorbic Acid
+10μM Cupric Sulfate
Control
250mV
250mV
Retention time (minutes)
C
GTP (nmoles)
Control
1mM L-Ascorbic Acid
+10μM Cupric Sulfate
D
Oxo⁸GTP (pmoles)
Control
1mM L-Ascorbic Acid
+10μM Cupric Sulfate

Figure 9. Chromatographic profiles of GTP exposed to oxidizing conditions

Chromatograhic profiles of dephosphorylated GTP (A) and oxo^{8}GTP (B) after GTP exposure to control (1 mM L-ascorbic acid) or oxidizing conditions (1 mM L-ascorbic acid and 10 μM cupric sulfate). Bar graph shows nanomoles of GTP (C) and picomoles oxo^{8}GTP (D) in GTP samples exposed to control (black bar) or oxidizing conditions (white bar). Data expressed as the mean ± SEM (n =6-9, * $p < 0.05$).

Production of $OH^{\cdot}$ in mixtures of Cu^{2+} and ascorbate has been previously demonstrated, and therefore $OH^{\cdot}$ is likely the ROS responsible for producing oxo^{8}GTP via the same attack mechanism that produces oxo^{8}dG in DNA (Biaglow, Held et al. 1996). The average percent recovery of GTP incubated in PBS for 4 hours was 101% using this sample processing and HPLC-EC method which shows that no GTP is lost due to decomposition or due to the reaction conditions. Under oxidizing conditions, approximately four times more oxo^{8}GTP was formed as compared to control reactions that were incubated with L-ascorbic acid alone (Fig. 9D). Pre-treatment of reagents with the Chelex 100 resin (sodium form) to remove any trace metals did not affect oxo^{8}GTP levels under control conditions. Oxo^{8}GTP was undetectable in untreated GTP reactions (data not shown). GTP also showed a small, although significant decrease in concentration after incubation under oxidizing conditions due to its direct oxidation (Fig. 9C).

To determine if the same oxidation conditions can induce oxo^{8}GTP in a cell culture system, we exposed HEK 293T cells to similar conditions as the ones described above (1 mM L-ascorbic acid, 10 μM cupric sulfate). Figure 10A and 10B are representative chromatograms of alkaline treated cytosolic extracts from HEK 293T cells under control and oxidizing conditions.

FIGURE 10

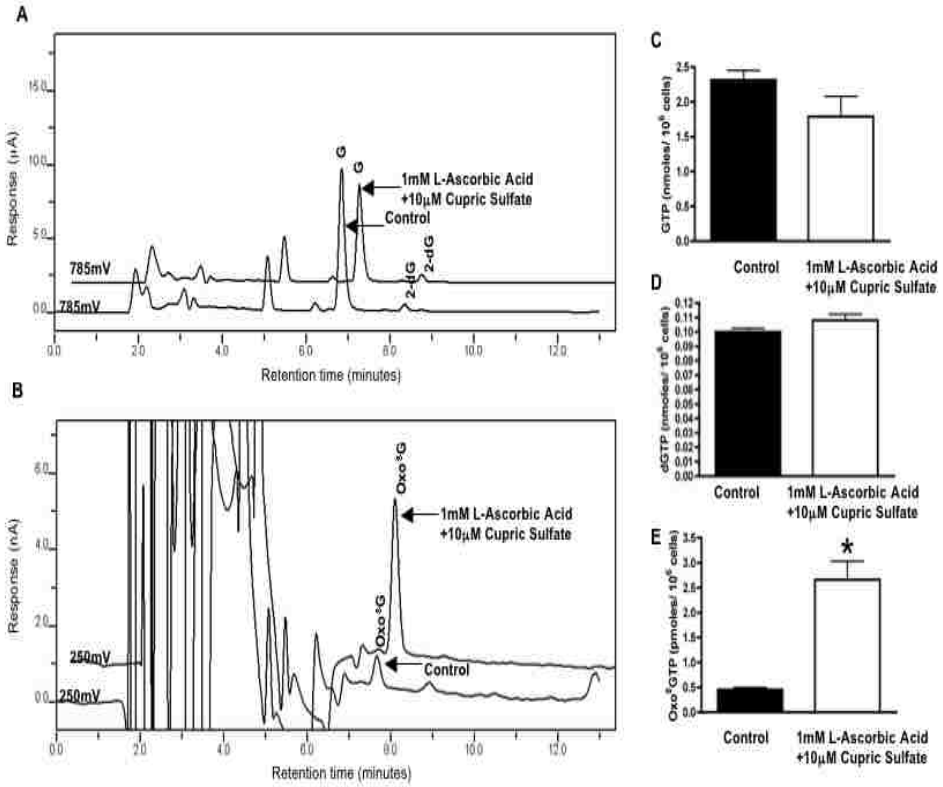
A
Response (nA)
Retention time (minutes)
G
G
1mM L-Ascorbic Acid
+10μM Cupric Sulfate
Control
2-dG
2-dG
785mV
785mV
B
Response (nA)
Retention time (minutes)
Oxo⁸G
1mM L-Ascorbic Acid
+10μM Cupric Sulfate
Oxo⁸G
Control
250mV
250mV
C
GTP (nmoles/ 10⁶ cells)
Control
1mM L-Ascorbic Acid
+10μM Cupric Sulfate
D
dGTP (nmoles/ 10⁶ cells)
Control
1mM L-Ascorbic Acid
+10μM Cupric Sulfate
E
Oxo⁸GTP (pmoles/ 10⁶ cells)
*
Control
1mM L-Ascorbic Acid
+10μM Cupric Sulfate

Figure 10. Chromatographic profiles of GTP in oxidized HEK 293T cells

Chromatographic profiles of alkaline phosphatase treated cytosolic cellular extracts obtained from HEK 293T cells in control (1 mM L-ascorbic acid) or oxidizing (1 mM L-ascorbic acid, 10 μM cupric sulfate) conditions. Typical elution profiles for the generated G and 2-dG (A) and typical elution profile for the oxo^{8}G generated (B). Bar graphs represent cellular levels of GTP (C), dGTP (D), and oxo^{8}GTP (E) in control (black bar and treated cell populations (white bar). Data expressed as levels per 10^{6} cells. Data expressed as the mean ± SEM (n =3, ***** $p < 0.05$).

Oxo^{8}GTP extracted from HEK 293T cells exposed to L-ascorbic acid and cupric sulfate were six times higher than control populations exposed to L-ascorbic acid alone (Fig. 10E). Exposure to L-ascorbic acid alone (control) decreased oxo^{8}GTP levels as compared to untreated cells (data not shown). GTP concentrations in oxidized populations were apparently decreased from controls although the difference was not significant (Fig. 10C). This is likely due to the normal increase in the variability of data obtained from cell cultures as compared to purified reagents. dGTP levels were unaffected in all groups (Fig. 10D) and oxo^{8}dGTP was undetectable in all groups.

Oxidation to guanosine moiety in nuclear DNA of HEK 293T cells

To test whether similar free radical conditions had an effect in the levels of oxidized guanosine in DNA, we measured oxo^{8}dG level in DNA from HEK 293T cells that were exposed to L-ascorbic acid and cupric sulfate. Figure 11 demonstrates that nuclear DNA extracted from HEK 293T cells treated under the same oxidation conditions did not show an increase in oxidation to the guanosine moiety. This suggests the nucleotide pool, specifically GTP, is the primary target for oxidation after exposure to mild oxidizing conditions.

FIGURE 11

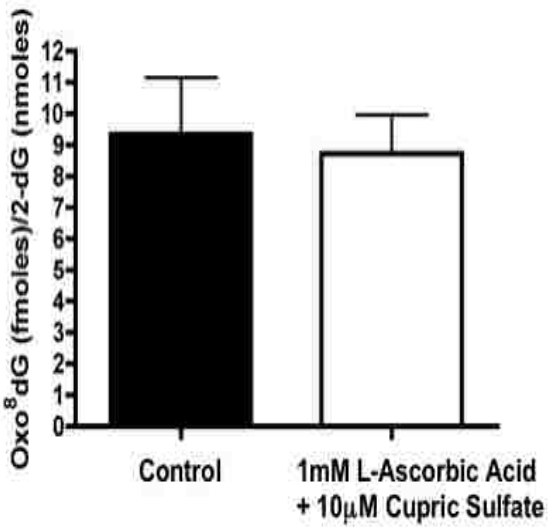
Oxo8dG (fmoles)/2-dG (nmoles)
12
11
10
9
8
7
6
5
4
3
2
1
0
Control
1mM L-Ascorbic Acid
+ 10μM Cupric Sulfate

Figure 11. Levels of oxo^{8}dG in DNA isolated from oxidized HEK 293T Cells

Levels of oxo^{8}dG, as compared to the levels of 2-dG, in DNA isolated from HEK 293T cells exposed to 1 mM L-ascorbic acid (control, black bar) or 1 mM L-ascorbic acid, 10 μM cupric sulfate (oxidizing conditions, white bar). Data expressed femtomoles of oxo^{8}dG per nanomoles of 2-dG in DNA. Bars represent mean ± SEM (n =4).

Discussion

The GTP pool has not been adequately investigated as a target of oxidation and therefore as a biomarker of oxidative stress. Until now, this paucity of information is in part due to the lack of a reliable method to assess oxidized guanosine moieties in the nucleotide pool. The present method for simultaneous detection of dGTP, GTP, oxo^{8}dGTP, and oxo^{8}GTP is the first report of a sensitive, reliable method for the direct determination of these guanosine triphosphates in cells. In addition, this method allows for the detection of the impact of ROS to cellular guanosine under conditions that do not evidence oxidation to DNA. Reports of oxidative damage to DNA in disease and after toxicological challenge have relied on assessments using antibodies against oxo^{8}dG (Degan, Shigenaga et al. 1991; Yin, Whyatt et al. 1995; Toyokuni, Tanaka et al. 1997; Kikuchi, Takeda et al. 2002). However, these antibodies are notorious for showing cross-reactivity with oxo^{8}G, G, and 2-dG (Degan, Shigenaga et al. 1991; Yin, Whyatt et al. 1995). Immunohistochemical studies using antibodies for oxo^{8}dG have also displayed high background reactivity in both the nucleus and cytosol in various cell types. This demonstrates unreliable discrimination between oxidized moieties in DNA and in the free guanosine nucleoside or guanosine nucleotide triphosphate forms (Toyokuni, Tanaka et al. 1997; Kikuchi, Furuta et al. 2002).

Determination of nucleotide concentrations has been investigated by several methods including gas chromatography (GC), bioluminescence, nuclear magnetic resonance spectroscopy (NMR), and high-performance liquid chromatography (HPLC) (Werner 1993). It has been generally established that the quantification of nucleoside and deoxynucleoside triphosphates is most reliably assessed via ion-pair HPLC with UV

detection (Huang, Zhang et al. 2003). However, HPLC with electrochemical detection (EC) is the most sensitive and reliable way of quantifying oxo^{8}dG (Bolin, Stedeford et al. 2004). The chemical properties of guanosine and oxidized guanosine in their triphosphate forms make reverse-phase HPLC-EC incapable of accurately detecting these analytes from biological samples. Incorporation of a preparative dephosphorylation step to overcome difficulties in detecting analytes eluting in the solvent front of the chromatogram ensured the ability to measure dGTP, GTP, oxo^{8}dGTP, and oxo^{8}GTP in cell extracts in a single run. Although basal oxo^{8}dGTP concentrations in biological samples were below the detection limit, sensitivity to this analyte was shown in Figure 6C. Free 2-dG, G, oxo^{8}dG, or oxo^{8}G were not detected in cell extracts that did not undergo the preparative dephosphorylation step, thus they do not interfere with measurements of their triphosphate forms via alkaline phosphatase dephosphorylation. Alkaline phosphatase cleaves the 5' phosphates in ribo and deoxyribonucleotide triphosphates with no activity on nucleotide diphosphates and little activity on nucleotide monophosphates (Humphreys, Kaysen et al. 1980). Given the substrate specificity of alkaline phosphatase for nucleotide triphophates and the inability of HPLC methods with similar extraction techniques to detect GDP or GMP, inflation of G levels using the presented method by interference of GDP or GMP is unlikely (Metz, Rabaglia et al. 1992). The reduction of GTP and oxo^{8}GTP by MPA, a specific inhibitor of de novo GTP synthesis in vivo, provided further validation of the sample preparation and HPLC-EC conditions presented.

The concentration of GTP in HEK 293T cells was found to be approximately ten-fold higher than the concentration of dGTP which corroborates earlier studies in various

normal and tumor cell lines (Huang, Zhang et al., 2003; Traut, 1994) (see Fig.8). The GTP pool also proved to exhibit higher basal levels of oxidation as compared to the dGTP pool which was undetectable under normal growth media conditions (see Fig. 8). The higher basal levels of oxo^{8}GTP, as compared to oxo^{8}dGTP, can be explained by the presence of a specific cellular repair mechanism for the removal of oxo^{8}dGTP from the deoxynucleotide pool. The MTH1 (EC 3.1.6.) protein is responsible for hydrolyzing oxo^{8}dGTP to oxo^{8}dGMP and thus preventing its incorporation into DNA (Mo, Maki et al. 1992). Although MTH1 also acts on oxo^{8}GTP, it has been shown that the rate of cleavage of oxo^{8}GTP by MTH1 is 50 times lower than that of oxo^{8}dGTP (Hayakawa, Hofer et al. 1999). No specific repair or removal mechanism for oxo^{8}GTP has been identified to compensate for this inefficiency of MTH1. This fact also can help explain why the levels of oxo^{8}GTP in HEK 293T cells exposed to oxidizing conditions represented an approximately 6-fold increase from control with no observable increase in oxo^{8}dGTP (see Fig. 10) . Interestingly, this increase in oxo^{8}GTP levels is approximately twice the magnitude of increase seen in oxo^{8}GTP from direct oxidation of GTP (see Fig. 9). Previous studies investigating 1mM ascorbate as a free radical scavenger in solutions of purified 2-dG and calf thymus DNA exposed to radiation have also demonstrated discrepancies in the degree of oxidation to the guanosine moiety (Svoboda and Harms-Ringdahl 1999). Although these particular experiments suggested free 2-dG was more susceptible to oxidation as compared to 2-dG incorporated into DNA, they support the fact that oxidation of the guanine base is highly dependent on the moiety it is contained within the cell (free nucleoside, DNA, nucleotide triphosphate, etc.).

Oxidation of the guanosine moiety in DNA is one of the most widely reported biomarkers of oxidative stress due to its implications in mutagenesis as well as ease and reliability of assessment methods. However, the percent of oxidized guanosine relative to unmodified guanosine in DNA in tissues from pathologies such as Alzheimer's Disease and Parkinson's Disease ranges between 0.002 and 1%. The percent of oxo^{8}GTP relative to GTP in HEK 293T cells exposed to mild oxidizing conditions used in this study was 0.15%. This is at the upper end of this range for oxo^{8}dG/ 2-dG seen in neurodegenerative diseases and an order of magnitude higher than the average percent of oxo^{8}dG relative to 2-dG found in the DNA isolated from the blood of patients with diabetes mellitus (Dandona, Thusu et al. 1996). Oxo^{8}dG measured in naked DNA under similar copper and ascorbate oxidation conditions, 500 μM and 50 μM respectively, reflects only a 0.1% oxidation of the total 2-dG (Spear and Aust 1995). Our in vitro oxidations of GTP demonstrated that 6.6% of the guanosine moiety in its nucleotide triphosphate form was oxidized to oxo^{8}GTP. This is over 60 times more oxidation to the GTP pool as compared to DNA treated under more severe oxidative conditions (Spear and Aust 1995). The magnitude of oxidation we observe both in vitro and in cell culture in the GTP pool under mild oxidative conditions that do not produce any measurable increase in oxidation to guanosine in DNA evidences the importance of evaluating this guanosine pool as an previously overlooked, important marker of oxidative stress.

Conclusions

In conclusion, dephosphorylation of dGTP and GTP and their oxidized counterparts via alkaline phosphatase coupled to HPLC-EC analysis has proven to be a valid method for the detection and analysis of oxidative modification to the guanosine triphosphate pool. This method can be extended to studies evaluating biomarkers of oxidative stress and their pathophysiological role in cancer, neurological disease, and toxicological insult.

References

Alam, Z. I., A. Jenner, et al. (1997). "Oxidative DNA damage in the parkinsonian brain: an apparent selective increase in 8-hydroxyguanine levels in substantia nigra." J Neurochem 69(3): 1196-203.

Allison, A. C. and E. M. Eugui (2000). "Mycophenolate mofetil and its mechanisms of action." Immunopharmacology 47(2-3): 85-118.

Beal, M. F. (2003). "Mitochondria, oxidative damage, and inflammation in Parkinson's disease." Ann N Y Acad Sci 991: 120-31.

Biaglow, J. E., K. D. Held, et al. (1996). "Role of guanosine triphosphate in ferric ion-linked Fenton chemistry." Radiat Res 145(5): 554-62.

Bolin, C., T. Stedeford, et al. (2004). "Single extraction protocol for the analysis of 8-hydroxy-2'-deoxyguanosine (oxo8dG) and the associated activity of 8-oxoguanine DNA glycosylase." J Neurosci Methods 136(1): 69-76.

Buettner, G. R. (1993). "The pecking order of free radicals and antioxidants: lipid peroxidation, alpha-tocopherol, and ascorbate." Arch Biochem Biophys 300(2): 535-43.

Cheng, K. C., D. S. Cahill, et al. (1992). "8-Hydroxyguanine, an abundant form of oxidative DNA damage, causes G----T and A----C substitutions." J Biol Chem 267(1): 166-72.

Chiou, C. C., P. Y. Chang, et al. (2003). "Urinary 8-hydroxydeoxyguanosine and its analogs as DNA marker of oxidative stress: development of an ELISA and measurement in both bladder and prostate cancers." Clin Chim Acta 334(1-2): 87-94.

Cohen, M. B., J. Maybaum, et al. (1981). "Guanine nucleotide depletion and toxicity in mouse T lymphoma (S-49) cells." J Biol Chem 256(16): 8713-7.

Dandona, P., K. Thusu, et al. (1996). "Oxidative damage to DNA in diabetes mellitus." Lancet 347(8999): 444-5.

Daxecker, H., M. Raab, et al. (2001). "Determination of the effects of mycophenolic acid on the nucleotide pool of human peripheral blood mononuclear cells in vitro by high-performance liquid chromatography." Clin Chim Acta 310(1): 81-7.

Degan, P., M. K. Shigenaga, et al. (1991). "Immunoaffinity isolation of urinary 8-hydroxy-2'-deoxyguanosine and 8-hydroxyguanine and quantitation of 8-hydroxy-2'-deoxyguanosine in DNA by polyclonal antibodies." Carcinogenesis 12(5): 865-71.

Devasagayam, T. P., S. Steenken, et al. (1991). "Formation of 8-hydroxy(deoxy)guanosine and generation of strand breaks at guanine residues in DNA by singlet oxygen." Biochemistry 30(25): 6283-9.

Dizdaroglu, M., P. Jaruga, et al. (2002). "Free radical-induced damage to DNA: mechanisms and measurement." Free Radic Biol Med 32(11): 1102-15.

Gu, J. J., K. Gathy, et al. (2003). "Induction of apoptosis in IL-3-dependent hematopoietic cell lines by guanine nucleotide depletion." Blood 101(12): 4958-65.

Haghdoost, S., S. Czene, et al. (2005). "Extracellular 8-oxo-dG as a sensitive parameter for oxidative stress in vivo and in vitro." Free Radic Res 39(2): 153-62.

Halliwell, B. and J. M. Gutteridge (1986). "Oxygen free radicals and iron in relation to biology and medicine: some problems and concepts." Arch Biochem Biophys 246(2): 501-14.
Hayakawa, H., A. Hofer, et al. (1999). "Metabolic fate of oxidized guanine ribonucleotides in mammalian cells." Biochemistry 38(12): 3610-4.
Hayakawa, H., A. Taketomi, et al. (1995). "Generation and elimination of 8-oxo-7,8-dihydro-2'-deoxyguanosine 5'-triphosphate, a mutagenic substrate for DNA synthesis, in human cells." Biochemistry 34(1): 89-95.
Hollstein, M., D. Sidransky, et al. (1991). "p53 mutations in human cancers." Science 253(5015): 49-53.
Huang, D., Y. Zhang, et al. (2003). "Analysis of intracellular nucleoside triphosphate levels in normal and tumor cell lines by high-performance liquid chromatography." J Chromatogr B Analyt Technol Biomed Life Sci 784(1): 101-9.
Humphreys, M. H., G. A. Kaysen, et al. (1980). "Anion-stimulated phosphohydrolase activity of intestinal alkaline phosphatase." Am J Physiol 238(1): G3-9.
Kasai, H. and S. Nishimura (1983). "Hydroxylation of the C-8 position of deoxyguanosine by reducing agents in the presence of oxygen." Nucleic Acids Symp Ser(12): 165-7.
Kikuchi, A., A. Takeda, et al. (2002). "Systemic increase of oxidative nucleic acid damage in Parkinson's disease and multiple system atrophy." Neurobiol Dis 9(2): 244-8.
Kikuchi, H., A. Furuta, et al. (2002). "Impairment of mitochondrial DNA repair enzymes against accumulation of 8-oxo-guanine in the spinal motor neurons of amyotrophic lateral sclerosis." Acta Neuropathol (Berl) 103(4): 408-14.
Kornberg, A., and Baker, T.A. (1992). DNA replication. New York, W.H. Freeman and Co.
Metz, S. A., M. E. Rabaglia, et al. (1992). "Selective inhibitors of GTP synthesis impede exocytotic insulin release from intact rat islets." J Biol Chem 267(18): 12517-27.
Milligan, J. R., J. A. Aguilera, et al. (2001). "Redox reactivity of guanyl radicals in plasmid DNA." Int J Radiat Biol 77(3): 281-93.
Mo, J. Y., H. Maki, et al. (1992). "Hydrolytic elimination of a mutagenic nucleotide, 8-oxodGTP, by human 18-kilodalton protein: sanitization of nucleotide pool." Proc Natl Acad Sci U S A 89(22): 11021-5.
Proteggente, A. R., T. G. England, et al. (2002). "Gender differences in steady-state levels of oxidative damage to DNA in healthy individuals." Free Radic Res 36(2): 157-62.
Sanchez-Ramos, J., Overvik, Eva., Ames, B. (1994). "A Marker of Oxyradical-Mediated DNA Damage (8-Hydroxy-2'-Deoxyguanosine) is Increased in Nigro-Striatum of Parkinson's Disease Brain." Neurodegeneration 3: 197-204.
Sies, H. (1991). "Role of reactive oxygen species in biological processes." Klin Wochenschr 69(21-23): 965-8.
Spear, N. and S. D. Aust (1995). "Hydroxylation of deoxyguanosine in DNA by copper and thiols." Arch Biochem Biophys 317(1): 142-8.
Steenken, S. (1997). "Electron transfer in DNA? Competition by ultra-fast proton transfer?" Biol Chem 378(11): 1293-7.

Svoboda, P. and M. Harms-Ringdahl (1999). "Protection or sensitization by thiols or ascorbate in irradiated solutions of DNA or deoxyguanosine." Radiat Res 151(5): 605-16.

Toyokuni, S., T. Tanaka, et al. (1997). "Quantitative immunohistochemical determination of 8-hydroxy-2'-deoxyguanosine by a monoclonal antibody N45.1: its application to ferric nitrilotriacetate-induced renal carcinogenesis model." Lab Invest 76(3): 365-74.

Traut, T. W. (1994). "Physiological concentrations of purines and pyrimidines." Mol Cell Biochem **140**(1): 1-22.

Tsao, Y. S., R. G. Condon, et al. (2000). "Biomass and aggregation analysis of human embryonic kidney 293 suspension cell cultures by particle size measurement." Biotechnol Prog **16**(5): 809-14.

Wang, J., S. Xiong, et al. (2005). "Increased oxidative damage in nuclear and mitochondrial DNA in Alzheimer's disease." J Neurochem 93(4): 953-62.

Werner, A. (1993). "Reversed-phase and ion-pair separations of nucleotides, nucleosides and nucleobases: analysis of biological samples in health and disease." J Chromatogr 618(1-2): 3-14.

Yin, B., R. M. Whyatt, et al. (1995). "Determination of 8-hydroxydeoxyguanosine by an immunoaffinity chromatography-monoclonal antibody-based ELISA." Free Radic Biol Med 18(6): 1023-32.

CHAPTER TWO

A mechanism for the production of oxidized guanosine 5'-triphosphate (oxo^{8}GTP): hydroxyl radical production by a GTP-Cu(II) complex in the presence of L-ascorbic acid

Abstract

Levels of oxidized guanosine (G) base in DNA have become a hallmark biomarker in assessing oxidative stress implicated in a variety of disease and toxin-induced states. However, there is evidence that the G in the nucleotide triphosphate pool (GTP) is more susceptible to oxidation than Gs incorporated into nucleic acids and this causes a substantial amounts of the oxidized product, 8-oxoguanosine 5'-triphosphate (oxo^{8}GTP), to accumulate in cell-free and in cell culture preparations. Electron paramagnetic resonance (EPR) spectroscopy and direct EPR analysis of free radical production by copper sulfate and L-ascorbic acid demonstrates that the hydroxyl radical ($^{\bullet}$OH) is produced via oxidation of Cu^{+} to Cu^{2+} while in a complex with GTP. This $^{\bullet}$OH production is dependent on the availability of oxygen and the presence of GTP in the reaction milieu. Verification of free radical-mediated production of oxo^{8}GTP is presented using HPLC with electrochemical (EC) detection and matrix-assisted laser desorption/ionization linear time-of-flight mass spectrometry (MALDI-LTOF-MS). The sum of these results is presented in a novel mechanism of GTP oxidation by Cu^{2+} and L-ascorbic acid. A better understanding of the chemistry involved in this oxidative modification of GTP facilitates a more comprehensive understanding of its potential physiological consequences.

Introduction

Oxidative stress is defined as the deleterious impact on cell function or viability as a consequence of the loss in balance between reactive oxygen species (ROS) and antioxidants in the cellular milieu (Sies 1991). ROS are formed continuously as a result of normal cellular respiration, enzymatic metabolism, and exogenous insults (Halliwell and Gutteridge 1986). An excess of ROS is known to induce damage to DNA and the cellular nucleotide pool, yielding DNA strand breaks as well as specific oxidized bases in DNA. 8-oxo-7,8-dihydro-2`-deoxyguanosine ($oxo^{8}dG$) is the most prevalent form of oxidative base modifications produced by the reaction of a hydroxyl radical ($^{\bullet}OH$) at the C8 position of 2`-deoxyguanosine (dG) incorporated into DNA or in the guanine incorporated in the cytosolic nucleotide triphosphates form (dGTP and GTP) (Hayakawa, Taketomi et al. 1995; Einolf, Schnetz-Boutaud et al. 1998; Russo, Blasi et al. 2004). The nucleotide pool has been recently been investigated as a significant target for oxidative stress given that GTP is more accessible for $OH^{\bullet}$-mediated oxidative modification than the deoxynucleoside form, dG, incorporated into DNA (Svoboda and Harms-Ringdahl 1999; Haghdoost, Sjolander et al. 2006; Bolin and Cardozo-Pelaez 2007). Substantial evidence has been presented that much of the biologically relevant oxidation occurs in the cytosol at the nucleotide pool level (Haghdoost, Sjolander et al. 2006).

GTP comprises nearly 25% of the intracellular nucleotide triphosphate pool, it acts as a versatile nucleotide participating in many critical physiological functions including RNA synthesis, cell signaling through activation of GTP-binding proteins, as well as the production of the second messenger cyclic guanosine monophosphate (cGMP) (Strader, Fong et al. 1994). It has been previously shown that $^{\bullet}OH$ is produced by

electron transfer by Fe(II), Fe(III), and Cu(II) complexed with nucleotide triphosphates such as GTP in the presence of the abundant cellular reductant ascorbate (Biaglow, Held et al. 1996). Additionally, such Cu complexes are known to affect signal transduction by interfering with second messenger systems, and depending on their concentration and the target, these Cu complexes may be a major factor influencing cell survival or cell death responses (Filomeni, Rotilio et al. 2005; Filomeni, Cerchiaro et al. 2007). Oxidation to the GTP pool produces the oxidized adduct 8-oxoguanosine 5'-triphosphate (oxo^{8}GTP) (Figure 3). It is unknown how the increase in $^{\bullet}$OH by Cu complexes such as Cu(II)-GTP in the presence of reductants might effect the various cellular targets of GTP either directly or indirectly due to the oxidation of GTP itself. Despite the high cellular abundance of GTP and the availability of Cu, the specific mechanism of $^{\bullet}$OH production by GTP in the presence of Cu(II) and ascorbate has not been investigated.

Copper is contained within all respiring tissues as an essential trace element, a micronutrient essential for cell survival, as well as a cofactor for several metalloenzymes (e.g. Cu,Zn-SOD, cytochrome c oxidase) (Kaim and Rall 1996; Solomon, Sundaram et al. 1996). However, in some pathological conditions, copper homeostasis is lost and the toxicological consequences have been ascribed to its potential to act as a catalyst for oxidative damage by redox cycling between univalent (Cu(I)) and divalent (Cu(II)) oxidation states (Klomp, Lin et al. 1997; Rossi, Lombardo et al. 2004; Rossi, Arciello et al. 2006). In particular, redox cycling in the presence of partially reduced oxygen species such as hydrogen peroxide (H_20_2) and superoxide anion ($O_2^{\bullet -}$) is believed to result in the generation of the highly reactive and damaging $^{\bullet}$OH via the Haber-Weiss cycle (eq. 1-3) [15]. Hence, the copper ion has been highly implicated in ROS-mediated damage in the

high concentrations that occur in diseases such as Alzheimer's Disease, familial amyotrophic lateral sclerosis, and Creutzfeldt-Jacob Disease (Rossi, Arciello et al. 2006).

$$Cu^{2+} + H_2O_2 \rightarrow Cu^{+} + O_2^{\bullet -} \quad (1)$$

$$2\ O_2^{\bullet -} + 2H^{+} \rightarrow H_2O_2 + O_2 \quad (2)$$

$$Cu^{+} + H_2O_2 \rightarrow Cu^{2+} + {}^{\bullet}OH + {}^{-}OH \quad (3)$$

The goal of this study is to identify the free radical chemistry of $^{\bullet}OH$ production by Cu(II) complexed with GTP in the presence of ascorbate. In order to assess the mechanism by which copper ions catalyze the oxidation of GTP in the presence of L-ascorbic acid, we detected the generation of ROS by EPR spin trapping. We also evaluated the influence of pH, copper and GTP concentration, and oxygen consumption on the production of $^{\bullet}OH$ and oxo^{8}GTP along with verification of the Cu(II)-GTP complex formed during the oxidation process. Our results are compiled to propose a mechanism for this reaction.

Materials and Methods

Materials

All reagents were purchased from Sigma-Aldrich (St. Louis, MO), Merck & Co. Inc. (Whitehouse Station, NJ) or Fisher Scientific (Pittsburgh, PA) and were analytical grade or better. 8-oxoguanosine-5'-triphosphate (oxo^{8}GTP) was purchased from TriLink Biotechnologies (San Diego, CA). 8-oxoguanosine (oxo^{8}G) was obtained from Cayman Chemical (Ann Arbor, MI). Cu(II) isatin-diimine complex [Cu(Imine)] used in the control reaction was synthesized by condensation reaction of the amine ligand 2-aminoethyl pyridine with isatin, followed by metallation with Cu(II) ions added as perchlorate salt, according to the procedures in the literature (Cerchiaro, Aquilano et al. 2005). All buffers were pre-treated with Chelex-100 to remove metal ion contamination. All solutions were prepared with distilled water purified in Milli-Q UF-Plus apparatus (Millipore Corp., Bedford, MA).

EPR Spin-Trapping Instrument Conditions

Electronic spectra were recorded on a Shimadzu 1500 spectrophotometer with temperature regulated cell compartment. EPR spectra were recorded in a Bruker EMX Plus Electron-Spin Resonance Spectrometer System instrument, operating at X-band frequency. We utilized standard Wilmad quartz tubes maintained at 77 K for frozen solutions or a flat 200 μL quartz cell for spin trapping experiments at room temperature. DPPH (α,α′-diphenyl-β-picrylhydrazyl) was used as frequency calibrant (g = 2.0036) with samples in frozen water solution at 77 K. Typical conditions used in these measurements were 2.00 x 10^{4} gain, and 10 G modulation amplitude.

Reaction Conditions for EPR Analysis

To examine the production of radicals during the incubations of copper, GTP and ascorbic acid, EPR spin trapping experiments were performed utilizing 5,5-dimethylpyrroline N-oxide (DMPO) as a spin trap. A typical incubation mixture contained 10 μM copper sulfate ($CuSO_4.5H_2O$), 1 mM GTP, and 1 mM L-ascorbic acid maintained in phosphate buffered acid solution (pH 4). Reactions were diluted in 10mM phosphate buffered saline (PBS) with the addition of 80 mM DMPO, pH 7.4. The reaction mixtures were monitored over several time points between one and 30 minutes. The spectra were recorded at room temperature (22 ± 1 °C) on a Bruker EMX Plus Electron-Spin Resonance Spectrometer System instrument at X-Band equipped with a high sensitivity cavity (4119HS). The magnetic field and the quantification of radical production were measured with a standard aqueous solution of 4-hydroxy-2,2,6,6-tetrametyl-1-piperidiniloxy (TEMPOL, $g = 2.0056$). All EPR spin trapping experiments were conducted in replicates of three.

Oxymetry Conditions

Oxygen measurements were carried out in a GILSON oxygraph apparatus (Medical Electronics Inc. USA). A Clark platinum electrode was used as an O_2 probe with an internal reference probe containing a Ag/AgCl solution and a YSI membrane (Yellow Spring Instruments, Yellow Sprins, OH). A saturated KCl solution was maintained between the electrode and the membrane. A 1.5 mL volume standard cell was utilized in these experiments enclosed with a capillary cap, ensuring no oxygen was exchanged with the atmosphere, and incubated in a water bath maintained at 22.0 ± 0.2 °C with constant stirring. Sodium dithionite was used to calibrate the oxygraph. Oxymetry experiments were conducted in replicates of three.

Quantification of Oxo^{8}GTP by HPLC-EC

Oxo^{8}GTP was quantified using HPLC-EC with preparative dephosphorylation as described previously (Bolin and Cardozo-Pelaez 2007). A typical reaction contained 10 μM Cu(II) sulfate, 1mM GTP, and 1 mM L-Ascorbic Acid diluted in PBS, pH 7.4 exactly as described above. Incubations were maintained at 37ºC for four hours. Oxo^{8}GTP was then dephosphorylated to it's nucleoside form, 8-oxoguanosine (oxo^{8}G), for detection via HPLC-EC. On ice, 25 Units of alkaline phosphatase (dissolved in Tris-HCl pH 8.0), 1.8 mM sodium acetate, and 100 mM Tris-HCl, were added to 10 μL of sample in total volume of 10 μL. After incubation at 37ºC for 1 hour, the dephosphorylation reaction was stopped by placing on ice. This was followed by filtering through Ultrafree-MC (30-kD) tubes (Millipore Corp., Bedford, MA). Detection of the generated nucleoside oxo^{8}G was carried out by injecting 10 μL of the filtrate into the HPLC. Oxo^{8}G was resolved by HPLC with a reverse phase YMC basic column (4.6 x 150 mm; particle size 3-micron) (YMC Inc., Wilmington, NC) and quantified using a CoulArray electrochemical detection (EC) system (ESA, Inc., Chelmsford, MA). An isocratic mobile phase consisting of 100 mM sodium acetate, pH 5.2, 4% Methanol (HPLC Grade) diluted in water polished with C18 Sep-Pak cartridges (Waters Corp., Milford, MA) was utilized to elute oxo^{8}G from the column. The mobile phase was filtered using 0.2 μm nylon filters and degassed by sonication before use with the HPLC. Potentials of the twelve coulometric analytical cells of the CoulArray system, placed in series, were as follows: 50, 125, 175, 200, 250, 380, 500, 700, 785, 850, 890, 900 mV. Data were recorded, analyzed, and stored using CoulArray for Windows data analysis software (ESA Inc., Chelmsford, MA). Oxo^{8}G was monitored in the 250 mV channel and injected amounts

were graphed relative to peak area. A calibration curve for oxo^{8}G was generated from known quantities ranging from 10.0 picomoles to 500 picomoles. Oxo^{8}G quantified in reactions were reported as oxo^{8}GTP.

Verification of Oxo^{8}GTP formation by MALDI-LTOF

GTP reactions and standards were analyzed using negative-mode, matrix-assisted laser desorption/ionization linear time-of-flight mass spectrometry (MALDI-LTOF-MS) as previously described with minor modifications (Edwards and Kennedy 2005). Standards and reaction mixtures diluted in methanol were mixed in a 1:1 ratio with 9 mg/mL of 9-aminoacridine (9-AA) matrix in acetone for deposition. An aliquot of 1 μL of these mixtures were deposited onto a single spot on a 96-well, stainless steel (SS), MALDI sample plate and allowed to dry at room temperature (Applied Biosystems, Foster City, CA). Analysis was performed using a Voyager-DE Pro MALDI-TOF mass spectrometer using the negative linear mode of operation (Applied Biosystem, Foster City, CA). The following settings were used for each analysis: accelerating voltage of 20,000V, acquisition mass range between 60 and 600 Dalton, laser intesity of 2000, and laser repetition rate of 20.0Hz. Data was acquired with 50 laser shots/spectrum. Spectra were analyzed using Data Exploreer Version 4.0.0.0 (Aplied Applied Biosystem, Foster City, CA). The oxo^{8}GTP analyte was confirmed by comparing spectra to standard preparations of purified oxo^{8}GTP and GTP.

Statistical Analysis

All data were analyzed using GraphPad 4.0 software (GraphPad Software Inc., San Diego, CA). A one-way ANOVA with a Newman–Keuls multiple comparison test post-

hoc analysis was performed on the oxo^{8}GTP data presented; values denoted with an asterisk are significantly different from their corresponding control ($p < 0.05$).

Results

Production of $^{\bullet}$OH by Cu(II)-GTP

Figure 12 shows representative EPR spectra from reactions of GTP and copper sulfate diluted in PBS at pH 7.4 in the presence of equimolar L-ascorbic acid. A constant ascorbyl radical background signal was detected in control experiments containing only L-ascorbic acid and DMPO (Figure 12, spectra A-B).

FIGURE 12

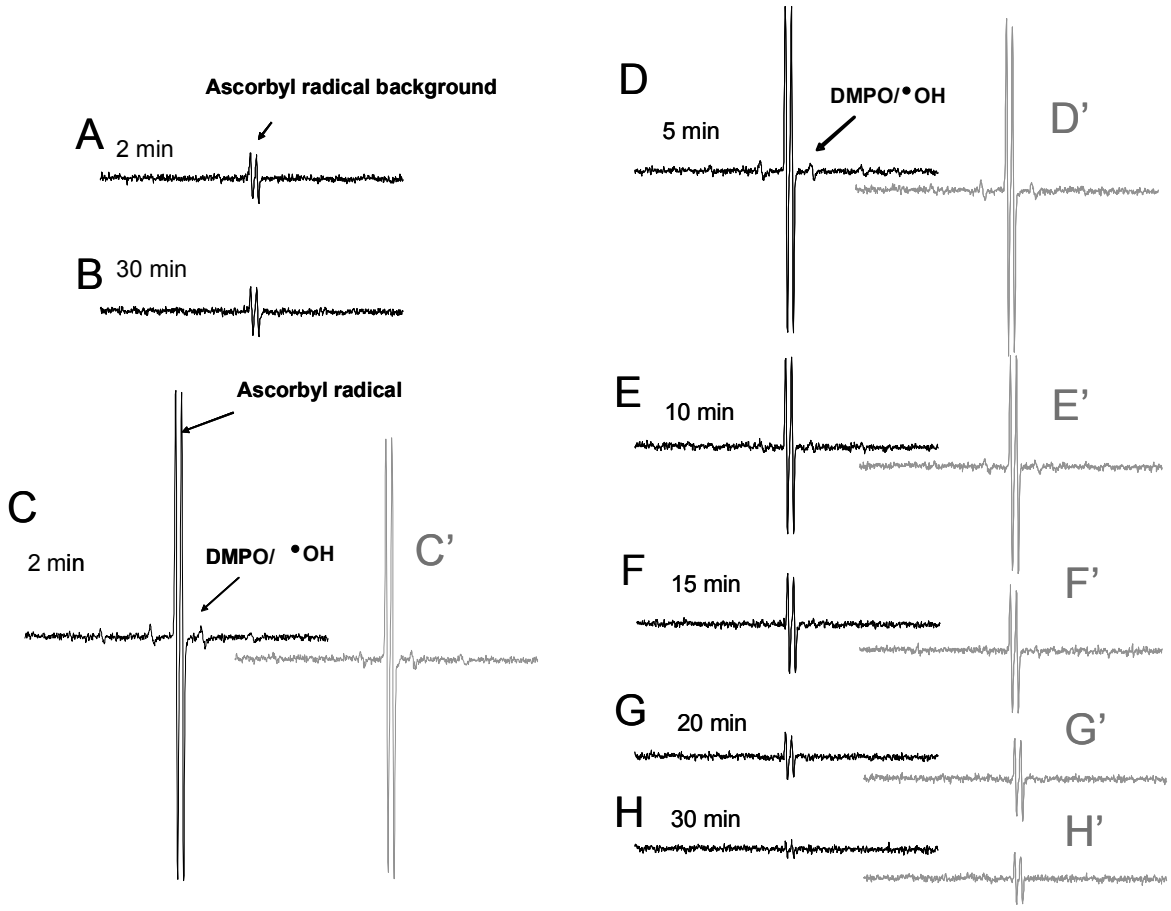
Ascorbyl radical background
A
2 min
B
30 min
Ascorbyl radical
C
2 min
DMPO/ •OH
C'
D
5 min
DMPO/•OH
D'
E
10 min
E'
F
15 min
F'
G
20 min
G'
H
30 min
H'

Figure 12. EPR spectra of GTP, L-ascorbic acid, and Cu(II)

A) and **B**) EPR spectra of control experiments in PBS, pH =7.4, 1 mM L-ascorbic acid, and 80mM DMPO incubated for 2 min (A) and 30 min (B). **C**) to **H**) EPR spectra of reactions of 1 mM GTP, 1 mM L-ascorbic acid, 10 μM Cu(II) sulfate, and 80mM DMPO in air-saturated PBS, pH 7.4 solution. **C'**) to **H'**) EPR spectra of reactions exactly as in C to H, with the exception that the PBS pH 7.4 solution is devoid of oxygen by saturation with argon for 30 minutes. All spectra were collected at room temperature (22 °C) and plotted on the same scale (magnetic field and intensity of EPR) for comparison. EPR conditions: receiver gain 5.02 x 10^4, modulation amplitude 1 G, time constant 163.84 ms, frequency 9.687 GHz, power 20 mW and 1024 points resolution.

Interestingly, in our reactions under experimental conditions (copper/GTP/L-ascorbic acid) the signal from the ascorbyl radical increased in the first 2-5 minutes and then decreased over the course of 30 minute incubation (Figure 12, spectra C to H). We also confirmed the initial formation of DMPO/$^{\bullet}$OH adduct, characterized by $a_N = a_H$ EPR hyperfine parameters of 14.9 G (Figure 12, spectra C). After 10 minutes, this signal is no longer detected (Figure 12, spectrum E). The relatively small signal from DMPO/$^{\bullet}$OH is due to the low concentration of GTP and Cu(II) ion. We also performed experiments under low oxygen conditions by bubbling Argon into the solution during the 30 minute incubation as well into all stock solutions included in the reactions (Figure 12, spectra C' to H'). This resulted in a lower concentration of DMPO/$^{\bullet}$OH adduct at the early time points of incubation, and greater ascorbyl radical detection at later time points as compared to PBS and stock solutions saturated in atmospheric oxygen (Figure 12, spectrum C' to H'). This finding indicates that oxygen participates directly in the reaction mechanism. Low oxygen concentration resulted in a slower extinction of the ascorbyl radical and a decrease in $^{\bullet}$OH production as compared to reactions saturated in higher, atmospheric oxygen. Hydroxyl radicals react with dimethyl sulfoxide (DMSO) at a high velocity with second order rate constant of about 10^9 M^{-1} s^{-1}, generating a methyl radical trapped by DMPO (DMPO/$^{\bullet}CH_3$) (Figure 13) (Zhang, Joseph et al. 2000).

FIGURE 13

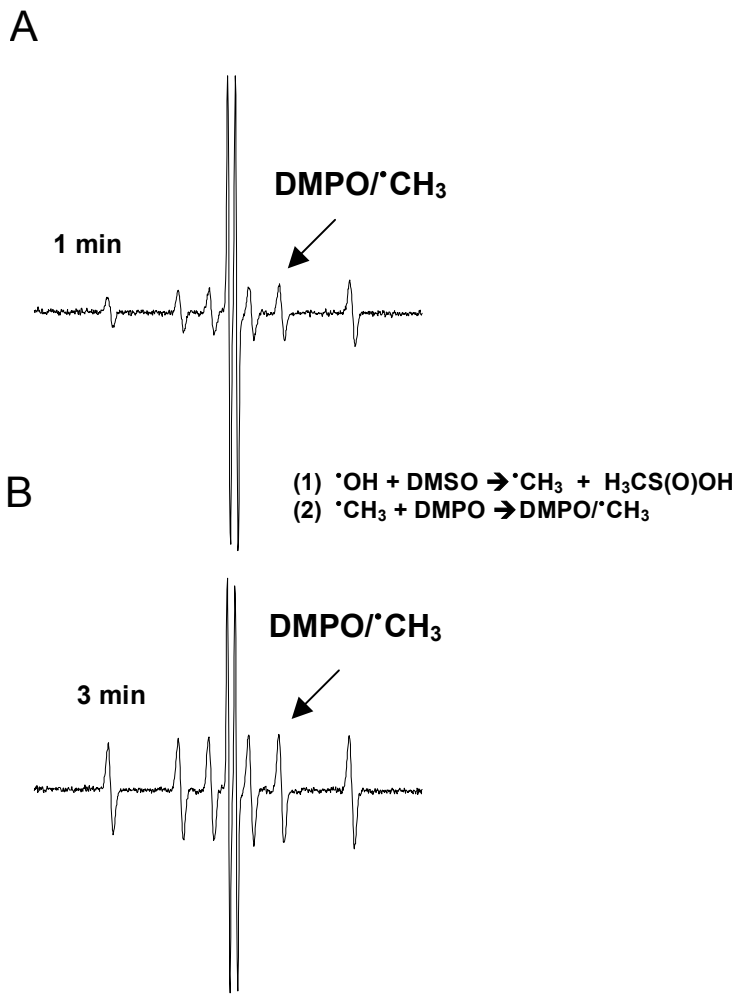
A
DMPO/˙CH3
1 min
B
(1) ˙OH + DMSO → ˙CH3 + H3CS(O)OH
(2) ˙CH3 + DMPO → DMPO/˙CH3
DMPO/˙CH3
3 min

Figure 13. EPR spectra of GTP, L-ascorbic acid, and Cu(II) with DMSO

Experiment conducted in PBS, pH =7.4, 1mM L-ascorbic acid, and 80 mM DMPO incubated for 1 min (A) or 3 min (B). EPR conditions: receiver gain 5.02 x 10^4, modulation amplitude 1 G, time constant 163.84 ms, frequency 9.687 GHz, power 20 mW and 1024 points resolution.

To confirm the formation of •OH, DMSO was added into the incubations mixtures and the DMPO/•CH_3 adduct (a_N = 16.4 G and a_H = 23.4 G) was detected while the ascorbyl radical signal remained unchanged (Figure 13).

To compare the differences in the radical generation during GTP oxidation, between Cu(II) ion free in solution and Cu complexed with GTP, an organic Cu(II) complex [Cu(Imine)] was used as model of a stable Cu(II) complex in the reaction. In these experiments, the Cu(II) sulfate solution was substituted with Cu(Imine) which contains an imine ligand derivate from the oxindole isatin (Cerchiaro, Aquilano et al. 2005; Filomeni, Cerchiaro et al. 2007). The resulting EPR spectra from spin trapping experiments were very similar to those using Cu(II) sulfate as a catalyst. This suggests that the Cu(II) ion in this reaction is complexed and the electron recycling between Cu(II) and Cu(I) is facilitated while in this complex (data not shown).

Control experiments were also performed in order to identify the individual influence of copper, ascorbic acid and GTP on the production of •OH (Figure 14).

FIGURE 14

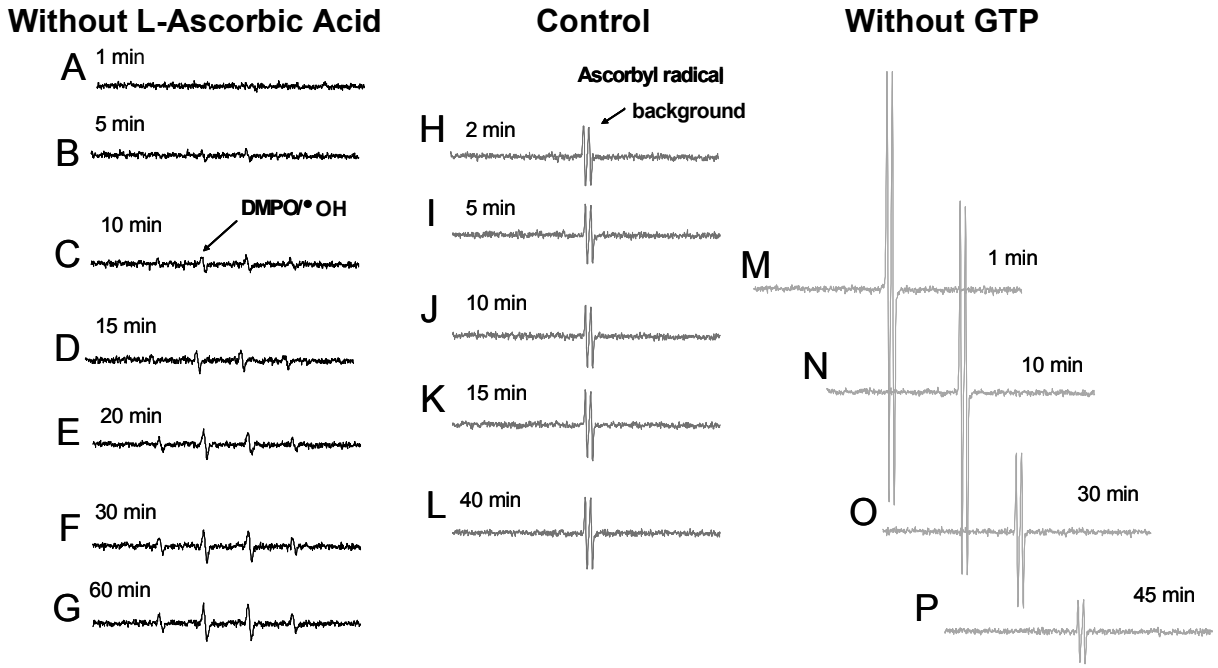
Without L-Ascorbic Acid
Control
Without GTP
A
1 min
B
5 min
C
10 min
DMPO/•OH
D
15 min
E
20 min
F
30 min
G
60 min
Ascorbyl radical
background
H
2 min
I
5 min
J
10 min
K
15 min
L
40 min
M
1 min
N
10 min
O
30 min
P
45 min

Figure 14. EPR spectra of GTP and Cu(II) or L-ascorbic acid

A) to **G**) EPR spectra of the reaction of 1mM GTP, 10 μM Cu(II) sulfate, and 80 mM DMPO in air-saturated PBS, pH=7.4 solution (without L-ascorbic acid). **H**) to **L**) EPR spectra of the reaction of 1 mM GTP, 1 mM L-ascorbic acid, and 80 mM DMPO in air-saturated PBS, pH 7.4 solution (control). **M**) to **P**) EPR spectra of the reaction of 1mM L-ascorbic acid, 10 μM Cu(II) sulfate, and 80 mM DMPO in air-saturated PBS, pH=7.4 solution (without GTP). All spectra were collected at room temperature (22 °C) and plotted on the same scale (magnetic field and intensity of EPR) for comparison. EPR conditions: receiver gain 5.02 x 10^4, modulation amplitude 1 G, time constant 163.84 ms, frequency 9.687 GHz, power 20 mW and 1024 points resolution.

In reactions without the reducing agent L-ascorbic acid, production of the DMPO/•OH adduct starts at time points beginning at 10 minutes, rises slowly, and persists for about 1 hour (Figure 14, spectra A to G). This demonstrates that the L-ascorbic acid rapidly regenerates the Cu(II) species from Cu(I) formed during the reaction, resulting in a major production of •OH in the beginning of the reaction (Figure 14, spectra 2C). In the absence of Cu(II) ions, there is no detectable •OH formed , and the time course and amplitude of the ascorbyl radical is exactly as control reactions containing L-ascorbic acid in PBS solution alone (Figure 14, spectra H to L and Fig. 1, spectra A). Without the substrate GTP, we observed only the high-amplitude ascorbyl radical peak due to recycling with the copper ions. This diminishes over time in a similar fashion as reactions containing GTP (Figure 14, spectra M to P and Fig. 1, spectra D to H).

With the aim of evaluating the effect of pH on •OH formation, we also analyzed reactions at pH 7.0 and pH 5.7 (Figure 15).

FIGURE 15

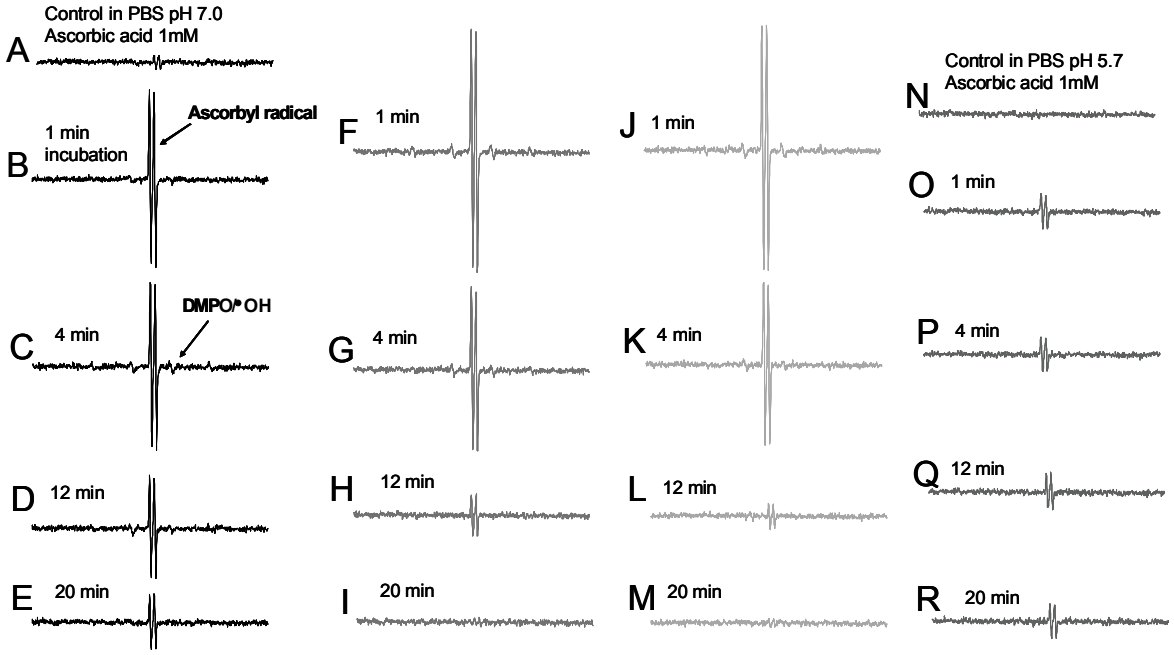
Control in PBS pH 7.0
Ascorbic acid 1mM
A
1 min
incubation
B
Ascorbyl radical
C
4 min
DMPO/•OH
D
12 min
E
20 min
F
1 min
G
4 min
H
12 min
I
20 min
J
1 min
K
4 min
L
12 min
M
20 min
Control in PBS pH 5.7
Ascorbic acid 1mM
N
O
1 min
P
4 min
Q
12 min
R
20 min

Figure 15. Effects of pH and reactant concentrations on free radical generation

A) and **N**) EPR spectra of 1 mM L-ascorbic and 80 mM DMPO in PBS, pH 7.0 (A) and PBS, pH 5.7 (N); **B**) to **E**) EPR spectra of the reaction of 1 mM GTP, 1 mM L-ascorbic acid, 10 μM Cu(II) sulfate, and 80 mM DMPO, in air-saturated PBS, pH 7.0 solution. **F**) to **I**) EPR spectra of the reaction of 2 mM GTP, 1 mM L-ascorbic acid, 30 μM Cu(II) sulfate, and 80 mM DMPO, in air-saturated PBS, pH=7.0 solution. **J**) to **M**) EPR spectra of the reaction of 3 mM GTP, 1mM L-ascorbic acid, 40 μM Cu(II) sulfate, and 80 mM DMPO, in air-saturated PBS, pH 7.0 solution. **O**) to **P**) EPR spectra of the reaction of 1 mM GTP, 1 mM L-ascorbic acid, 10 μM Cu(II) sulfate, and 80 mM DMPO, in air-saturated PBS, pH 5.7 solution. All spectra were collected at room temperature (22 °C) and plotted on the same scale (magnetic field and intensity of EPR) for comparison. EPR conditions: receiver gain 5.02 x 10^4, modulation amplitude 1 G, time constant 163.84 ms, frequency 9.687 GHz, power 20 mW and 1024 points resolution.

The production of both the ascorbyl radical and the DMPO/•OH adduct were decreased by lowering the pH of the PBS in the reaction solution from control, pH 7.4, to pH 7.0 and pH 5.7 (Figure 12, Figure 15, spectra A to E and N to R). We also evaluated the effects of varying Cu(II) and GTP concentrations in solution on radical formation. Spectra F to I and J to M are from reactions containing 1 mM L-ascorbic acid and 2 mM GTP/30 μM Cu(II) sulfate and 3 mM GTP/40 μM Cu(II) sulfate respectively (Figure 15, Spectra F to I and J to M). Increased concentrations of GTP and Cu(II) sulfate allowed for the reactions to proceed faster as compared to reactions with 1mM GTP and 10 μM Cu(II) sulfate, as demonstrated by the disappearance of the ascorbyl radical after 20 minutes (Figure 15, Spectra I and M).

Cu(II)-GTP complex

We performed direct EPR and UV-vis analysis of Cu(II) sulfate in PBS solution and Cu(II) sulfate combined with GTP and detected changes in the Cu(II) center which indicate a complexation of Cu(II) with GTP (Figure 16).

FIGURE 16

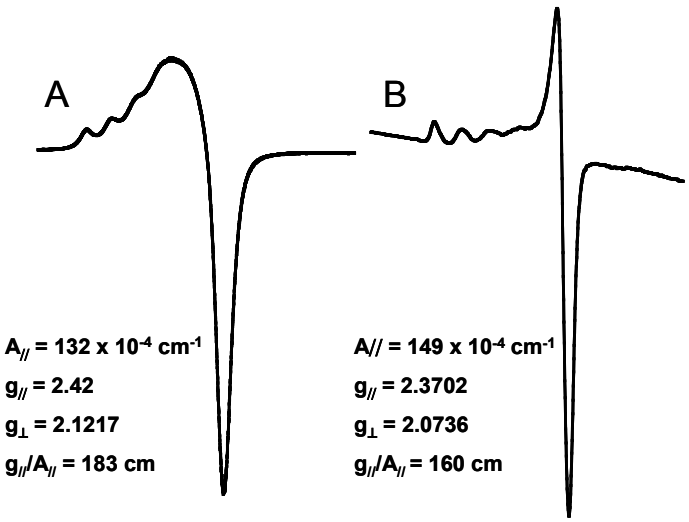
A
B
$A_{//}$ = 132 x 10^{-4} cm^{-1}
$g_{//}$ = 2.42
$g_{\perp}$ = 2.1217
$g_{//}/A_{//}$ = 183 cm
A// = 149 x 10^{-4} cm^{-1}
$g_{//}$ = 2.3702
$g_{\perp}$ = 2.0736
$g_{//}/A_{//}$ = 160 cm

Figure 16. Direct EPR analysis of Cu(II) and GTP

A) EPR spectrum of 2 mM Cu(II) sulfate. **B**) EPR spectrum of 500 μM Cu(II) sulfate with 2 mM of GTP. All solutions diluted in water, PBS, and 5% glycerol. EPR conducted at 77K.

EPR spectra of Cu(II) sulfate in PBS solution and Cu(II) sulfate combined with GTP were collected from frozen solutions of each and showed a characteristic profile of an axial environment around the Cu(II) center, as shown by the relationship of the electron g-factors (g) $g_{//} > g_{\perp}$ (Figure 16, A-B). However, it was observed that a great structural change on the Cu(II) center took place in the presence of GTP in solution. Specifically, the EPR hyperfine parameters $A_{//}$, $g_{//}$ and $g_{\perp}$ changed from 132 x 10^{-4} cm^{-1}, 2.42 and 2.1217 respectively, in an aqueous solution of Cu(II) sulfate, to 149 x 10^{-4} cm^{-1}, 2.37 and 2.0736 respectively, in solution where GTP was present (Figure 16, A-B). Additionally, electronic spectra of Cu(II) sulfate alone and in the presence of GTP carried out under the same conditions of EPR analysis, showed a slight change on d-d absorption band (data not shown).

Oxygen consumption

To confirm the participation of molecular oxygen in the GTP oxidation we monitored oxygen consumption in reaction of GTP, Cu(II) sulfate, and L-ascorbic acid using a Clark electrode. Figure 17 shows representative curves of O_2 consumption when either Cu(II) sulfate or Cu(II) imine are added as the Cu(II) catalysts in solutions containing GTP and L-ascorbic acid. Oxygen consumption over time was very similar for the two Cu(II) compounds which indicates that Cu(II) sulfate acts as a stable complex in solutions with GTP.

FIGURE 17

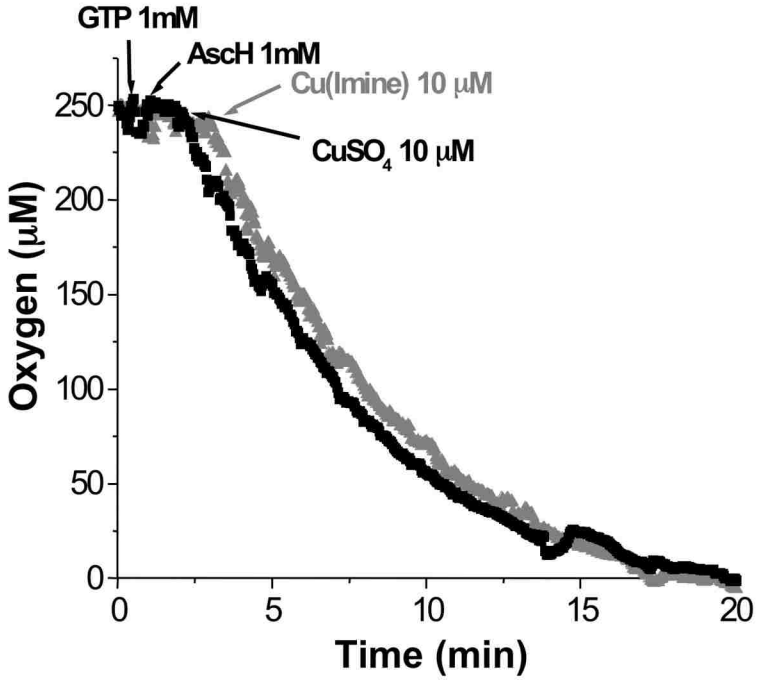
GTP 1mM
AscH 1mM
Cu(Imine) 10 μM
CuSO4 10 μM
Oxygen (μM)
250
200
150
100
50
0
0
5
10
15
20
Time (min)

Figure 17. Oxygen consumption by GTP, Cu(II), and L-ascorbic acid

Oxygen measurements using a Clark electrode of the reaction of 1 mM GTP, 1 mM L-ascorbic acid, 10 μM Cu(II) sulfate (■) or Cu(Imine) (▲), in air-saturated PBS, pH 7.4 solution in a total cell volume of 1.5 mL at (22.0 ± 0.2) °C.

Total consumption of O_2 was observed within approximately 20 minutes. This corroborates the EPR spin trapping results presented in Figure 12 which shows that the DMPO/•OH adduct formed during the reaction is undetectable and the ascorbyl radical is at background levels after 20 minutes.

Oxo^{8}GTP production

In order to verify and quantify the levels of oxo^{8}GTP produced by the copper/GTP/L-ascorbic acid system, we utilized HPLC-EC and MALDI-TOF. Figure 18 includes representative chromatograms and spectra from four-hour incubations at 37^{o}C of GTP under control conditions (1 mM L-ascorbic acid), incubations of GTP with10 μM Cu(II) sulfate only, and incubations of GTP with both L-ascorbic acid and Cu(II) sulfate.

FIGURE 18

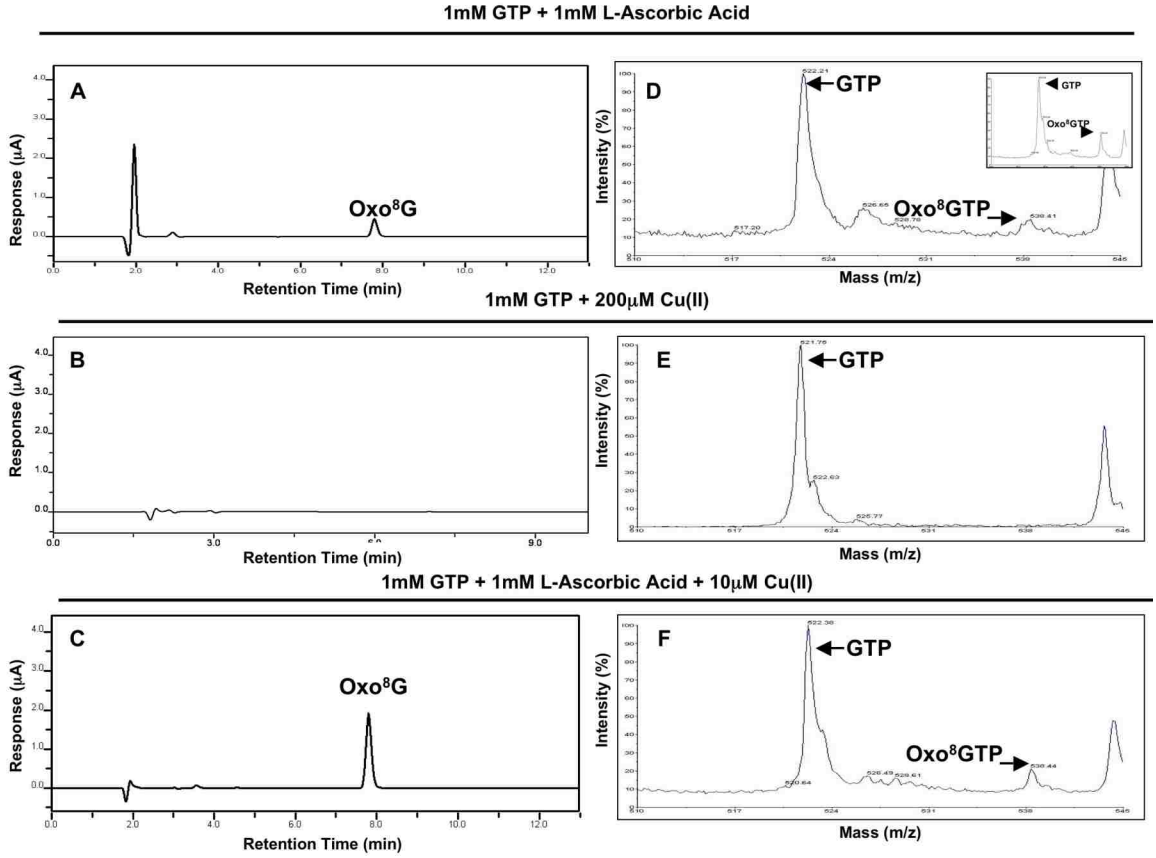
1mM GTP + 1mM L-Ascorbic Acid
A
Response (μA)
Oxo8G
Retention Time (min)
D
Intensity (%)
GTP
Oxo8GTP
Mass (m/z)
1mM GTP + 200μM Cu(II)
B
Response (μA)
Retention Time (min)
E
Intensity (%)
GTP
Mass (m/z)
1mM GTP + 1mM L-Ascorbic Acid + 10μM Cu(II)
C
Response (μA)
Oxo8G
Retention Time (min)
F
Intensity (%)
GTP
Oxo8GTP
Mass (m/z)

Figure 18. Oxo^{8}GTP formation analysis by HPLC-EC and MALDI-TOF

A) and D) are HPLC-EC chromatogram and MALDI-TOF spectra of oxo^{8}G (reported as oxo^{8}GTP, see Methods) and GTP respectively, in a four-hour incubation of 1 mM GTP and 1 mM L-ascorbic acid at 37^{o}C. Inset of D) is from a standard solution containing 1:1 GTP:Oxo^{8}GTP. **B) and E)** is a four-hour incubation of 1mM GTP and 200 μM Cu(II) sulfate at 37^{o}C. **C) and F)** is a four-hour incubation of 1mM GTP, 1mM L-ascorbic acid, and 10 μM Cu(II) sulfate at 37^{o}C. HPLC-EC chromatograms show traces collected at 250 mV EC channel. MALDI-TOF spectra are normalized to % Intensity of signal and baselines were corrected for noise.

The highest levels of oxo^{8}GTP, approximately 430 picomoles, were produced with a four-hour incubation of 1 mM GTP with both 1 mM L-ascorbic acid and 10 μM Cu(II) sulfate (Figure 18C and 19C). L-ascorbic acid alone was able to oxidize GTP due to the presence of the ascorbyl radical confirmed by EPR analysis although the oxo^{8}GTP produced was four times lower than incubations that included 10 μM Cu(II) sulfate (Figure 18A and 19C).

FIGURE 19

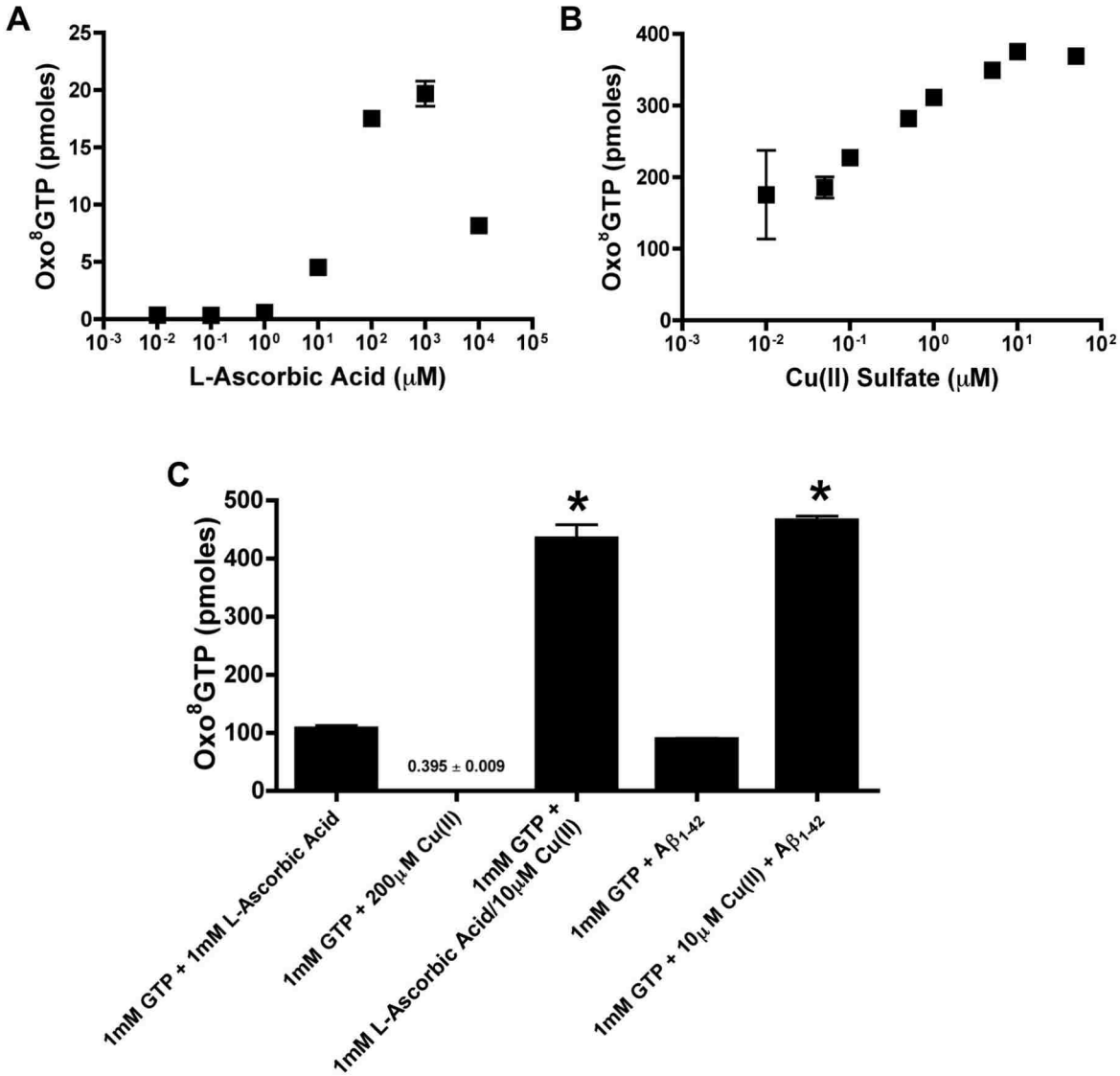
A
Oxo8GTP (pmoles)
25
20
15
10
5
0
10-3 10-2 10-1 100 101 102 103 104 105
L-Ascorbic Acid (μM)
B
Oxo8GTP (pmoles)
400
300
200
100
0
10-3 10-2 10-1 100 101 102
Cu(II) Sulfate (μM)
C
Oxo8GTP (pmoles)
500
400
300
200
100
0
0.395 ± 0.009
*
*
1mM GTP + 1mM L-Ascorbic Acid
1mM GTP + 200μM Cu(II)
1mM GTP + 1mM L-Ascorbic Acid/10μM Cu(II)
1mM GTP + Aβ1-42
1mM GTP + 10μM Cu(II) + Aβ1-42

Figure 19. Oxo^{8}GTP in GTP, Cu(II), L-ascorbic acid and A$\beta_{1\text{-}42}$ reactions

A) Oxo^{8}GTP levels quantified by HPLC-EC in one-hour incubations of 1mM GTP and increasing concentrations of L-ascorbic acid. **B)** Oxo^{8}GTP levels quantified by HPLC-EC in four-hour incubations of 1 mM GTP, 1 mM L-ascorbic acid, and increasing concentrations of Cu(II) sulfate. **C)** Oxo^{8}GTP levels quantified by HPLC-EC in four-hour incubations of 1 mM GTP and 1 mM L-ascorbic acid, 200 μM Cu(II) sulfate, 1mM L-ascorbic acid/ 10 μM Cu(II) sulfate, 100 nM A$\beta_{1\text{-}42}$, and 10 μM Cu(II) sulfate/100 nM A$\beta_{1\text{-}42}$ at 37^{o}C. Data represent mean ± SEM. *n= 2-9.* * $p < 0.05$ applying a one-way ANOVA with Newman-Keuls Multiple Comparison Test post-hoc analysis.

However, oxo^{8}GTP is undetectable in incubations of GTP with10 μM Cu(II) sulfate alone in the μAmpere (μA) scale used to report oxo^{8}GTP under control and 1 mM-ascorbic acid/10 μM Cu(II) sulfate conditions (Figure 8B). When quantified using the nanoampere (nA) scale, oxo^{8}GTP levels in incubations without 1 mM L-ascorbic acid are detectable although three orders of magnitude lower than those that include the reductant in the presence of 10 μM Cu(II) sulfate (Figure 19C). These results confirm the EPR analysis of GTP incubations where the highest levels of the most oxidizing radical •OH were observed in reactions that included both L-ascorbic acid and copper. MALDI-TOF spectra confirmed the presence of oxo^{8}GTP in these four-hour incubations (Figure 18, D to F). Mass to charge (m/z) ratios for standard mixtures of GTP and oxo^{8}GTP were 522.20 and 538.33 respectively, which were also detected in our incubations of GTP under control (1 mM L-ascorbic acid) and 1 mM L-ascorbic acid/10 μM Cu (II) sulfate conditions.

L-ascorbic acid alone was able to increase oxo^{8}GTP levels in a dose-dependent manner during one-hour incubations at 37^{o}C with the highest oxidation seen at 1 mM and a decrease in oxo^{8}GTP observed at concentrations of 10 mM (Figure 19A). Increasing concentrations of Cu(II) sulfate in the presence of 1 mM L-ascorbic acid also dose-dependently increased oxo^{8}GTP levels reaching the highest values at 10 μM with no additional oxidation seen at 100 μM (Figure 19B).

To emphasize the specificity of our oxo^{8}GTP-generating system, we included another endogenous biological oxidant, the aggregated peptide found in the senile plaques of AD brains, amyloid beta peptide ($A\beta_{1-42}$). Our results included in Figure 19

indicate that $A\beta_{1-42}$ alone is not capable of producing ROS at a level that oxidizes GTP to a detectable degree.

Mechanism proposed

The results presented herein indicate a mechanism involving ROS and the ascorbyl radical in the oxidation of GTP by copper. As shown in the proposed mechanism in Figure 20, key factors in this oxidative modification of GTP is the requirement for oxygen and the complexation of Cu(II) with GTP.

FIGURE 20

Proposed mechanism of GTP oxidation by Cu(II) ions

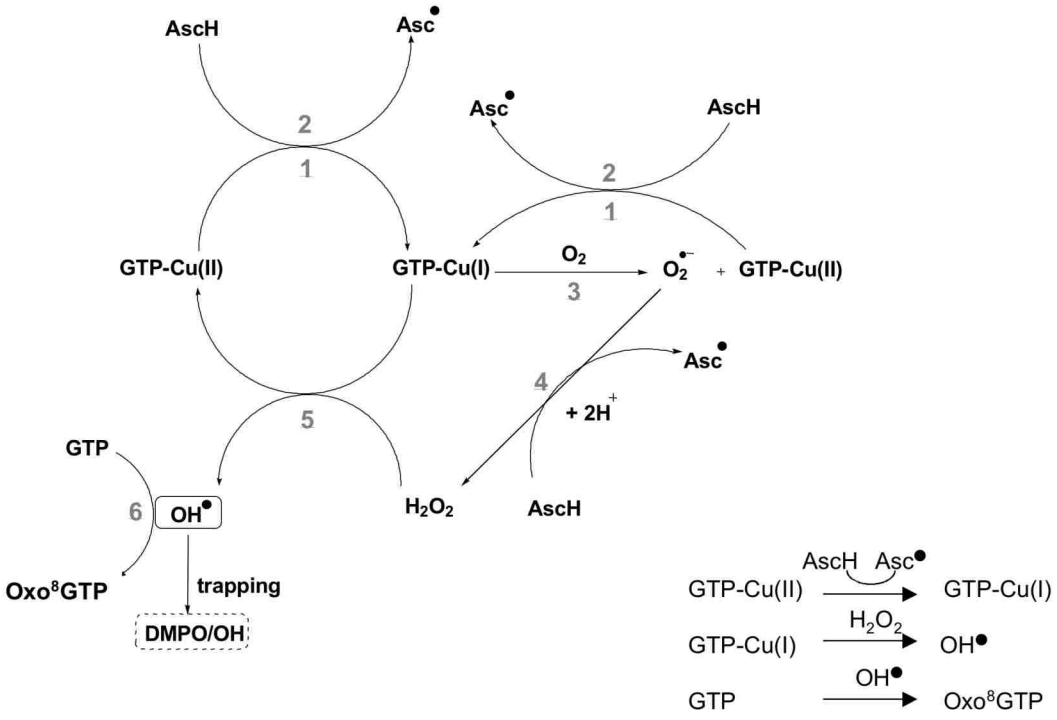

The $^{\bullet}OH$ produced in our solutions, via Fenton reactions involving Cu(II) is likely responsible for the production of oxo^{8}GTP because of its high oxidation potential (E^{o} = 2.31 V, pH 7.0) (Halliwell and Gutteridge 1986). In the first step of our proposed mechanism, the Cu(II) ion forms a complex with GTP and in step 2, is reduced to Cu(I)-GTP via electron transfer from the oxidation of ascorbic acid to the ascorbyl radical. This is followed by step 3 in which the Cu(I)-GTP reacts with molecular oxygen present in the solution to generate $O_2^{-\bullet}$ by electron transfer, and Cu(II)-GTP is regenerated and enters the cycle to produce another ascorbyl radical. The generated $O_2^{-\bullet}$ is subsequently reduced (E^{o} = 0.94 V) in the presence of the ascorbyl radical to H_2O_2 in step 4. The ascorbyl radical is also converted back to ascorbate in this step (E^{o} = 0.28 V). The reaction of the ascorbyl radical and $O_2^{-\bullet}$, generating ascorbate and H_2O_2 has a second order rate constant of 2.3 x 10^{8} M^{-1} s^{-1} (Scarpa, Stevanato et al. 1983). The other important reaction that can happen in this system is the oxidation of ascorbic acid by $O_2^{-\bullet}$ which proceeds with a second order rate constant of about 2.7 x 10^{5} M^{-1} s^{-1} (Nishikimi 1975). Thus, the ascorbyl radical produced in the first step of this reaction acts as an important agent in the reduction of $O_2^{-\bullet}$ to H_2O_2 which enters the Fenton reaction with Cu(I)-GTP in step 5 to produce •OH. Finally, this generated •OH goes on to oxidize GTP to oxo^{8}GTP in step 6. The reaction stops when available oxygen is consumed in the reactions or all available GTP is oxidized. Based on the results presented in this work, we propose a •OH-mediated mechanism for GTP oxidation by Cu(II) in the presence of L-ascorbic acid.

Discussion

We have previously demonstrated that the Cu/L-ascorbic acid system leads to the formation of the oxo^{8}GTP cell-free preparation as well as in cells in culture (Bolin and Cardozo-Pelaez 2007). It has been proposed that oxidation of the G moiety is mainly due to attack by •OH (Breen and Murphy 1995). In order to verify the chemical generation of •OH and consequent oxidation of GTP by Cu(II)-GTP complexes, we investigated free radical production by the copper/GTP/L-ascorbic acid system. In general, these EPR spin trapping experiments confirmed the production of •OH and the ascorbyl radical in reactions containing GTP, Cu(II), and ascorbate (Figure 12). The results also suggest that copper(II) catalyzes the formation of •OH while complexed, stabilizing the copper ion. The empirical ratio $g_{//}/A_{//}$ is frequently used to evaluate tetrahedral distortions in tetragonal structures of Cu(II) compounds. A ratio $g_{//}/A_{//}$ close to 100 cm indicates a square planar or tetragonal structure around the Cu(II) ion, and values from 175 to 250 cm are indicative of a distorted tetrahedral symmetry (Muller, Felix et al. 1995). Based on this designation, our data revealed a change to a more tetragonal structure when Cu(II) is combined with GTP in solution and strongly suggests the complexation of Cu(II) with GTP. The maximum wavelength for Cu(II) sulfate in aqueous PBS solution decreased from 750 nm to 830 nm in presence of GTP thus corroborating the changes on the Cu(II) center observed by EPR. The formation of a Cu(II) complex with GTP favors the formation of a more efficient catalyst for the observed oxidation of GTP, by facilitating Cu(II)/Cu(I) redox potential changes (Azzellini, Bagatin et al. 2006). When a redox active metal like copper is bound to a biological molecule such as GTP, known to be susceptible to oxidation, the oxidative-reduction reaction between ion states of the metal

can generate ROS locally that modify the molecule to which the metal is bound most efficiently. Our finding that L-ascorbic acid alone generates detectable levels of the ascorbyl radical and consequently leads to the oxidation of GTP in the absence of copper is not unsual. The dual-role of L-ascorbic acid as an oxidant at lower concentrations and antioxidant at higher concentrations has been previously reported and is due to the decrease in the rate of antioxidant reactions by ascorbate at low concentrations as compared to the rate of radical chain reactions initiated by catalytic metals such as copper (Buettner and Jurkiewicz 1996).

The •OH-producing system of GTP/1 mM L-ascorbic acid/ 10 μM Cu(II) sulfate presented in this study has been shown to generate significant levels of oxo^{8}GTP in cell culture (Bolin and Cardozo-Pelaez 2007). Interestingly, the increase in the percent of oxo^{8}GTP produced relative to GTP in HEK 293T cells exposed to 1 mM L-ascorbic acid/ 10 μM Cu(II) sulfate as compared to control is nearly twice as high as that observed in cell-free preparations of GTP like those reported here. This is likely due to higher availability of oxygen for this •OH-producing system in a respiring cell as compared to a cell-free, closed reaction with high oxygen demand but limited oxygen supply.

In order to evaluate this mechanism of oxidation in regards to a disease pathology known to be associated with oxidative stress, we decided to include the aggregated peptide $A\beta_{1-42}$ found in senile AD plaques (Gaggelli, Kozlowski et al. 2006). There has been some debate as to whether aggregated $A\beta_{1-42}$ can spontaneously produce ROS (Hensley, Carney et al. 1994; Turnbull, Tabner et al. 2001). Our results indicate that $A\beta_{1-42}$ alone is not capable of producing ROS at a level that oxidizes GTP to a detectable degree. This finding lends support to the hypothesis that Fenton-reactive metals such as

copper that from complexes with these senile plaques, at concentrations estimated to be as high as 400 μM in AD brain, and copper-complexing biomolecules such as GTP are likely the source of ROS which cause measurable oxidative modification to biomolecules in pathologies such as AD (Lovell, Robertson et al. 1998; Huang, Atwood et al. 1999; Huang, Cuajungco et al. 1999; Dikalov, Vitek et al. 2004).

Conclusions

In this study we report that GTP oxidation by copper is promoted by the production of ROS (summarized in Figure 20). Complexation of Cu(II) with GTP is an integral step in this mechanism of oxidation to produce oxo^{8}GTP as is the availability of a cellular reductant such as L-ascorbic acid and oxygen. An endogenous environment that fulfills these oxidative requirements is found in the brains of patients with neurodegenerative disease pathologies such as AD where copper, L-ascorbic acid, GTP, and oxygen are all within the range used in the cell-free experiments presented herein. Insight into the mechanism of GTP oxidation could lend important clues as to how oxidative damage from aging or disease pathologies might impair neuronal cell processes necessary for proper brain function. The influence of pH on the level of the generated radicals suggest that H_2O_2 is involved in the •OH production. This H_2O_2 is likely formed by the reaction of $O_2^{\bullet-}$, generated initially by copper in the presence of O_2, with available hydrogen in the reaction milieu (Fig. 20).

References

Azzellini, M. A., I. A. Bagatin, et al. (2006). "Di-imine copper(II) complexes as redox mediator and modulator in 2-deoxy-D-ribose oxidative damage." Redox Rep **11**(1): 25-37.

Biaglow, J. E., K. D. Held, et al. (1996). "Role of guanosine triphosphate in ferric ion-linked Fenton chemistry." Radiat Res **145**(5): 554-62.

Bolin, C. and F. Cardozo-Pelaez (2007). "Assessing biomarkers of oxidative stress: analysis of guanosine and oxidized guanosine nucleotide triphosphates by high performance liquid chromatography with electrochemical detection." J Chromatogr B Analyt Technol Biomed Life Sci **856**(1-2): 121-30.

Breen, A. P. and J. A. Murphy (1995). "Reactions of oxyl radicals with DNA." Free Radic Biol Med **18**(6): 1033-77.

Buettner, G. R. and B. A. Jurkiewicz (1996). "Catalytic metals, ascorbate and free radicals: combinations to avoid." Radiat Res **145**(5): 532-41.

Cerchiaro, G., K. Aquilano, et al. (2005). "Isatin-Schiff base copper(II) complexes and their influence on cellular viability." J Inorg Biochem **99**(7): 1433-40.

Dikalov, S. I., M. P. Vitek, et al. (2004). "Cupric-amyloid beta peptide complex stimulates oxidation of ascorbate and generation of hydroxyl radical." Free Radic Biol Med **36**(3): 340-7.

Edwards, J. L. and R. T. Kennedy (2005). "Metabolomic analysis of eukaryotic tissue and prokaryotes using negative mode MALDI time-of-flight mass spectrometry." Anal Chem **77**(7): 2201-9.

Einolf, H. J., N. Schnetz-Boutaud, et al. (1998). "Steady-state and pre-steady-state kinetic analysis of 8-oxo-7,8-dihydroguanosine triphosphate incorporation and extension by replicative and repair DNA polymerases." Biochemistry **37**(38): 13300-12.

Filomeni, G., G. Cerchiaro, et al. (2007). "Pro-apoptotic activity of novel Isatin-Schiff base copper(II) complexes depends on oxidative stress induction and organelle-selective damage." J Biol Chem **282**(16): 12010-21.

Filomeni, G., G. Rotilio, et al. (2005). "Disulfide relays and phosphorylative cascades: partners in redox-mediated signaling pathways." Cell Death Differ **12**(12): 1555-63.

Gaggelli, E., H. Kozlowski, et al. (2006). "Copper homeostasis and neurodegenerative disorders (Alzheimer's, prion, and Parkinson's diseases and amyotrophic lateral sclerosis)." Chem Rev **106**(6): 1995-2044.

Haghdoost, S., L. Sjolander, et al. (2006). "The nucleotide pool is a significant target for oxidative stress." Free Radic Biol Med **41**(4): 620-6.

Halliwell, B. and J. M. Gutteridge (1986). "Oxygen free radicals and iron in relation to biology and medicine: some problems and concepts." Arch Biochem Biophys **246**(2): 501-14.

Hayakawa, H., A. Taketomi, et al. (1995). "Generation and elimination of 8-oxo-7,8-dihydro-2'-deoxyguanosine 5'-triphosphate, a mutagenic substrate for DNA synthesis, in human cells." Biochemistry **34**(1): 89-95.

Hensley, K., J. M. Carney, et al. (1994). "A model for beta-amyloid aggregation and neurotoxicity based on free radical generation by the peptide: relevance to Alzheimer disease." Proc Natl Acad Sci U S A **91**(8): 3270-4.

Huang, X., C. S. Atwood, et al. (1999). "The A beta peptide of Alzheimer's disease directly produces hydrogen peroxide through metal ion reduction." Biochemistry **38**(24): 7609-16.
Huang, X., M. P. Cuajungco, et al. (1999). "Cu(II) potentiation of alzheimer abeta neurotoxicity. Correlation with cell-free hydrogen peroxide production and metal reduction." J Biol Chem **274**(52): 37111-6.
Kaim, W. and J. Rall (1996). Angew. Chem. Int. Ed. Engl. **35**(43-XX).
Klomp, L. W., S. J. Lin, et al. (1997). "Identification and functional expression of HAH1, a novel human gene involved in copper homeostasis." J Biol Chem **272**(14): 9221-6.
Lovell, M. A., J. D. Robertson, et al. (1998). "Copper, iron and zinc in Alzheimer's disease senile plaques." J Neurol Sci **158**(1): 47-52.
Muller, J., K. Felix, et al. (1995). Inorg. Chem. Acta. **233**: 11-19.
Nishikimi, M. (1975). "A function of tetrahydropteridines as cofactors for indoleamine 2,3-dioxygenase." Biochem Biophys Res Commun **63**(1): 92-8.
Rossi, L., M. Arciello, et al. (2006). "Copper imbalance and oxidative stress in neurodegeneration." Ital J Biochem **55**(3-4): 212-21.
Rossi, L., M. F. Lombardo, et al. (2004). "Mitochondrial dysfunction in neurodegenerative diseases associated with copper imbalance." Neurochem Res **29**(3): 493-504.
Russo, M. T., M. F. Blasi, et al. (2004). "The oxidized deoxynucleoside triphosphate pool is a significant contributor to genetic instability in mismatch repair-deficient cells." Mol Cell Biol **24**(1): 465-74.
Scarpa, M., R. Stevanato, et al. (1983). "Superoxide ion as active intermediate in the autoxidation of ascorbate by molecular oxygen. Effect of superoxide dismutase." J Biol Chem **258**(11): 6695-7.
Sies, H. (1991). "Role of reactive oxygen species in biological processes." Klin Wochenschr **69**(21-23): 965-8.
Solomon, E. I., U. M. Sundaram, et al. (1996). "Multicopper Oxidases and Oxygenases." Chem Rev **96**(7): 2563-2606.
Strader, C. D., T. M. Fong, et al. (1994). "Structure and function of G protein-coupled receptors." Annu Rev Biochem **63**: 101-32.
Svoboda, P. and M. Harms-Ringdahl (1999). "Protection or sensitization by thiols or ascorbate in irradiated solutions of DNA or deoxyguanosine." Radiat Res **151**(5): 605-16.
Turnbull, S., B. J. Tabner, et al. (2001). "New evidence that the Alzheimer beta-amyloid peptide does not spontaneously form free radicals: an ESR study using a series of spin-traps." Free Radic Biol Med **30**(10): 1154-62.
Zhang, H., J. Joseph, et al. (2000). "Bicarbonate enhances the hydroxylation, nitration, and peroxidation reactions catalyzed by copper, zinc superoxide dismutase. Intermediacy of carbonate anion radical." J Biol Chem **275**(19): 14038-45.

CHAPTER THREE

Characterization of Oxidized Guanosine 5'-Triphosphate (oxo^{8}GTP) as a viable inhibitor of soluble guanylyl cyclase (sGC)

Abstract

We have recently characterized oxidation of guanosine (G) in the nucleotide triphosphate pool, yielding oxidized guanosine 5'-triphoshate (oxo^{8}GTP), is an important biomarker of oxidative stress. Oxo^{8}GTP has been shown to precede oxidation to G incorporated into DNA and modulate cell processes such as G-protein signaling and RNA synthesis. This study demonstrates significant induction of oxo^{8}GTP in cell-free preparation as well as in PC12 cells exposed to physiologically relevant oxidative conditions generated with 10 μM copper sulphate and 1 mM L-Ascorbic Acid (Cu/Asc). We also present data identifying soluble guanyly cyclase (sGC) as important target of oxo^{8}GTP using purified sGC and endogenous sGC in PC12 cells. Oxo^{8}GTP is characterized as a competitive inhibitor of sGC and evidence is presented of Cu/Asc causing elevations in oxo^{8}GTP significant enough to result in a reduction of the sGC product cGMP by as much as half in pure sGC and PC12 cells. GTP is protected from oxidation in the presence of reduced glutathione and this subsequently rescues sGC activity. This suggests that oxo^{8}GTP is produced by free radicals *in vivo* and can have significant impact on cell functions regulated by sGC activity such as synaptic plasticity in the central nervous system. Alterations in copper homeostasis and oxidative stress have been implicated in several neurodegenerative disorders including Alzheimer's, Prion, and Parkinson's diseases as well as Amyotrophic Lateral Sclerosis. Thus, it is

possible that neuronal deficiencies in such disorders might be due to oxidation of the GTP pool and the ensuing effects in neuronal function.

Introduction

Oxidative stress has been implicated in the onset and development of several pathological processes including cancer and age-related neurodegenerative diseases such as Alzheimer's Disease (AD) and Parkinson's Disease (Hollstein, Sidransky et al. 1991; Sanchez-Ramos 1994; Alam, Jenner et al. 1997; Gabbita, Lovell et al. 1998; Wang, Xiong et al. 2005). Oxidative stress is often accomplished by probing cellular DNA for modified guanine, reported as 8-oxo-2'-deoxyguanosine (oxo^{8}2dG), a cellular biomarker (Dizdaroglu, Jaruga et al. 2002; Proteggente, England et al. 2002; Chiou, Chang et al. 2003). However, the percent of oxo^{8}dG relative to unmodified 2'-deoxyguanosine (2-dG) in DNA in tissues from pathologies such as Alzheimer's Disease and Parkinson's Disease is quite low, as little as 0.002 to 1% (Te Koppele, Lucassen et al. 1996; Alam, Jenner et al. 1997; Gabbita, Lovell et al. 1998). This implies that nuclear guanosine (G) moieties found in DNA may not be the best place to quantify oxidative insult. Increases in oxo^{8}dG levels in DNA can also occur after hydroxyl radical ($OH^{\cdot}$) attack on the cytosolic pool of G incorporated into 2-dG 5'- triphosphate (dGTP) or guanosine 5'-triphosphate (GTP). This oxidative modification produces the respective oxidized 2-dG and G triphosphate adducts, oxo^{8}dGTP and oxo^{8}GTP (Hayakawa, Taketomi et al. 1995). We have recently validated a novel method to measure oxidized guanosine triphosphate moieties using HPLC with electrochemical (EC) detection (Bolin and Cardozo-Pelaez 2007). Using this method, we have shown that the percent of cytosolic oxo^{8}GTP relative to GTP in human embryo kidney 293T (HEK 293T) cells under normal growth conditions was greater than 400 times the percent of oxo^{8}2dG to 2-dG in nuclear DNA under the conditions (Bolin and Cardozo-Pelaez 2007).

GTP participates in several critical physiological functions including RNA synthesis, cell signaling through activation of GTP-binding proteins, as well as the production of the second messenger cyclic guanosine monophosphate (cGMP) (Waldman and Murad 1987; Jayaram, Cooney et al. 1999; Metaye, Gibelin et al. 2005). Recent studies have shown that addition of oxo^{8}GTP to *in vitro* transcription reactions reduces the total amount of mRNA synthesized as well as increasing the number of mutations in the mRNA (Kamiya, Suzuki et al. 2007). Additionally, oxo^{8}GTP was shown to increase the activity of the GTP-binding protein Ras as well as downstream activators of the Ras-ERK pathway in HEK293T cells while the opposite effect was observed with the GTP-binding protein Rac1 (Yoon, Hyun et al. 2005). Given these reported effects of oxo^{8}GTP and our verification of its formation in cells, we opted to determine the role of oxo^{8}GTP on the activity of soluble guanylyl cyclase (sGC) [E.C. 4.6.1.2.]. sGC facilitates the conversion of GTP to cGMP, a pathway important for a range of physiological processes such as vasodilation, platelet aggregation, and neurotransmission (Moncada, Palmer et al. 1991). Alterations in the capacity of sGC to respond to NO, level of expression of sGC, as well as sGC activity have been associated with physiological deficiencies that may play a role in the pathologies of a variety of disorders including cardiovascular disease and neurological diseases including Alzheimer's Disease (AD) and Creutzfeldt-Jakob disease (Bonkale, Winblad et al. 1995; Baltrons, Pifarre et al. 2004; Puzzo, Vitolo et al. 2005; Moncada and Higgs 2006). Despite evidence of oxidative stress as a major player in these pathologies and evidence of GTP being a target for free radical attack, there have been no studies aimed at identifying the consequences of oxo^{8}GTP on sGC activity (Gaggelli, Kozlowski et al. 2006). We hypothesize that the GTP pool is vulnerable to

conditions of oxidative stress and formation of oxo^{8}GTP will impact cellular function, specifically the activity of sGC. We present evidence of oxo^{8}GTP as a viable inhibitor of purified sGC and endogenous sGC in PC12 cells. Our results support evidence of oxo^{8}GTP being a critical cellular biomarker of oxidative stress with deleterious biological consequences.

The goal of this study was to investigate the effects of oxo^{8}GTP on sGC activity *in vitro* and in rat pheochromocytoma (PC12) cells. We present evidence of oxo^{8}GTP as a viable inhibitor of purified sGC as well as endogenous sGC in PC12 cells. Our results support evidence of oxo^{8}GTP being a critical cellular biomarker of oxidative stress with deleterious biological consequences. Several synthetic stimulators and inhibitors of sGC have been used for experimental and therapeutic investigations although the effects of the endogenous product of GTP oxidation, oxo^{8}GTP, on sGC activity has never been evaluated until now (Gruetter, Kadowitz et al. 1981; Garthwaite, Southam et al. 1995; Schrammel, Behrends et al. 1996; Olesen, Drejer et al. 1998; Hobbs 2002).

Materials and Methods

Materials

All reagents were purchased from Sigma-Aldrich (St. Louis, MO), unless otherwise indicated. 8-oxoguanosine-5'-triphosphate (oxo^{8}GTP) was purchased from TriLink Biotechnologies (San Diego, CA). 8-hydroxy guanosine (oxo^{8}G) was obtained from Cayman Chemical (Ann Arbor, MI). Soluble guanylyl cyclase (sGC) isolated from bovine lung, DEA NONOate (DEA/NO), and 3-isobutyl-1-methylxanthine (IBMX) were purchased from Alexis Biochemicals (Lausen, Switzerland). Ultrapure water was obtained from a Milli-Q UF-Plus apparatus (Millipore, Billerica, MA).

cGMP Deterimination by HPLC-EC

cGMP was resolved by HPLC with a reverse phase YMC basic column (4.6 x 150 mm; particle size 3-micron) (YMC Inc., Wilmington, NC) and quantified using a CoulArray electrochemical detection system (ESA, Inc., Chelmsford, MA). An isocratic mobile phase consisting of 100 mM sodium acetate, pH 5.2, 4% Methanol (HPLC Grade) diluted in water polished with C18 Sep-Pak cartridges (Waters Corp., Milford, MA) was utilized to elute cGMP from the column. The mobile phase was filtered using 0.2 μm nylon filters and degassed by sonication before use with the HPLC. Potentials of the twelve coulometric analytical cells of the CoulArray system, placed in series, were as follows: 50, 125, 175, 200, 250, 380, 500, 700, 785, 850, 890, 900 mV. Data were recorded, analyzed, and stored using CoulArray for Windows data analysis software (ESA Inc., Chelmsford, MA). A calibration curve was generated from standards of cGMP ranging from 5 nanograms (13.6 picomoles) to 1 milligram (2.7 nanomoles).

Elution of the cGMP analyte was monitored in the 700, 785, and 850 mV channels and injected amounts were plotted relative to the sum of the peak areas.

Measurement sGC activity in cell-free and PC12 extract samples

5 ng of purified sGC from bovine lung was incubated with 1 mM GTP and stimulated with increasing concentrations of DEA/NO (0.001 μM to 100 μM diluted in ice-cold 10 mM NaOH) in buffer containing 3 mM $MgCl_2$, 0.5 g/L BSA, 50 mM TEA, 3 mM DTT, pH 7.4 at 37°C for 10 minutes. The reaction was stopped by placing on ice and immediately adding 0.5 N $HClO_4$ to a final concentration of 0.05 N $HClO_4$. Samples were mixed and centrifuged at 14,000 x g at 4°C for 15 minutes. Supernatants were then subjected to 0.45 μm filtration and 10 μL was then immediately injected into the HPLC-EC.

PC12 cells were seated at a density of 5-7 x 10^7 cells per plate in 10 mL of RPMI 1640 medium containing 5% fetal bovine serum (FBS), 10% horse serum (HS), 2 mM L-glutamine, 1mM sodium pyruvate, 25 units penicillin G, and 25 μL/mL of streptomyocin. Cells were grown until 80-90% confluent (about 4 days) on collagen coated 100 mM petri dishes maintained at 37°C, 5% CO_2, and 95% air atmosphere. Following a 10 minute incubation at 37°C with media containing 1mM IBMX, cells are incubated with increasing concentrations of DEA/NO (0.001 μM to 100 μM) at 37°C for 10 minutes. Prior to cGMP extraction, these PC12 cells were assessed for viability using the trypan blue exclusion method. The media was then replaced with 5 mL of ice-cold phosphate-buffered saline (PBS) containing 1mM IBMX prior to collecting cells and centrifuging at 1500 rpm at 4°C for 5 minutes. The cells were then washed with 300 μL of ice-cold PBS, sonicated, mixed, and centrifuged at 14,000 x g at 4°C for 15 minutes. A 10 μL

aliquot was set aside for Bradford protein analysis and 30 μL of 0.5 N $HClO_4$ was then added to remaining supernatant and centrifuged at 14, 000 x g, 4°C for 15 minutes. After 0.45 μm filtering, the 27 μL of supernatant was immediately injected into the HPLC-EC. cGMP was quantified in each sample based on calibration curves generated from known quantities of cGMP.

Measurement of GTP and Oxo^{8}GTP

GTP and Oxo^{8}GTP were isolated and quantified using HPLC-EC with preparative dephosphorylation as described previously (Bolin and Cardozo-Pelaez 2007). Briefly, PC12 cells grown under standard conditions described above were exposed to normal media (control) or media containing 1mM L-ascorbic acid and 10 μM copper sulfate (Cu/Asc) for 4 hours. After washing three times with ice-cold PBS, cells were collected in 300 μL of PBS. Following centrifugation, protein was precipitated using 30 μL of 60% Trichloroacetic Acid (TCA), vortex-mixed for 20s, placed in an ice-bath for 10 minutes, and vortex-mixed again for 20s. Cell extracts were then centrifuged at 13,000 rpm for 10 minutes at 4°C. The resulting supernatant was neutralized to pH 6.0 with a solution containing 3 M KOH and 3 M $KHCO_3$. GTP and oxo^{8}GTP were then dephosphorylated to their respective nucleosides guanosine (G) and 8-oxoguanosine (oxo^{8}G) for detection via HPLC-EC. On ice, 25 Units of alkaline phosphatase (dissolved in Tris-HCl pH 8.0), 1.8 mM sodium acetate, and 100mM Tris-HCl, were added to 30μL of sample in total volume of 60 μL. After incubation at 37°C for 1 hour, the dephosphorylation reaction was stopped by placing on ice. This was followed by filtering through Ultrafree-MC (30-kD) tubes (Millipore Corp., Bedford, MA). Detection of the generated nucleosides (G and oxo^{8}G) was carried out by injecting 27 μL of the

filtrate into the HPLC-EC using exactly the same HPLC-EC conditions described above. Guanosine elution was monitored in the 700, 785, and 850 mV channels and injected amounts were graphed relative to the sum of peak areas. Oxo^{8}G was monitored in the 250 mV channel and injected amounts were graphed relative to peak area. Calibration curves for G and Oxo^{8}G were generated from known quantities of each analyte ranging from 120 pmoles to 1.92 nmoles for G and 2.4 pmoles and 38.4 pmoles for oxo^{8}G. G and oxo^{8}G quantified in samples were reported as GTP and oxo^{8}GTP respectively.

Statistical Analysis

All data were analyzed using Prism GraphPad 4.0 software (Graph pad Software Inc., San Diego, CA). Calibration curve parameters for each of the analytes were obtained by linear regression analysis. Double reciprocal kinetic plots (Lineweaver-Burke) were analyzed using linear regression analysis. An unpaired t-test was performed on GTP, oxo^{8}GTP, and cGMP values collected from PC12 cells exposed to Cu/Asc; values denoted with an asterisk are significantly different from their corresponding controls ($P < 0.05$). A one-way ANOVA with Newman-Keuls Multiple Comparison Test post-hoc analysis was performed on *in vitro* GTP oxidation experiments with and without GSH; values denoted with an asterisk are significantly different from their corresponding controls ($P < 0.05$).

Results

Assay for sGC Activity Using HPLC-EC

Previous *in vitro* and *in vivo* studies of sGC activity have primarily utilized radioimmunoassay for detection of cGMP although HPLC methods have been previously presented (Yamamoto, Shimizu et al. 1984; Goossens, Leroux et al. 1994; Yonekura, Iwasaki et al. 1994; Pietta, Mauri et al. 1997; Seya, Furukawa et al. 1999; Diaz Enrich, Villamarin et al. 2000; Soda, Ohba et al. 2001). In order to measure sGC activity with the highest specificity and sensitivity, we developed a chromatographic analysis protocol employing HPLC-EC, to detect cGMP and determine sGC activity in cell-free preparations with purified sGC and in cell culture, using PC12 cells. sGC activity was defined as the amount of cGMP formed in a 10 minute reaction at 37^{o}C after the addition of DEA/NO to activate sGC. Figure 21A was obtained by injection of a standard containing 40 ng (108.9 pmoles) of purified cGMP eluting in the 785, 850, and 890 mV channels at approximately 6.0 minutes. Figure 21B demonstrates the linearity of the EC detector at these specific voltages for cGMP. The response was linear up to 4 milligrams (10.9 nanomoles) of injected cGMP with a minimum detection limit of 5 picograms (13.6 femtomoles).

FIGURE 21

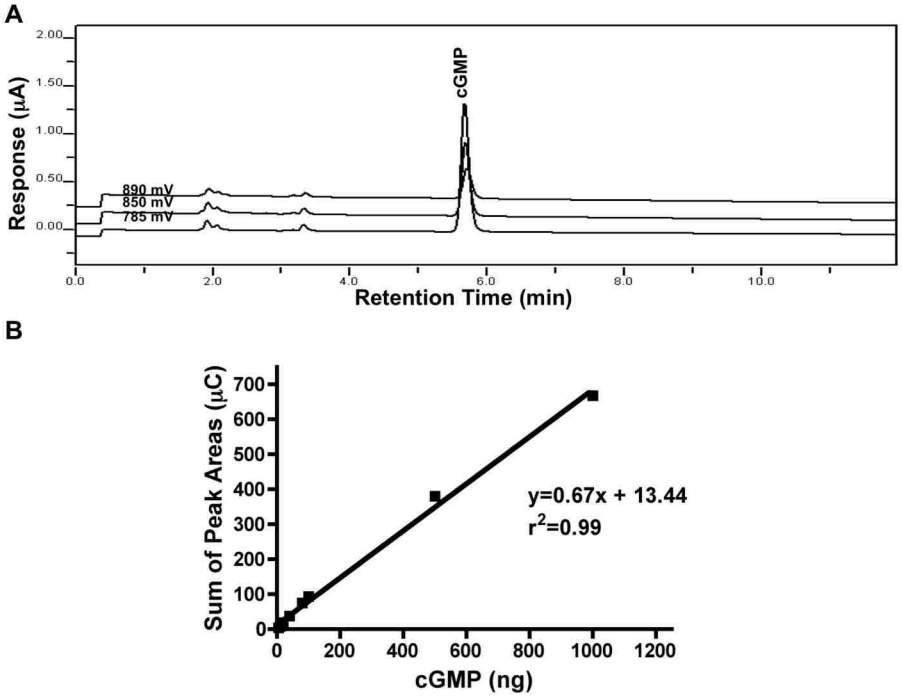
A
Response (μA)
2.00
1.50
1.00
0.50
0.00
cGMP
890 mV
850 mV
785 mV
0.0
2.0
4.0
6.0
8.0
10.0
Retention Time (min)
B
Sum of Peak Areas (μC)
700
600
500
400
300
200
100
0
y=0.67x + 13.44
r2=0.99
0
200
400
600
800
1000
1200
cGMP (ng)

Figure 21. Chromatographic profile for cGMP

cGMP detected and quantified based on the sum of peak areas of channels set at 785, 850, and 890 mV (A). Calibration curve showing the dynamic range of cGMP from 5 ng to 1 μg (B).

To test the validity of this approach to determine sGC activity, we stimulated purified sGC and PC12 cells with the NO donor DEA/NO. Figure 22A demonstrates that levels of cGMP detected using this method increased in a sigmoidal fashion with increasing concentrations of the NO donor DEA/NO using purified, cell–free sGC. cGMP was produced in a dose-dependent manner with maximal stimulation at 10 μM DEA/NO and an EC_{50} of 266 nM, values similar to previously reported values of sGC activity measured in cell-free preparations by radioimmunoassay (Bellamy, Griffiths et al. 2002). Figure 22B demonstrates that exposure of PC12 cells yields a similar concentration-response with increasing concentrations of DEA/NO with maximal stimulation at 50 μM DEA/NO and an EC_{50} of 5.7 μM. Addition of 50 μM DEA/NO to PC12 cells for 10 minutes resulted in an approximately 10-fold increase in intracellular cGMP levels (4.2 ± 0.37 nmoles/ mg total protein). This demonstrates that under our experimental conditions, PC12 cells produce a strong increase of detectable cGMP after NO stimulation.

FIGURE 22

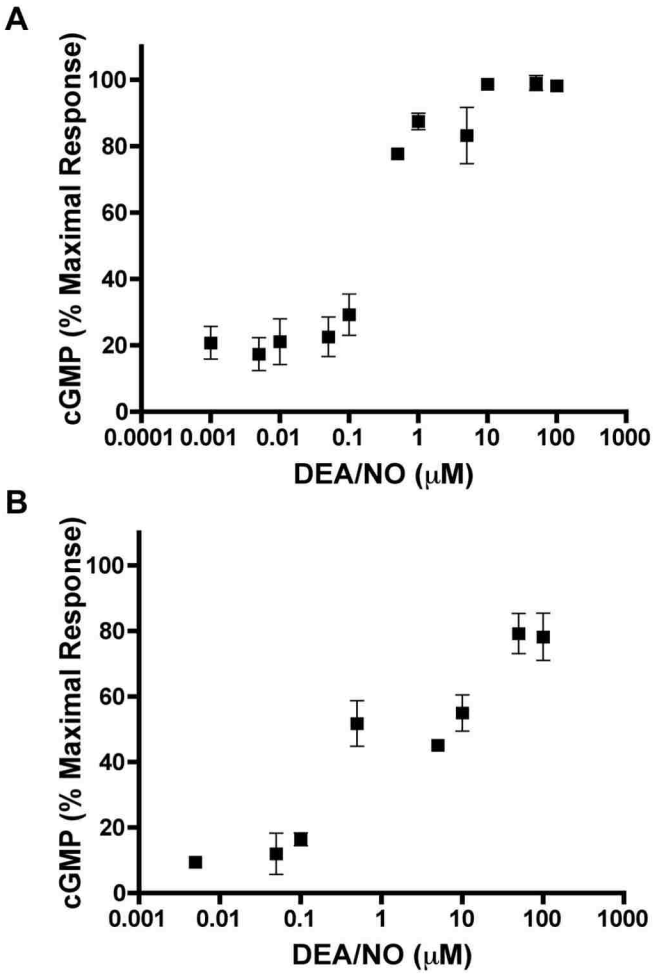
A
cGMP (% Maximal Response)
0
20
40
60
80
100
0.0001 0.001 0.01 0.1 1 10 100 1000
DEA/NO (μM)
B
cGMP (% Maximal Response)
0
20
40
60
80
100
0.001 0.01 0.1 1 10 100 1000
DEA/NO (μM)

Figure 22. sGC activity with increasing NO concentrations

cGMP levels in purified sGC(A) and cellular extracts from PC12 cells (B). Data are expressed as the mean amount of product (cGMP) ± SEM (n = 3-6) normalized to the maximal response observed in each experiment. x-axis is (log_{10} scale).

Kinetic Characterization of Oxo^{8}GTP as an Inhibitor of sGC

In order to determine the role of oxo^{8}GTP in the activity of sGC, we performed kinetic studies of sGC activity in presence of increasing levels of oxo^{8}GTP. Oxo^{8}GTP was found to inhibit the conversion of GTP to cGMP at low and high concentrations of GTP. Oxo^{8}GTP was added to incubations of purified sGC and stimulated with 10 μM DEA/NO and increasing concentrations of GTP (0.5 μM to 2 mM). Figure 23A shows cGMP levels produced by sGC after stimulation with DEA/NO (10 μM) in presence of 500 μM or 50 μM GTP with increasing levels of oxo^{8}GTP.

FIGURE 23

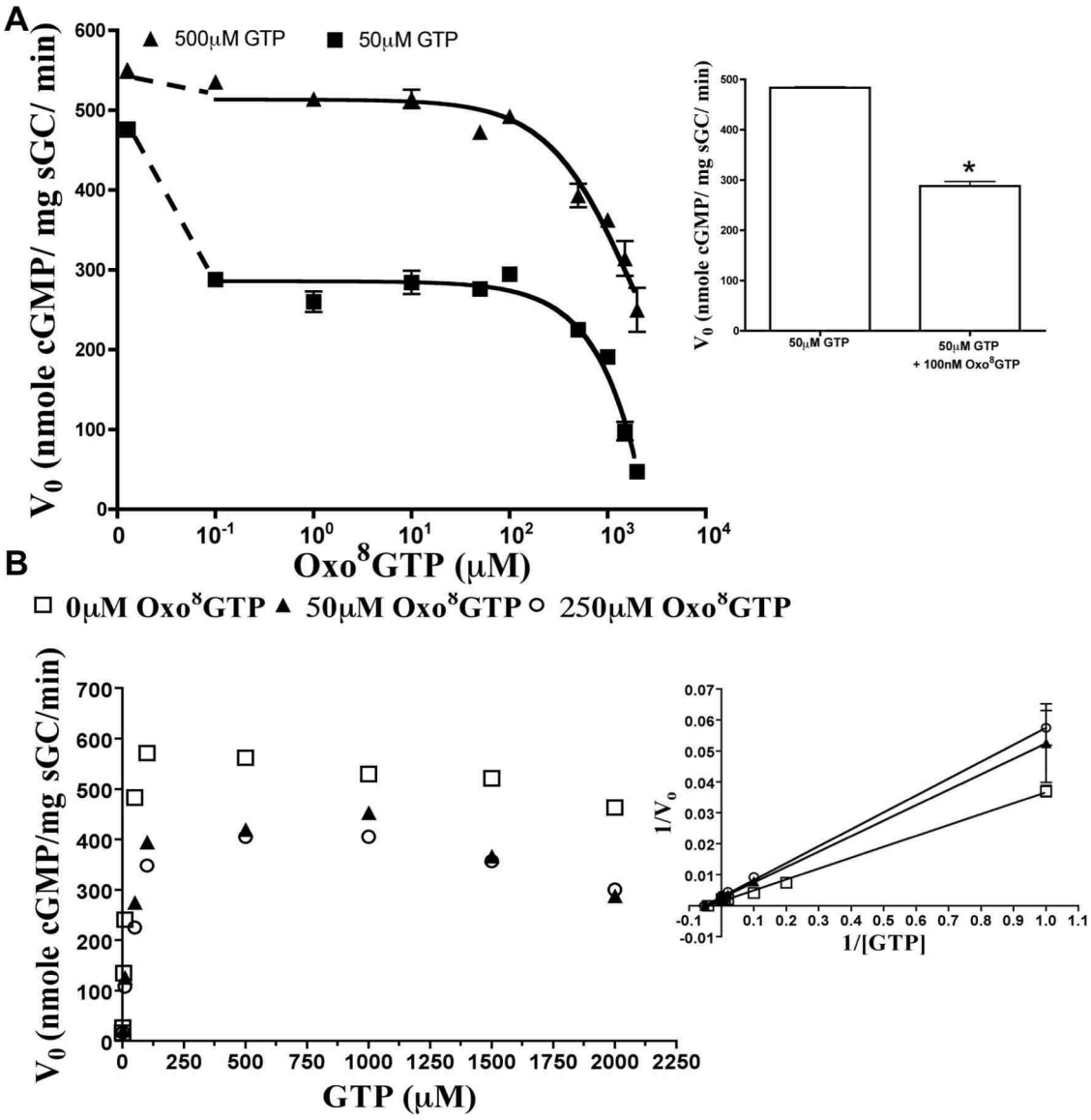
A
500μM GTP
50μM GTP
V0 (nmole cGMP/ mg sGC/ min)
Oxo8GTP (μM)
50μM GTP
50μM GTP + 100nM Oxo8GTP
*
B
0μM Oxo8GTP
50μM Oxo8GTP
250μM Oxo8GTP
V0 (nmole cGMP/mg sGC/min)
GTP (μM)
1/V0
1/[GTP]

Figure 23. **Inhibition of sGC by oxo^{8}GTP**

Oxo^{8}GTP-induced inhibition was determined in DEA/NO-stimulated, purified sGC in the presence of two different concentrations of the substrate (GTP) (A) and significant reduction in initial velocity (V_o) is demonstrated with as low as 100 nM oxo^{8}GTP (A, inset). Data represented as 1/velocity vs. 1/[GTP] indicate a noncompetitive, mixed type of inhibition by oxo^{8}GTP (B) as shown by a decreasing maximal velocity (V_{max}) with increasing oxo^{8}GTP concentrations (B, inset). Data are expressed as the means ± SEM (n = 3, * $p < 0.05$).

At both concentrations of GTP, oxo^{8}GTP was shown to inhibit sGC at concentrations greater than 100 μM. Values for IC_{50} were calculated to be 1.8mM for 500 μM GTP and 288 μM for 50 μM GTP. Despite the high IC_{50} values, inhibition of sGC incubated in the presence of 50 μM GTP was significant at levels of oxo^{8}GTP as low as 100 nM (Figure 23A, inset). Addition of as much as 100 μM DEA/NO to our cell-free sGC preparations with oxo^{8}GTP was ineffective at overcoming inhibition of the enzyme (Figure 24).

FIGURE 24

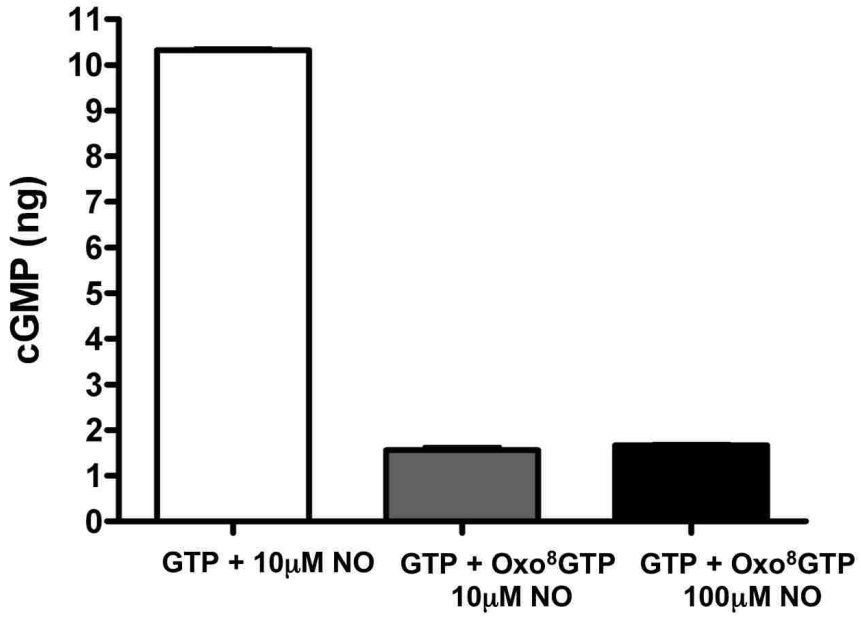
cGMP (ng)
11
10
9
8
7
6
5
4
3
2
1
0
GTP + 10μM NO
GTP + Oxo8GTP 10μM NO
GTP + Oxo8GTP 100μM NO

Figure 24. Effect of NO on sGC inhibition by oxo^{8}GTP

sGC activity, as assessed by total amount of cGMP product formed (ng), in reactions containing GTP and increasing concentrations of DEA/NO with or without oxo^{8}GTP. Data are expressed as means ± SEM (n = 3).

To identify the nature of the inhibition of sGC by oxo^{8}GTP, we determined Michaelis-Menten kinetic characteristics of the enzyme by plotting the substrate (GTP) versus the initial velocity (V_o). The percent conversion of substrate (GTP) to product (cGMP) was found to be between 0.1 and 16%, the production of cGMP was linear with time, purified sGC was stable during the 10 minute reaction period and therefore the Michaelis-Menten model is assumed (Marangoni 2003). We found the Michaelis constant (K_m) for GTP with purified sGC stimulated with 10 μM DEA/NO to be 24 μM, similar to previously published studies using cell-free, human sGC and synthetic NO donors (Table 8, Figure 23B) (Lee, Martin et al. 2000). The addition of 50 μM or 250 μM oxo^{8}GTP resulted in a very small change from K_m values calculated in sGC stimulated with 10 μM DEA/NO (Table 8, Figure 23B).

Table 8. Kinetic parameters of sGC inhibition by oxo^{8}GTP

	Oxo^{8}GTP (μM)		
	0	**50**	**250**
K_m, (μM)	**24.07**	**19.24**	**18.9**
V_{max}	**683.06**	**385.20**	**346.14**

However, the maximum reaction velocity (V_{max}) of sGC decreased from 683.06 μM GTP without inhibitor present to 346.14 μM GTP with 250 μM oxo^{8}GTP included in the reactions (Table 8, Figure 23B). The transformation of the same data into double-reciprocal plots at increasing concentrations of oxo^{8}GTP indicate that oxo^{8}GTP behaves as a noncompetitive, mixed type inhibitor of sGC (Figure 23B, inset).

Oxidative stress induces oxo^{8}GTP formation and sGC inhibition reversible by GSH

The direct addition of oxo^{8}GTP tells us very little of the consequences linked to its formation in biological systems. We have previously shown that a mixture of L-ascorbic acid (1 mM) and Copper Sulfate (10 μM) are sufficient to induce oxo^{8}GTP levels in cell-free reactions of GTP as well as in cell culture (Bolin and Cardozo-Pelaez 2007). To further investigate if the free radical-induced formation of oxo^{8}GTP can result in biological levels that decrease sGC activity, we exposed GTP to the Cu/As mixture before assessment of sGC activity. Figure 25A indicates that a four hour exposure of pure GTP to Cu/Asc results in a increase in oxo^{8}GTP that is three orders of magnitude higher than control.

FIGURE 25

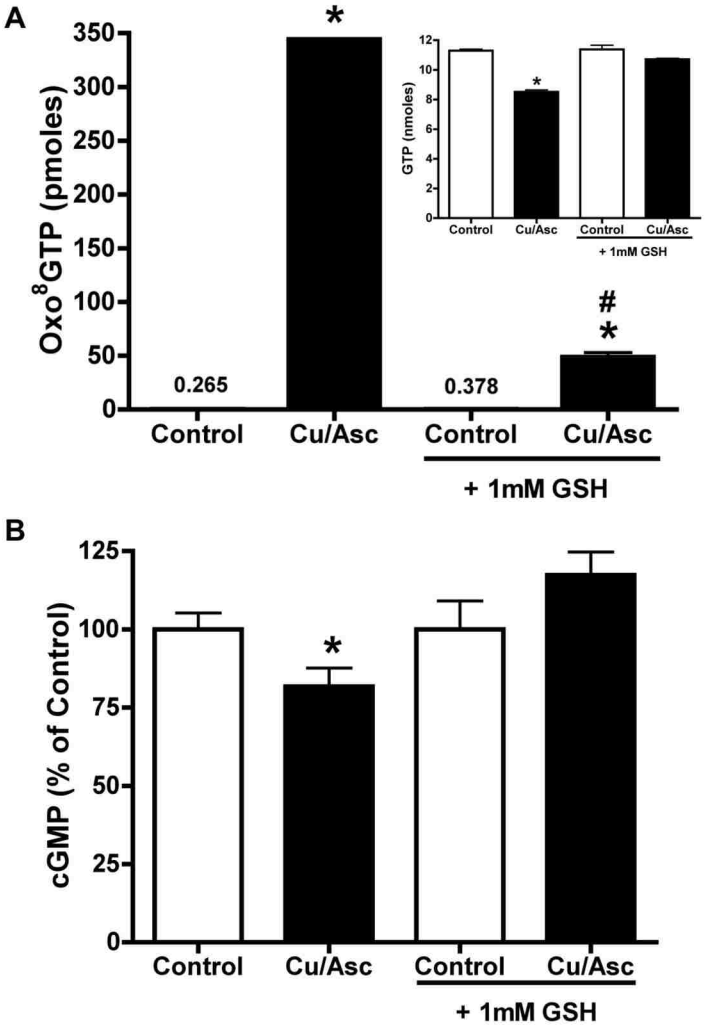
A
Oxo8GTP (pmoles)
350
300
250
200
150
100
50
0
0.265
0.378
*
#
*
Control
Cu/Asc
Control
Cu/Asc
+ 1mM GSH
GTP (nmoles)
12
10
8
6
4
2
0
*
Control
Cu/Asc
Control
Cu/Asc
+ 1mM GSH
B
cGMP (% of Control)
125
100
75
50
25
0
*
Control
Cu/Asc
Control
Cu/Asc
+ 1mM GSH

Figure 25. Induction of Oxo^{8}GTP with Cu/Asc and the effect of GSH

Increase in cell-free oxo^{8}GTP formation after incubation of GTP (inset) with Cu/Asc (black bars) as compared to control (white bar) conditions and the reduction of this oxidation by equimolar amount of GSH present in the incubations (A). Resulting reduction in DEA/NO-stimulated purified sGC activity with 1mM of GTP from (A) pre-incubated with Cu/Asc (black bars) as compared to control (white bars) and the rescue of this activity with GTP protected from oxidation by the presence of equimolar amounts of GSH (B) during four-hour incubations reported in (A). Data expressed as the means ± SEM (n =3, * $p < 0.05$ compared to control, $^{\#}$ $p<0.05$ compared to Cu/Asc without GSH).

It should be noted that incubations of pure GTP with L-ascorbic acid alone also shows a statistically significant increase in oxo^{8}GTP which is not due to trace metal contaminants, used as pre-treatment of all buffers with Chelex resin had no effect on oxo^{8}GTP levels (Figure 26).

FIGURE 26

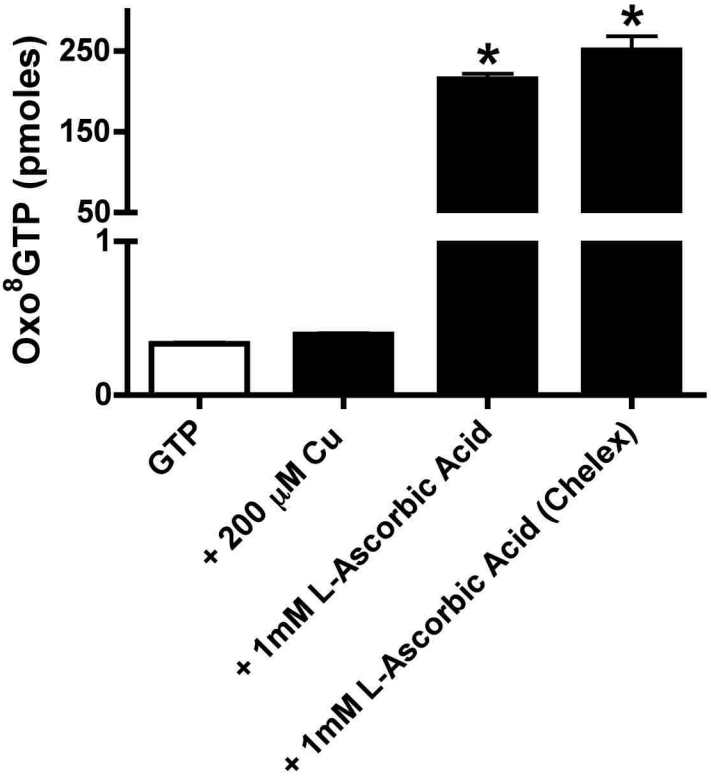
Oxo8GTP (pmoles)
250
150
50
1
0
*
*
GTP
+ 200 μM Cu
+ 1mM L-Ascorbic Acid
+ 1mM L-Ascorbic Acid (Chelex)

Figure 26. Levels of oxo^{8}GTP induced Cu and Asc independently

Amount of oxo^{8}GTP formed (pmoles) in four-hour incubations at 37^{o}C of 1mM pure GTP, 1 mM GTP exposed to 200 μM copper sulfate or 1mM L-ascorbic acid, and 1mM GTP exposed to 1 mM L-ascorbic acid in Chelex resin-treated buffers. Data are expressed as means ± SEM (n=2-6, ***** $p < 0.05$ as compared to pure GTP).

However as much as 200 μM copper sulfate does not increase oxo^{8}GTP above the small amounts produced in a four-hour incubation of pure GTP at 37ºC (Figure 26). This oxidation of GTP by Cu/Asc in combination also results in significantly reduced levels of recovered GTP from 11.295 ± 0.102 to 8.518 ± 0.135 nmoles (Figure 25A, inset). sGC reactions using 1 mM of this GTP pre-incubated with Cu/Asc, exhibited a significant reduction in 100 nM DEA/NO-stimulated sGC activity as compared to control reactions with unmodified GTP (Figure 25B). Incubation of purified sGC with Cu/Asc prior to stimulation with as much as 1 μM DEA/NO did not show any reduction in activity demonstrating that there is no direct effect of these oxidation conditions on sGC and inhibition is likely due to elevations in cellular oxo^{8}GTP (Figure 27).

FIGURE 27

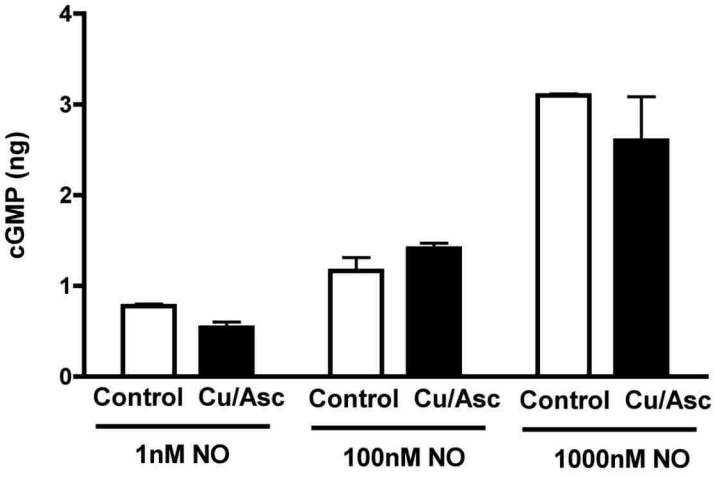
cGMP (ng)
4
3
2
1
0
Control
Cu/Asc
Control
Cu/Asc
Control
Cu/Asc
1nM NO
100nM NO
1000nM NO

Figure 27. sGC activity of purified sGC incubated with Cu/Asc

sGC activity, as assessed by total amount of cGMP product formed (ng), in purified sGC incubated with Cu/Asc (black bars) or PBS (white bars) before exposure to 1 mM GTP and stimulation with 1, 100, or 1000 nM DEA/NO. Data are expressed as means ± SEM (n=2).

It has been previously demonstrated that either Cu or Ascorbate alone can inhibit sGC and this inhibition is prevented by the antioxidant reduced glutathione (GSH) (Schrammel, Koesling et al. 1996; Schrammel, Koesling et al. 2000). Addition of equimolar amounts of GSH to GTP before incubation with Cu/Asc significantly reduced the levels of oxo^{8}GTP formed and rescued sGC activity (Figure 25). GSH had no effect on recovered GTP (Figure 25).

Increase in Oxo^{8}GTP in PC12 Cells Exposed to Cu/Asc: Effect on cellular sGC

Despite these previous results and other reported effects of oxo^{8}GTP, little is known of its role in cellular systems. We have recently shown that the known ROS producing system of 10 μM copper sulfate and 1 mM L-ascorbic acid (Cu/Asc) is capable of increasing oxo^{8}GTP in cell-free incubations of GTP alone as well as in HEK 293T cells (Figure 5A) (Biaglow, Held et al. 1996; Bolin and Cardozo-Pelaez 2007). In order to determine whether a similar challenge can affect the GTP pool in PC12 cells, we exposed PC12 cells to similar oxidizing conditions. Figures 28A and 28B are representative chromatograms of cytosolic extracts from PC12 cells under control and Cu/Asc-exposed, oxidizing conditions.

FIGURE 28

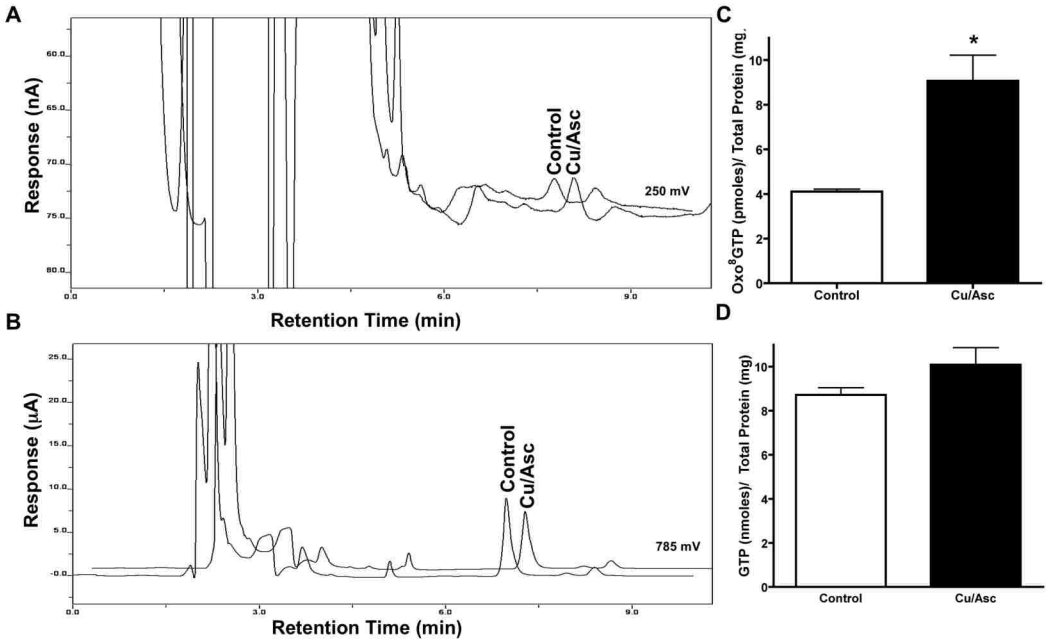
A
Response (nA)
Control
Cu/Asc
250 mV
Retention Time (min)
B
Response (μA)
Control
Cu/Asc
785 mV
Retention Time (min)
C
Oxo8GTP (pmoles)/ Total Protein (mg)
*
Control
Cu/Asc
D
GTP (nmoles)/ Total Protein (mg)
Control
Cu/Asc

Figure 28. **Chromatographic profiles of GTP in oxidized PC12 cells**

Alkaline phosphatase -treated cellular extracts obtained from PC12 cells under control or Cu/Asc –exposed (1mM L-ascorbic acid, 10 μM copper sulfate) conditions. Typical elution profiles for oxo^{8}G (A) and G (B) detected at 250mV and 785mV respectively. Bar graphs demonstrate increases in cellular levels of oxo^{8}G, reported as oxo^{8}GTP (C), in Cu/Asc –exposed cell populations (black bars) as compare to control (white bars) and constant levels of G, reported as GTP (D), in both groups. Data expressed as the mean molar quantities of analyte per total protein (mg) ± SEM (n =6, * $p < 0.05$).

We found that a four-hour incubation with Cu/Asc significantly increased cellular oxo^{8}GTP two-fold from basal levels in PC12 cells (Figure 28B). Detected levels of G and oxo^{8}G were expressed as GTP and oxo^{8}GTP respectively and normalized to total protein. Levels of GTP were unchanged between control and Cu/Asc-exposed cell populations (Figure 28D). GTP levels in untreated PC12 cells (1.5 nmoles GTP/ 10^6 cells) were similar to basal levels we previously reported in untreated HEK 293T cells (2.3 nmoles GTP/ 10^6 cells) using this method (Bolin and Cardozo-Pelaez 2007).

To determine if the increase in oxo^{8}GTP in PC12 cells with Cu/Asc would have an effect on sGC activity, we exposed a population of PC12 cells to Cu/Asc for four hours. After exposure to Cu/Asc, PC12 cells were stimulated with DEA/NO and cGMP formation by intracellular sGC was measured by HPLC-EC. Both 1 μM and 0.5 μM DEA/NO–stimulated PC12 cell populations had a two-fold reduction in cGMP formation after Cu/Asc exposure (Figure 29).

FIGURE 29

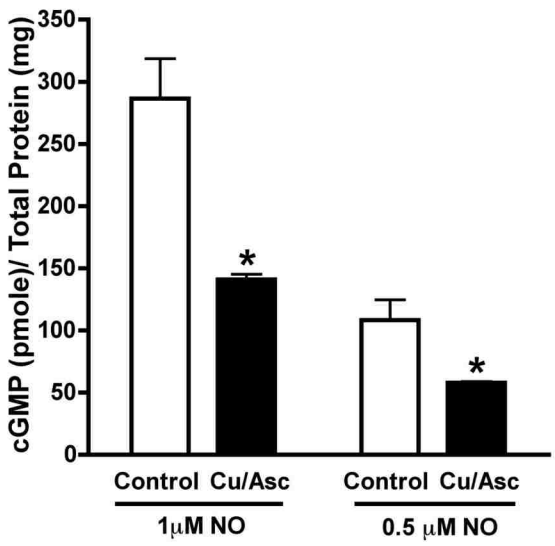
cGMP (pmole)/ Total Protein (mg)
350
300
250
200
150
100
50
0
*
*
Control
Cu/Asc
Control
Cu/Asc
1μM NO
0.5 μM NO

Figure 29. Inhibition of sGC activity in NO-stimulated, oxidized PC12 cells

Inhibition of sGC activity in DEA/NO-stimulated PC12 cells under control or Cu/Asc – exposed (1 mM L-ascorbic acid, 10 μM copper sulfate) conditions. Data expressed as the mean molar quantities of analyte per total protein (mg) ± SEM (n =2-9, * $p < 0.05$).

In order to reproduce the protective effects of GSH in cell-free preparations, we incubated PC12 cells with 1mM or 5 mM of a cell permeable GSH, glutathione ethyl ester, twenty minutes prior to the addition of Cu/Asc. Neither concentration of GSH was able to protect GTP from oxidative modification and only at 5mM was a protective effect on sGC activity observed (Figure 30).

FIGURE 30

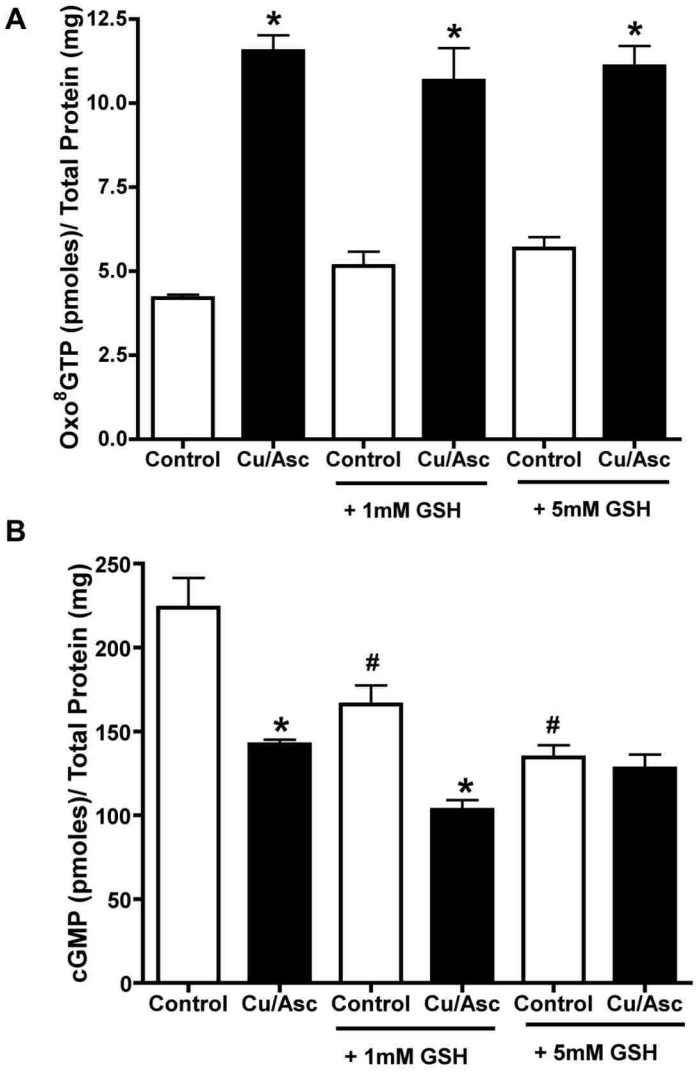
A
Oxo8GTP (pmoles)/ Total Protein (mg)
12.5
10.0
7.5
5.0
2.5
0.0
*
*
*
Control
Cu/Asc
Control
Cu/Asc
Control
Cu/Asc
+ 1mM GSH
+ 5mM GSH
B
cGMP (pmoles)/ Total Protein (mg)
250
200
150
100
50
0
*
#
*
#
Control
Cu/Asc
Control
Cu/Asc
Control
Cu/Asc
+ 1mM GSH
+ 5mM GSH

Figure 30. Effects of GSH on oxidation and sGC activity in PC12 cells

Increase in oxo^{8}GTP formation after incubation of PC12 cells with Cu/Asc (black bars) as compared to control (white bar) conditions including subsets of cells receiving 1 mM or 5mM glutathione ethyl ester (GSH) (A). Resulting reduction in DEA/NO-stimulated endogenous sGC activity in the same populations of PC12 cells as (A) incubated with Cu/Asc (black bars) as compared to control (white bars) with or without pretreatment with GSH (B). Data expressed as the means ± SEM (n =3, ***** $p < 0.05$ compared to control, $^{\#}$ $p<0.05$ compared to control without GSH).

It is important to note the confounding finding that GSH alone resulted in a significant reduction in cGMP produced in PC12 cells stimulated with NO (Figure 30B). Therefore, further investigation of the reversal of oxo^{8}GTP production and subsequent sGC inhibition in PC12 cells needs to be evaluated with alternative antioxidants such as mannitol or oxycoumarin previously shown to reduce oxidative stress in this cell type (Jones, Underwood et al. 2007).

Discussion

We have found that under oxidizing conditions the guanine (Gua) base incorporated into GTP is sensitive to free radical attack causing the formation of oxo^{8}GTP. Accumulation of this damaged form of GTP can have deleterious effects on cell function as evidenced by a reduction in purified sGC activity as well as endogenous sGC in PC12 cells. Conditions of oxidative stress induced by 1 mM L-ascorbic acid and 10 μM copper sulfate are sufficient to induce formation of oxo^{8}GTP without oxidation of the Gua incorporated into DNA (Bolin and Cardozo-Pelaez 2007).

To accurately report sGC activity, we developed a novel HPLC-EC methodology for quantifying cGMP which can be used as a supporting, functional assay for investigating changes in cytosolic oxo^{8}GTP levels using the same instrumentation in one cellular extract. We have previously reported the first biomarker assay of this kind for the measurement of oxidized guanosine triphosphates (oxo^{8}GTP and oxo^{8}dGTP) simultaneously with their unmodified triphosphate forms (GTP and dGTP) (Bolin and Cardozo-Pelaez 2007). In order to extend this methodology into an assay of cell function, we utilized these same HPLC-EC conditions and probed for cGMP. The most widely used assay for determining the conversion of GTP to cGMP by NO-stimulated sGC *in vitro* and *in vivo* is by radioimmunoassay with commercially available kits (e.g., Amersham International, Arlington Heights, IL). However, reverse phase and ion-exchange HPLC methods for the detection of cGMP using fluorometric, diode array, UV, and EC detection have all been described (Yamamoto, Shimizu et al. 1984; Smith, Wales et al. 1993; Goossens, Leroux et al. 1994; Yonekura, Iwasaki et al. 1994; Pietta, Mauri et al. 1997; Seya, Furukawa et al. 1999; Diaz Enrich, Villamarin et al. 2000; Soda, Ohba et

al. 2001). Our detection limit of 13.6 femtomoles is competitive with the most sensitive of these HPLC methods, that have a detection range between 5 femtomoles and 10 picomoles. The reliability of the method is demonstrated by an average percent recovery for cGMP standards of 99.8% and a coefficient of variation of less than 5% between replicate injections. Additionally, under our experimental conditions, sGC activity produces a strong increase of detectable cGMP stimulated by DEA/NO both in cell-free preparations of purified sGC and in PC12 cells similar to previously published studies (Figure 22) (Lee, Martin et al. 2000; Watjen, Benters et al. 2001; Bellamy, Griffiths et al. 2002). Our detected values of cGMP are close to cGMP values previously reported in this cell type although higher due to our use of a phosphodiesterase inhibitor, more potent NO donor, and our more sensitive detection methodology (Watjen, Benters et al. 2001). The advantage of our method lies within our ability to analyze the unmodified and oxidized substrates (GTP and oxo^{8}GTP) of NO-stimulated sGC along with the enzymatic product (cGMP) within the same sample.

Employing our sGC assay *in vitro* we were able to characterize oxo^{8}GTP as a potent, endogenous inhibitor of NO-stimulated sGC. The most characterized and widely used inhibitors of sGC to date are methylene blue, LY-83583, ODQ and NS 2028. These exogenous inhibitors act by either directly or indirectly interfering with NO binding to the ferrous heme iron which prevents the change in conformation of sGC and subsequent enzyme activation (Luo, Das et al. 1995; Schrammel, Behrends et al. 1996; Olesen, Drejer et al. 1998). This type of synthetic inhibition is partially overcome upon competitive addition of NO donors such as DEA/NO (Schrammel, Behrends et al. 1996). Due to the fact that high concentrations of DEA/NO were not able to overcome the

inhibition of sGC by oxo^{8}GTP, we suggest oxo^{8}GTP is not acting at the NO-binding site (Figure 24). Analysis of double reciprocal plots of substrate (GTP) versus the velocity of sGC demonstrated a decrease in V_{max} with increasing oxo^{8}GTP concentration with little effect on K_m (Table 1). This suggests a noncompetitive, mixed type of inhibition of oxo^{8}GTP with GTP. However, further analysis of inhibition is necessary to accurately characterize the specifics of oxo^{8}GTP inhibition on sGC activity.

Interestingly, L-ascorbic acid and cupper sulfate, independently, have been found to inhibit sGC in a similar cell-free system as the one used in our studies (Schrammel, Koesling et al. 1996; Schrammel, Koesling et al. 2000). Schrammel et. al. presented data showing that both copper ions and L-ascorbic acid act as inhibitors of sGC via NO-independent mechanisms and the inhibition is prevented by the addition of GSH. However, they failed to establish a role for the GTP pool. We report that exposure of pure GTP to L-ascorbic acid alone leads to an approximately 600 fold increase in oxo^{8}GTP although incubations of GTP with copper alone do not affect oxo^{8}GTP levels (Figure 26). Our results suggest that the previously reported observations of sGC inhibition by L-ascorbic acid and copper sulfate could be due in part to oxidative modification of GTP present in the reactions, producing the inhibitor oxo^{8}GTP, as opposed to direct effects on NO binding or direct modification of the sGC protein. This is further supported by the successful reduction of oxo^{8}GTP levels produced by the combination of L-ascorbic acid and copper sulfate in our reactions by GSH and consequent rescue of sGC activity (Figure 26).

Corroboration of our cell-free sGC activity results with findings using the PC12 neuronal cell culture model demonstrates the physiological relevancy of our findings.

The levels of oxo^{8}GTP induced with Cu/Asc correspond to approximately 24 nM oxo^{8}GTP in the cell extracts and approximately 50 μM GTP which resulted in a 50% reduction in cGMP produced by NO-stimulated, native sGC (Figures 24 and 25). This is very similar to the magnitude of reduction in cGMP in cell-free, NO-stimulated sGC inhibition observed (Figure 23A, inset). Therefore, although oxo^{8}GTP may only represent between 0.048 and 0.2 % of the total cellular GTP present, it is able to reduce the amount of cGMP available via sGC activation by as much as half. This is an interesting result that might suggest that sGC has a higher affinity for oxo^{8}GTP than the endogenous GTP substrate. Consequences of lowered cGMP levels in the CNS include reduced neuronal activation, impairment of long term potentiation (LTP), and the disruption of neuritogenesis (Zhuo, Hu et al. 1994; Arancio, Kandel et al. 1995; Boulton, Southam et al. 1995; Tanaka, Markerink-van Ittersum et al. 1997; Bidmon, Starbatty et al. 2004; Boess, Hendrix et al. 2004; Monfort, Munoz et al. 2004; Yamazaki, Chiba et al. 2006). Further investigation of oxo^{8}GTP levels and resulting changes in sGC could provide key mechanistic insights into the pathology of normal developmental, aging, and disease processes known to be highly affected by oxidative stress. This is emphasized by the fact that the MTH1 protein, responsible for hydrolyzing oxo^{8}dGTP to oxo^{8}dGMP and thus preventing its incorporation into DNA, has a rate of cleavage 50 times lower for oxo^{8}GTP than that of oxo^{8}dGTP (Mo, Maki et al. 1992; Hayakawa, Hofer et al. 1999). No specific repair mechanism for sanitation of cellular oxo^{8}GTP has been identified to compensate for this inefficiency of MTH1.

Concentrations of L-ascorbic acid and copper sulfate used in this study are biologically relevant to those found in brain where copper reaches levels as high as 30

μM during normal neurotransmission (Haeffner, Smith et al. 2005). Additionally, evaluation of AD brains known to contain concentrations of copper as high as 400 μM in a cellular environment rich in reducing agents such as ascorbic acid could provide a novel approach to understand early biomarkers of oxidative stress that appear to precede gross neuronal death (Lovell, Robertson et al. 1998; Pratico, Clark et al. 2000; Pratico, Uryu et al. 2001). Further studies evaluating the consequences of oxidative stress induced elevated oxo^{8}GTP levels and resulting modulations in sGC activity in brain tissue is necessary to investigate physiological impacts of this novel biomarker. Additionally, it is necessary to confirm the presence of an oxidized cGMP product, as a result of oxo^{8}GTP being converted to oxo^{8}cGMP by sGC, and determine how this oxidized cGMP may behave in downstream processes requiring cGMP.

In conclusion, our results show oxo^{8}GTP to be a potent inhibitor of sGC, and that oxidative environments induced with Cu/Asc cause an elevation in oxo^{8}GTP that significantly lowers available cGMP. The methodology outlined within this study to quantify oxo^{8}GTP and sGC activity concomitantly can be applied to a variety of systems investigating oxidative stress as a component of pathologies including cardiovascular disease and neurodegenerative disease. Furthermore, investigating this previously overlooked biomarker and its cellular consequences may lead to novel therapeutic interventions for these diseases.

Conclusions

In this study we report oxo^{8}GTP as an endogenous product of GTP oxidation under conditions of oxidized stress induced by copper sulfate and L-ascorbic acid that is reversible with the antioxidant GSH. sGC, a previously uncharacterized target of oxo^{8}GTP, is also evaluated and shown to be inhibited by oxo^{8}GTP produced in cell-free preparations as well as oxo^{8}GTP induced in PC12 cells exposed to copper sulfate and L-ascorbic acid. Analysis of brains from patients with neurodegenerative disease pathologies such as AD, known to have elevated levels of endogenous copper in cellular environments rich in ascorbate and GTP, could yield a more relevant source of biomarkers for disease state than previously characterized oxidative lesions to G incorporated into DNA. Analysis of oxidative products such as oxo^{8}GTP could help facilitate the transition from G being regarded as an endpoint of cellular dysfunction that leads to carcinogenesis or apoptosis in a cellular state too compromised for effective intervention to a player in early mechanistic modulations in neurodegenerative disease such as neuronal signaling.

References

Alam, Z. I., A. Jenner, et al. (1997). "Oxidative DNA damage in the parkinsonian brain: an apparent selective increase in 8-hydroxyguanine levels in substantia nigra." J Neurochem **69**(3): 1196-203.

Alam, Z. I., A. Jenner, et al. (1997). "Oxidative DNA damage in the parkinsonian brain: an apparent selective increase in 8-hydroxyguanine levels in substantia nigra." J Neurochem **69**(3): 1196-203.

Arancio, O., E. R. Kandel, et al. (1995). "Activity-dependent long-term enhancement of transmitter release by presynaptic 3',5'-cyclic GMP in cultured hippocampal neurons." Nature **376**(6535): 74-80.

Baltrons, M. A., P. Pifarre, et al. (2004). "Reduced expression of NO-sensitive guanylyl cyclase in reactive astrocytes of Alzheimer disease, Creutzfeldt-Jakob disease, and multiple sclerosis brains." Neurobiol Dis **17**(3): 462-72.

Bellamy, T. C., C. Griffiths, et al. (2002). "Differential sensitivity of guanylyl cyclase and mitochondrial respiration to nitric oxide measured using clamped concentrations." J Biol Chem **277**(35): 31801-7.

Biaglow, J. E., K. D. Held, et al. (1996). "Role of guanosine triphosphate in ferric ion-linked Fenton chemistry." Radiat Res **145**(5): 554-62.

Bidmon, H. J., J. Starbatty, et al. (2004). "Cerebral expression of the alpha2-subunit of soluble guanylyl cyclase is linked to cerebral maturation and sensory pathway refinement during postnatal development." Neurochem Int **45**(6): 821-32.

Boess, F. G., M. Hendrix, et al. (2004). "Inhibition of phosphodiesterase 2 increases neuronal cGMP, synaptic plasticity and memory performance." Neuropharmacology **47**(7): 1081-92.

Bolin, C. and F. Cardozo-Pelaez (2007). "Assessing biomarkers of oxidative stress: analysis of guanosine and oxidized guanosine nucleotide triphosphates by high performance liquid chromatography with electrochemical detection." J Chromatogr B Analyt Technol Biomed Life Sci **856**(1-2): 121-30.

Bonkale, W. L., B. Winblad, et al. (1995). "Reduced nitric oxide responsive soluble guanylyl cyclase activity in the superior temporal cortex of patients with Alzheimer's disease." Neurosci Lett **187**(1): 5-8.

Boulton, C. L., E. Southam, et al. (1995). "Nitric oxide-dependent long-term potentiation is blocked by a specific inhibitor of soluble guanylyl cyclase." Neuroscience **69**(3): 699-703.

Chiou, C. C., P. Y. Chang, et al. (2003). "Urinary 8-hydroxydeoxyguanosine and its analogs as DNA marker of oxidative stress: development of an ELISA and measurement in both bladder and prostate cancers." Clin Chim Acta **334**(1-2): 87-94.

Diaz Enrich, M. J., J. A. Villamarin, et al. (2000). "Measurement of adenosine 3',5'-cyclic monophosphate and guanosine 3', 5'-cyclic monophosphate in mussel (Mytilus galloprovincialis lmk.) by high-performance liquid chromatography with diode array detection." Anal Biochem **285**(1): 105-12.

Dizdaroglu, M., P. Jaruga, et al. (2002). "Free radical-induced damage to DNA: mechanisms and measurement." Free Radic Biol Med **32**(11): 1102-15.

Gabbita, S. P., M. A. Lovell, et al. (1998). "Increased nuclear DNA oxidation in the brain in Alzheimer's disease." J Neurochem **71**(5): 2034-40.
Gaggelli, E., H. Kozlowski, et al. (2006). "Copper homeostasis and neurodegenerative disorders (Alzheimer's, prion, and Parkinson's diseases and amyotrophic lateral sclerosis)." Chem Rev **106**(6): 1995-2044.
Garthwaite, J., E. Southam, et al. (1995). "Potent and selective inhibition of nitric oxide-sensitive guanylyl cyclase by 1H-[1,2,4]oxadiazolo[4,3-a]quinoxalin-1-one." Mol Pharmacol **48**(2): 184-8.
Goossens, J. F., F. Leroux, et al. (1994). "High-performance liquid chromatographic determination of cyclic 3',5'-AMP with fluorescence detection. Vasoactive intestinal peptide-induced modification of its concentration in neuroblastoma cells." J Chromatogr B Biomed Appl **657**(1): 192-6.
Gruetter, C. A., P. J. Kadowitz, et al. (1981). "Methylene blue inhibits coronary arterial relaxation and guanylate cyclase activation by nitroglycerin, sodium nitrite, and amyl nitrite." Can J Physiol Pharmacol **59**(2): 150-6.
Haeffner, F., D. G. Smith, et al. (2005). "Model studies of cholesterol and ascorbate oxidation by copper complexes: relevance to Alzheimer's disease beta-amyloid metallochemistry." J Inorg Biochem **99**(12): 2403-22.
Hayakawa, H., A. Hofer, et al. (1999). "Metabolic fate of oxidized guanine ribonucleotides in mammalian cells." Biochemistry **38**(12): 3610-4.
Hayakawa, H., A. Taketomi, et al. (1995). "Generation and elimination of 8-oxo-7,8-dihydro-2'-deoxyguanosine 5'-triphosphate, a mutagenic substrate for DNA synthesis, in human cells." Biochemistry **34**(1): 89-95.
Hobbs, A. J. (2002). "Soluble guanylate cyclase: an old therapeutic target re-visited." Br J Pharmacol **136**(5): 637-40.
Hollstein, M., D. Sidransky, et al. (1991). "p53 mutations in human cancers." Science **253**(5015): 49-53.
Jayaram, H. N., D. A. Cooney, et al. (1999). "Consequences of IMP dehydrogenase inhibition, and its relationship to cancer and apoptosis." Curr Med Chem **6**(7): 561-74.
Jones, C. E., C. K. Underwood, et al. (2007). "Copper induced oxidation of serotonin: analysis of products and toxicity." J Neurochem **102**(4): 1035-43.
Kamiya, H., A. Suzuki, et al. (2007). "Effects of 8-hydroxy-GTP and 2-hydroxy-ATP on in vitro transcription." Free Radic Biol Med **43**(5): 837-43.
Lee, Y. C., E. Martin, et al. (2000). "Human recombinant soluble guanylyl cyclase: expression, purification, and regulation." Proc Natl Acad Sci U S A **97**(20): 10763-8.
Lovell, M. A., J. D. Robertson, et al. (1998). "Copper, iron and zinc in Alzheimer's disease senile plaques." J Neurol Sci **158**(1): 47-52.
Luo, D., S. Das, et al. (1995). "Effects of methylene blue and LY83583 on neuronal nitric oxide synthase and NADPH-diaphorase." Eur J Pharmacol **290**(3): 247-51.
Marangoni, A. G. (2003). Enzyme Kinetics. Hoboken, New Jersey, Wiley-Interscience.
Metaye, T., H. Gibelin, et al. (2005). "Pathophysiological roles of G-protein-coupled receptor kinases." Cell Signal **17**(8): 917-28.

Mo, J. Y., H. Maki, et al. (1992). "Hydrolytic elimination of a mutagenic nucleotide, 8-oxodGTP, by human 18-kilodalton protein: sanitization of nucleotide pool." Proc Natl Acad Sci U S A **89**(22): 11021-5.

Moncada, S. and E. A. Higgs (2006). "Nitric oxide and the vascular endothelium." Handb Exp Pharmacol(176 Pt 1): 213-54.

Moncada, S., R. M. Palmer, et al. (1991). "Nitric oxide: physiology, pathophysiology, and pharmacology." Pharmacol Rev **43**(2): 109-42.

Monfort, P., M. D. Munoz, et al. (2004). "Sequential activation of soluble guanylate cyclase, protein kinase G and cGMP-degrading phosphodiesterase is necessary for proper induction of long-term potentiation in CA1 of hippocampus. Alterations in hyperammonemia." Neurochem Int **45**(6): 895-901.

Olesen, S. P., J. Drejer, et al. (1998). "Characterization of NS 2028 as a specific inhibitor of soluble guanylyl cyclase." Br J Pharmacol **123**(2): 299-309.

Pietta, P. G., P. L. Mauri, et al. (1997). "Assay of soluble guanylate cyclase activity by isocratic high-performance liquid chromatography." J Chromatogr B Biomed Sci Appl **690**(1-2): 343-7.

Pratico, D., C. M. Clark, et al. (2000). "Increased 8,12-iso-iPF2alpha-VI in Alzheimer's disease: correlation of a noninvasive index of lipid peroxidation with disease severity." Ann Neurol **48**(5): 809-12.

Pratico, D., K. Uryu, et al. (2001). "Increased lipid peroxidation precedes amyloid plaque formation in an animal model of Alzheimer amyloidosis." J Neurosci **21**(12): 4183-7.

Proteggente, A. R., T. G. England, et al. (2002). "Gender differences in steady-state levels of oxidative damage to DNA in healthy individuals." Free Radic Res **36**(2): 157-62.

Puzzo, D., O. Vitolo, et al. (2005). "Amyloid-beta peptide inhibits activation of the nitric oxide/cGMP/cAMP-responsive element-binding protein pathway during hippocampal synaptic plasticity." J Neurosci **25**(29): 6887-97.

Sanchez-Ramos, J., Overvik, Eva., Ames, B. (1994). "A Marker of Oxyradical-Mediated DNA Damage (8-Hydroxy-2'-Deoxyguanosine) is Increased in Nigro-Striatum of Parkinson's Disease Brain." Neurodegeneration **3**: 197-204.

Schrammel, A., S. Behrends, et al. (1996). "Characterization of 1H-[1,2,4]oxadiazolo[4,3-a]quinoxalin-1-one as a heme-site inhibitor of nitric oxide-sensitive guanylyl cyclase." Mol Pharmacol **50**(1): 1-5.

Schrammel, A., D. Koesling, et al. (1996). "Inhibition of purified soluble guanylyl cyclase by copper ions." Biochem Pharmacol **52**(7): 1041-5.

Schrammel, A., D. Koesling, et al. (2000). "Inhibition of purified soluble guanylyl cyclase by L-ascorbic acid." Cardiovasc Res **47**(3): 602-8.

Seya, K., K. I. Furukawa, et al. (1999). "A fluorometric assay for cyclic guanosine 3',5'-monophosphate incorporating a Sep-Pak cartridge and enzymatic cycling." Anal Biochem **272**(2): 243-9.

Smith, B. J., M. R. Wales, et al. (1993). "Assays of cyclic nucleotides. A review of current techniques." Appl Biochem Biotechnol **41**(3): 189-218.

Soda, K., Y. Ohba, et al. (2001). "Assay of human platelet guanylate cyclase activity by high-performance liquid chromatography with fluorescence derivatization." J Chromatogr B Biomed Sci Appl **752**(1): 55-60.

Tanaka, J., M. Markerink-van Ittersum, et al. (1997). "Nitric oxide-mediated cGMP synthesis in oligodendrocytes in the developing rat brain." Glia **19**(4): 286-97.
Te Koppele, J. M., P. J. Lucassen, et al. (1996). "8OHdG levels in brain do not indicate oxidative DNA damage in Alzheimer's disease." Neurobiol Aging **17**(6): 819-26.
Waldman, S. A. and F. Murad (1987). "Cyclic GMP synthesis and function." Pharmacol Rev **39**(3): 163-96.
Wang, J., S. Xiong, et al. (2005). "Increased oxidative damage in nuclear and mitochondrial DNA in Alzheimer's disease." J Neurochem **93**(4): 953-62.
Watjen, W., J. Benters, et al. (2001). "Zn2+ and Cd2+ increase the cyclic GMP level in PC12 cells by inhibition of the cyclic nucleotide phosphodiesterase." Toxicology **157**(3): 167-75.
Yamamoto, T., H. Shimizu, et al. (1984). "Simultaneous determination of guanine nucleotides in rat brain by high-performance liquid chromatography with dual-electrochemical detection." Anal Biochem **142**(2): 395-9.
Yamazaki, M., K. Chiba, et al. (2006). "Differences in neuritogenic response to nitric oxide in PC12 and PC12h cells." Neurosci Lett **393**(2-3): 222-5.
Yonekura, S., M. Iwasaki, et al. (1994). "Determination of guanine and its nucleosides and nucleotides in human erythrocytes by high-performance liquid chromatography with postcolumn fluorescence derivatization using phenylglyoxal reagent." J Chromatogr B Biomed Appl **654**(1): 19-24.
Yoon, S. H., J. W. Hyun, et al. (2005). "In vitro evidence for the recognition of 8-oxoGTP by Ras, a small GTP-binding protein." Biochem Biophys Res Commun **327**(1): 342-8.
Zhuo, M., Y. Hu, et al. (1994). "Role of guanylyl cyclase and cGMP-dependent protein kinase in long-term potentiation." Nature **368**(6472): 635-9.

SUMMARY

The goal of this study was to test the hypothesis that oxo^{8}GTP is produced under physiological conditions, increased during oxidative stress, and a consequence of elevated oxo^{8}GTP levels is a reduction in available cGMP due to its activity as a pathological inhibitor of sGC. We set out to test this hypothesis by testing the following specific aims: (1) Determine the levels of oxo^{8}GTP produced in cell-free GTP preparations and cytosolic extracts from cells in culture under conditions of oxidative stress induced by L-ascorbic acid and copper using a novel HPLC-EC methodology, (2) determine the specific mechanism of oxidation to GTP induced by L-ascorbic acid and copper using EPR, and (3) evaluate the consequences of increased levels of oxo^{8}GTP on sGC activity in cell-free and cell culture conditions.

Results from experiments testing these specific aims yielded the following conclusions. In regards to aim 1, HPLC-EC, with preparative dephosphorylation, is a sensitive, reliable method for measuring GTP, dGTP, oxo^{8}GTP, and oxo^{8}dGTP. Oxo^{8}GTP is produced in cell-free preparation of GTP under oxidizing conditions (1mM L-ascorbic acid/10 μM $CuSO_4$) and significant elevations in oxo^{8}GTP are also observed under the same oxidizing conditions in HEK 293T and PC12 cells. Additionally, Oxidation of the GTP pool may occur independently of oxidation to 2dG in DNA.

Major results and conclusions from aim 2 are that the $^{\bullet}$OH radical is generated in reactions of 1 mM GTP/10 μM $CuSO_4$/1 mM L-ascorbic acid as assessed by EPR spectroscopy. Production of the $^{\bullet}$OH radical is dependent on the presence of GTP and O_2 and Cu(II) forms a necessary complex with GTP which facilitates its reduction to Cu(I).

Differences observed in the percent increase of oxo^{8}GTP in cell-free GTP as compared to cell culture models can be explained by available O_2 in the system.

From specific aim 3 we were able to determined that HPLC-EC is a sensitive, reliable method for quantifying sGC activity based on detection of the cGMP product. Oxo^{8}GTP is a potent inhibitor of sGC in cell-free preparations and increases in oxo^{8}GTP in cell-free preparations by oxidizing conditions (1mM L-ascorbic acid and 10μM $CuSO_4$) cause significant inhibition of sGC activity which can be recovered by pre-treatment with the antioxidant GSH. The observed increases in oxo^{8}GTP in PC12 cells by oxidizing conditions also causes significant inhibition of sGC activity.

Taken together, the results presented in the entirety of this study provide a new means of understanding oxidative stress in the normal and disease or toxin-exposed cellular environment. Application of these methods can provide the tools necessary to target oxo^{8}GTP as a key biomarker and cellular signal in pathological disease states such as AD.

APPENDIX A:

Age-dependent accumulation of 8-hydroxy 2'-deoxyguanosine triphosphate (oxo^8GTP) in mouse caudate putamen

Summary of Method and Results

Male mice both young (aged 2-4 months) and old (aged 22-28 months) SVJ/129 mice were euthanized by cervical dislocation and microdissections of the caudate putamen performed. Caudate putamen tissues were weighed and immediately placed in ice-cold, 0.05M perchloric acid. After sonication, samples were centrifuged at 14,000 x g, 4°C for 20 minutes, supernatants were filtered through 0.45μm syringe filters and samples stored at -80°C until analysis. On the day of analysis, extracts were neutralized with $KHCO_3/KCO_3$ buffer and subjected to the dephosphorylation procedure using alkaline phosphatasee exactly as cell extracts in Chapter 1. HPLC-EC analysis of dG, G, oxo^8dG, and oxo^8G was also carried out exactly as described in Chapter 1 in 27 μL of dephosphorylated extract. dGTP, GTP, oxo^8dGTP, and oxo^8GTP were quantified as picomoles (pmoles) and expressed per amount of tissue weight in milligrams (mg).

As shown in Figure 1A and 1B, all analytes were detectable in caudate putamen tissue extracts from a representative young mouse caudate putamen.

FIGURE 1

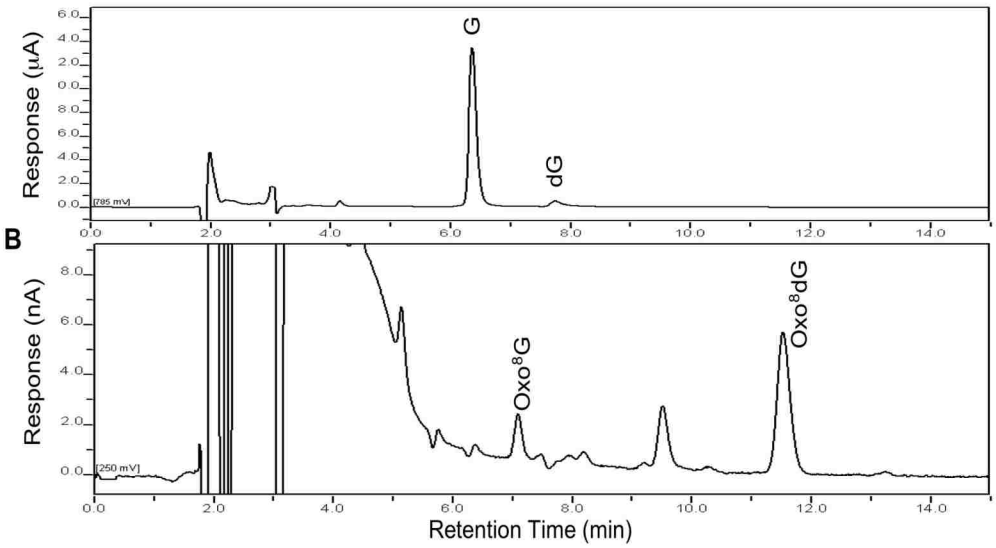
G
dG
Response (μA)
[785 mV]
B
Oxo8G
Oxo8dG
Response (nA)
[250 mV]
Retention Time (min)

Figure 1. Chromatographic profiles of caudate putamen extract.

Chromatograhic profiles of alkaline phosphatase treated caudate putament extracts in from young mice. Typical elution profiles for the generated G and 2-dG (A) and typical elution profile for the oxo^{8}G and oxo^{8}dG generated (B).

Figure 2 shows that GTP decreases significantly with age, rendering oxo^{8}GTP below detection limits in old animals. Conversely, dGTP appears to increase with age, and oxo^{8}dGTP is significantly elevated in old animals as compared to young animals (Figure 2).

FIGURE 2

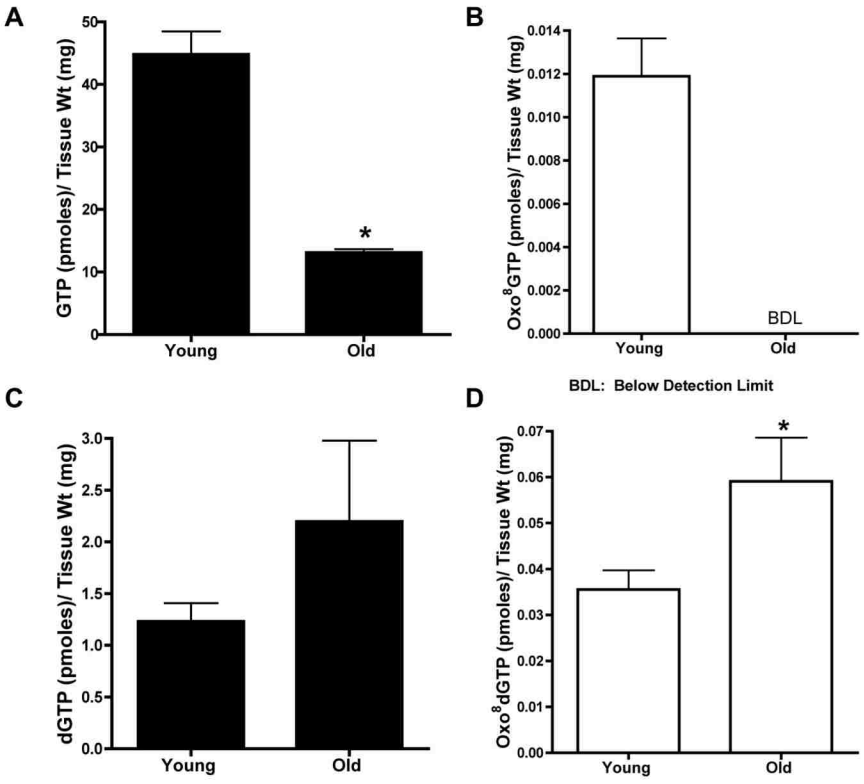
A
GTP (pmoles)/ Tissue Wt (mg)
50
40
30
20
10
0
*
Young
Old
B
Oxo8GTP (pmoles)/ Tissue Wt (mg)
0.014
0.012
0.010
0.008
0.006
0.004
0.002
0.000
BDL
Young
Old
BDL: Below Detection Limit
C
dGTP (pmoles)/ Tissue Wt (mg)
3.0
2.5
2.0
1.5
1.0
0.5
0.0
Young
Old
D
Oxo8dGTP (pmoles)/ Tissue Wt (mg)
0.07
0.06
0.05
0.04
0.03
0.02
0.01
0.00
*
Young
Old

Figure 2. **Quantitiation of GTP, dGTP, oxo^{8}GTP, and oxo^{8}dGTP in young and old mice.**

Levels of GTP (A) and oxo^{8}GTP (B) as well as dGTP (C) and oxo^{8}dGTP (D) from extracts of caudate putament from young (2-4 months) and old (22-28 months) mice. Data are expressed as mean ± SEM (n = 3-9), * $p<0.05$).

These findings are very interesting in terms of known oxidative accumulation to the guanosine moiety in DNA with age (Fraga, Shigenaga et al. 1990; Cardozo-Pelaez, Song et al. 1999; Izzotti, Cartiglia et al. 1999; Cardozo-Pelaez, Stedeford et al. 2002). It can be concluded from our data that the DNA precursor, dGTP, is also subject to an age-dependent increase in oxidation. This has never been directly quantified in brain tissue before. The results of these experiments verify that brain tissue is a viable source of these biomarkers of oxidation (oxo^{8}GTP and oxo^{8}dGTP) and further studies evaluating the effects of neurodegenerative disease such as AD or toxicological insult leading to neurological deficits are possible. The normal fluctuation in oxo^{8}GTP and oxo^{8}dGTP as well as their unmodified forms with observed with age differences in mouse brain caudate provide evidence of the vulnerability of this nucleotide pool that merits further investigation in murine and human brain tissue.

References

Cardozo-Pelaez, F., S. Song, et al. (1999). "Oxidative DNA damage in the aging mouse brain." Mov Disord **14**(6): 972-80.

Cardozo-Pelaez, F., T. J. Stedeford, et al. (2002). "Effects of diethylmaleate on DNA damage and repair in the mouse brain." Free Radic Biol Med **33**(2): 292-8.

Fraga, C. G., M. K. Shigenaga, et al. (1990). "Oxidative damage to DNA during aging: 8-hydroxy-2'-deoxyguanosine in rat organ DNA and urine." Proc Natl Acad Sci U S A **87**(12): 4533-7.

Izzotti, A., C. Cartiglia, et al. (1999). "Age-related increases of 8-hydroxy-2'-deoxyguanosine and DNA-protein crosslinks in mouse organs." Mutat Res **446**(2): 215-23.